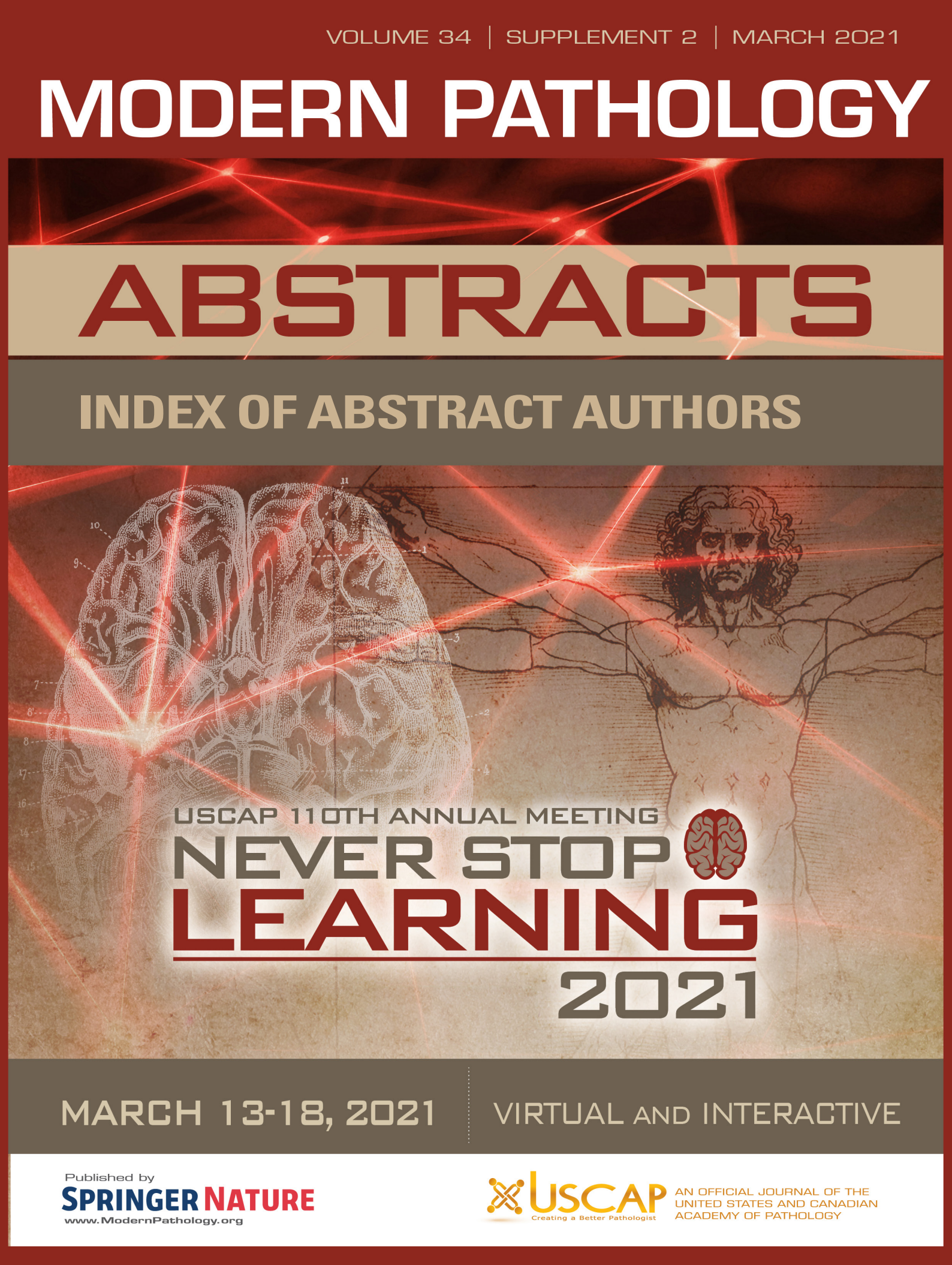


# MODERN PATHOLOGY

## ABSTRACTS

CYTOPATHOLOGY  
(158-237)



USCAP 110TH ANNUAL MEETING  
**NEVER STOP**  
**LEARNING**  
**2021**

MARCH 13-18, 2021

VIRTUAL AND INTERACTIVE

Published by  
**SPRINGER NATURE**  
[www.ModernPathology.org](http://www.ModernPathology.org)

 **USCAP** AN OFFICIAL JOURNAL OF THE  
UNITED STATES AND CANADIAN  
ACADEMY OF PATHOLOGY  
Creating a Better Pathologist



EDUCATION COMMITTEE

Jason L. Hornick  
Chair

Rhonda K. Yantiss, Chair  
Abstract Review Board and Assignment Committee

Kristin C. Jensen  
Chair, CME Subcommittee

Laura C. Collins  
Interactive Microscopy Subcommittee

Raja R. Seethala  
Short Course Coordinator

Ilan Weinreb  
Subcommittee for Unique Live Course Offerings

David B. Kaminsky  
(Ex-Officio)  
Zubair W. Baloch  
Daniel J. Brat  
Sarah M. Dry  
William C. Faquin  
Yuri Fedoriw  
Karen Fritchie  
Jennifer B. Gordetsky  
Melinda Lerwill  
Anna Marie Mulligan

Liron Pantanowitz  
David Papke,  
Pathologist-in-Training  
Carlos Parra-Herran  
Rajiv M. Patel  
Deepa T. Patil  
Charles Matthew Quick  
Lynette M. Sholl  
Olga K. Weinberg  
Maria Westerhoff  
Nicholas A. Zoumberos,  
Pathologist-in-Training

ABSTRACT REVIEW BOARD

Benjamin Adam  
Rouba Ali-Fehmi  
Daniela Allende  
Ghassan Allo  
Isabel Alvarado-Cabrero  
Catalina Amador  
Tatjana Antic  
Roberto Barrios  
Rohit Bhargava  
Luiz Blanco  
Jennifer Boland  
Alain Borczuk  
Elena Brachtel  
Marilyn Bui  
Eric Burks  
Shelley Caltharp  
Wenqing (Wendy) Cao  
Barbara Centeno  
Joanna Chan  
Jennifer Chapman  
Yunn-Yi Chen  
Hui Chen  
Wei Chen  
Sarah Chiang  
Nicole Cipriani  
Beth Clark  
Alejandro Contreras  
Claudiu Cotta  
Jennifer Cotter  
Sonika Dahiya  
Farbod Darvishian  
Jessica Davis  
Heather Dawson  
Elizabeth Demicco  
Katie Dennis  
Anand Dighe  
Suzanne Dintzis  
Michelle Downes

Charles Eberhart  
Andrew Evans  
Julie Fanburg-Smith  
Michael Feely  
Dennis Firchau  
Gregory Fishbein  
Andrew Folpe  
Larissa Furtado  
Billie Fyfe-Kirschner  
Giovanna Giannico  
Christopher Giffith  
Anthony Gill  
Paula Ginter  
Tamar Giorgadze  
Purva Gopal  
Abha Goyal  
Rondell Graham  
Alejandro Gru  
Nilesh Gupta  
Mamta Gupta  
Gillian Hale  
Suntrea Hammer  
Malini Harigopal  
Douglas Hartman  
Kammi Henriksen  
John Higgins  
Mai Hoang  
Aaron Huber  
Doina Ivan  
Wei Jiang  
Vickie Jo  
Dan Jones  
Kirk Jones  
Neerja Kambham  
Dipti Karamchandani  
Nora Katabi  
Darcy Kerr  
Francesca Khani

Joseph Khoury  
Rebecca King  
Veronica Klepeis  
Christian Kunder  
Steven Lagana  
Keith Lai  
Michael Lee  
Cheng-Han Lee  
Madelyn Lew  
Faqian Li  
Ying Li  
Haiyan Liu  
Xiuli Liu  
Lesley Lomo  
Tamara Lotan  
Sebastian Lucas  
Anthony Magliocco  
Kruti Maniar  
Brock Martin  
Emily Mason  
David McClintock  
Anne Mills  
Richard Mitchell  
Neda Moatamed  
Sara Monaco  
Atis Muehlenbachs  
Bitu Naini  
Dianna Ng  
Tony Ng  
Michiya Nishino  
Scott Owens  
Jacqueline Parai  
Avani Pendse  
Peter Pytel  
Stephen Raab  
Stanley Radio  
Emad Rakha  
Robyn Reed

Michelle Reid  
Natasha Rekhman  
Jordan Reynolds  
Andres Roma  
Lisa Rooper  
Avi Rosenberg  
Esther (Diana) Rossi  
Souzan Sanati  
Gabriel Sica  
Alexa Siddon  
Deepika Sirohi  
Kalliopi Siziopikou  
Maxwell Smith  
Adrian Suarez  
Sara Szabo  
Julie Teruya-Feldstein  
Khin Thway  
Rashmi Tondon  
Jose Torrealba  
Gary Tozbikian  
Andrew Turk  
Evi Vakiani  
Christopher VandenBussche  
Paul VanderLaan  
Hannah Wen  
Sara Wobker  
Kristy Wolniak  
Shaofeng Yan  
Huihui Ye  
Yunshin Yeh  
Anjana Yeldandi  
Gloria Young  
Lei Zhao  
Minghao Zhong  
Yaolin Zhou  
Hongfa Zhu

To cite abstracts in this publication, please use the following format: **Author A, Author B, Author C, et al. Abstract title (abs#). In "File Title." *Modern Pathology* 2021; 34 (suppl 2): page#**

**158 Cytological Findings in Bronchoalveolar Lavage of COVID-19 Positive Patients**

Andrea Agualimpia Garcia<sup>1</sup>, Sarah Al-Awami, Ya Xu<sup>1</sup>

<sup>1</sup>Baylor College of Medicine, Houston, TX

**Disclosures:** Andrea Agualimpia Garcia: None; Sarah Al-Awami: None; Ya Xu: None

**Background:** Histopathologic changes of lung described in COVID-19 autopsy cases have been reported. However, due to the highly contagious spread and invasiveness of the procedure bronchoalveolar lavage (BAL), rare reports exist regarding BAL findings.

**Design:** We reviewed 90 bronchoalveolar lavage (BAL) samples collected from 82 patients who presented to our hospital in the period of March to October 2020. There were 49 males (60%) and 33 females (40%) with an age range of 27-83 years old. 68 (82%) patients received RT-PCR COVID-19 test as send-out testing initially and later in house. The specimen collected for test was nasopharyngeal swab. The majority of the patients had COVID-19 test performed multiple times, ranging from 1-9 times. Clinical history and imaging findings were reviewed. The BAL samples were processed by ThinPrep method.

**Results:** There were 7 out of 68 tested patients positive for COVID-19. Three of these patients were positive for human immunodeficiency virus (HIV) with chest X-ray and/or CT showing bilateral infiltrates/haziness and nodules predominantly in the lower lobes. The other 4 patients presented with acute respiratory distress syndrome with imaging showing bilateral interstitial infiltrates with alveolar or hilar opacities. One positive patient (patient #7 in the Table 1) had the first BAL in January and COVID-19 test in March. The first BAL was also included in our study. The BAL specimens from COVID-19 positive patients had moderate to high cellularity with or without inflammatory necrotic debris. Bi- or multinucleated giant cells and hemosiderin laden-macrophages were present in 6 BALs (absent in a suboptimal sample). Atypical and apoptotic pneumocytes were seen in 3 BALs. The inflammatory cells were neutrophils predominant or mixed with lymphocytes. The cytological findings in BAL and clinico-pathological correlation of these 7 patients were summarized in Table 1.

Table 1. Cytological findings in bronchial alveolar lavage (BAL) and clinico-pathological correlation in seven patients with COVID 19 disease

COVID 19 cases	Gender	Age	Underlying disease	Cellularity/Inflammatory necrotic debris	Bi- or Multinucleated giant cells	Atypia and/or apoptosis	Inflammatory cells	Hemosiderin laden-macrophages	Follow up
1	M	57	HIV, DLBCL	Moderate/Absent	Present	Present	Lymphocytes & Neutrophils	Present	Died - 3 mon
2	M	59	HIV	High/Absent	Present	Present	Neutrophils	Present	4 mon
3	M	48	Multiple PE	Moderate/Absent	Present	Absent	Lymphocytes & Neutrophils	Present	2 mon
4	F	66	None	High/Present	Present	Absent	Lymphocytes & Neutrophils	Present	Died - 1 mon
5	F	59	None	High/Present	Absent	Present	Neutrophils	Absent	2 mon
6	M	55	None	Moderate/Present	Present	Absent	Lymphocytes & Neutrophils	Present	Died - 2 mon
7 (2 BAL)	M	33	HIV, DLBCL	High/Present	Present	Absent	Neutrophils	Present	9 mon
				Moderate/Absent	Present	Absent	Lymphocytes & Neutrophils	Present	

M: Male; F: Female; HIV: human immunodeficiency virus; PE: pulmonary embolism; DLBCL: diffuse large B cell lymphoma; Mon: months

**Conclusions:** There is no definite viral cytopathic effect identified in our BAL specimens from patients with COVID 19 disease. Features indicating pulmonary injury such as bi- or multinucleated giant cells and hemosiderin laden-macrophages are very frequently seen, which may be a hint of COVID -19 disease. The presence of cellular atypia and apoptosis of pneumocytes in BAL may mimic a neoplastic process. Further more extensive study is necessary to reveal other cytological findings in BAL in patients with COVID- 19 disease.

**159 Comparison of American College of Radiology (ACR) Thyroid Imaging Reporting and Data System (TI-RADS) with The Bethesda System for Reporting Thyroid Cytopathology (TBSRTC) in Predicting Risk of Malignancy in Surgically Resected Thyroid Nodules**

Imran Ajmal<sup>1</sup>, Fahd Hussain<sup>1</sup>, Varsha Manucha<sup>1</sup>

<sup>1</sup>University of Mississippi Medical Center, Jackson, MS

**Disclosures:** Imran Ajmal: None; Fahd Hussain: None; Varsha Manucha: None

**Background:** Ultrasound (USG) and Fine needle aspiration (FNA) play a critical role in the workup of a thyroid nodule (TN). The recently updated American College of Radiology Thyroid Imaging Reporting and Data Systems (ACR TI-RADS) and The Bethesda System for Reporting Thyroid Cytopathology (TBSRTC) are risk stratification systems that are used for classifying TN based on their risk of malignancy. In this retrospective study, we evaluated the risk of malignancy (ROM) and the risk of neoplasm (RON) for these reporting systems using the final histopathological diagnosis as the gold standard. The purpose of the study was to assess if ACR-TIRADS adds to the diagnostic value of thyroid FNAs.

**Design:** Of the 457 thyroidectomies that were performed during a period of three years (2017 to 2019), only cases with preceding FNA and concurrent USG examination using ACR-TIRADS scoring were included in the study. The TI-RADS category (TR) and TBSRTC categories were recorded for each case and compared with the final surgical pathology diagnosis (Figure 1). For this study all non-malignant follicular patterned neoplasms were categorized as benign neoplastic; multinodular goiters and Hashimotos thyroiditis were categorized as benign non-neoplastic. Using surgical pathology outcomes as the gold standard, ROM and RON were calculated for ACR TI-RADS and TBSRTC categories.

**Results:** Seventy-six cases fulfilled the inclusion criteria for this study. The majority (90%) of the patients were females. The average age was 52 years (range 13 to 74 y).

Fifty-one (67%) cases had a TR ≥ 4 (moderate to highly suspicious) of which 16 were malignant, 5 were benign neoplastic and 30 were non-neoplastic. Of the 30 non-neoplastic TN, 22 (73%) were downgraded on TBSRTC of ≤2. The ROM and RON for TR ≥ 4 were 31.4% and 41.3% respectively (Table 1).

Of the 25 (32%) cases that were categorized as TR ≤ 3 (benign to mildly suspicious), 7 of these were upgraded as TBSRTC category ≥ 3, resulting in a surgical resection with a diagnosis of neoplasm on all 7.

There were 15 (19%) cases that were assigned TBSRTC category V/VI (suspicious for malignancy /malignant). On surgical follow-up, 12 were malignant, 2 were benign neoplastic and 1 was non- neoplastic. The ROM and RON for TBSRTC category V/VI was 80% and 93.3% respectively.

In the 17 indeterminate TBSRTC category of III/IV, 12 cases were TR ≥ 4 and 5 cases were TR= 3. On surgical follow up, 10 (58.8%) were neoplastic and 7 (41.2%) were non-neoplastic. The sensitivity and negative predictive value of TBSRTC category of III/IV in detecting neoplasm is 62.5% and 86.36% respectively and did not change with or without the inclusion of TR.



Table 1: Comparison of ACR-TIRADS and TBSRTC with risk of malignancy and neoplasm

ACR-TIRADS	Histopathology			ROM	RON
	Benign Non-neoplastic (n)	Benign Neoplastic (n)	Malignant		
≤ 3 (n=25)	16	7	2	8%	36%
≥ 4 (n=51)	30	5	16	31.4%	41.3%
TBSRTC					
≤ II (n=44)	38	4	2	4.5%	13.6%
III-IV (n=17)	7	6	4	23.5%	58.8%
V-VI (n=15)	1	2	12	80%	93.3%

Abbreviation: ACR-TIRADS, American College of Radiology Thyroid Imaging Reporting and Data Systems; TBSRTC, The Bethesda System for Reporting Thyroid Cytopathology; ROM, Risk of Malignancy; RON, Risk of Neoplasm.

Figure 1 - 159

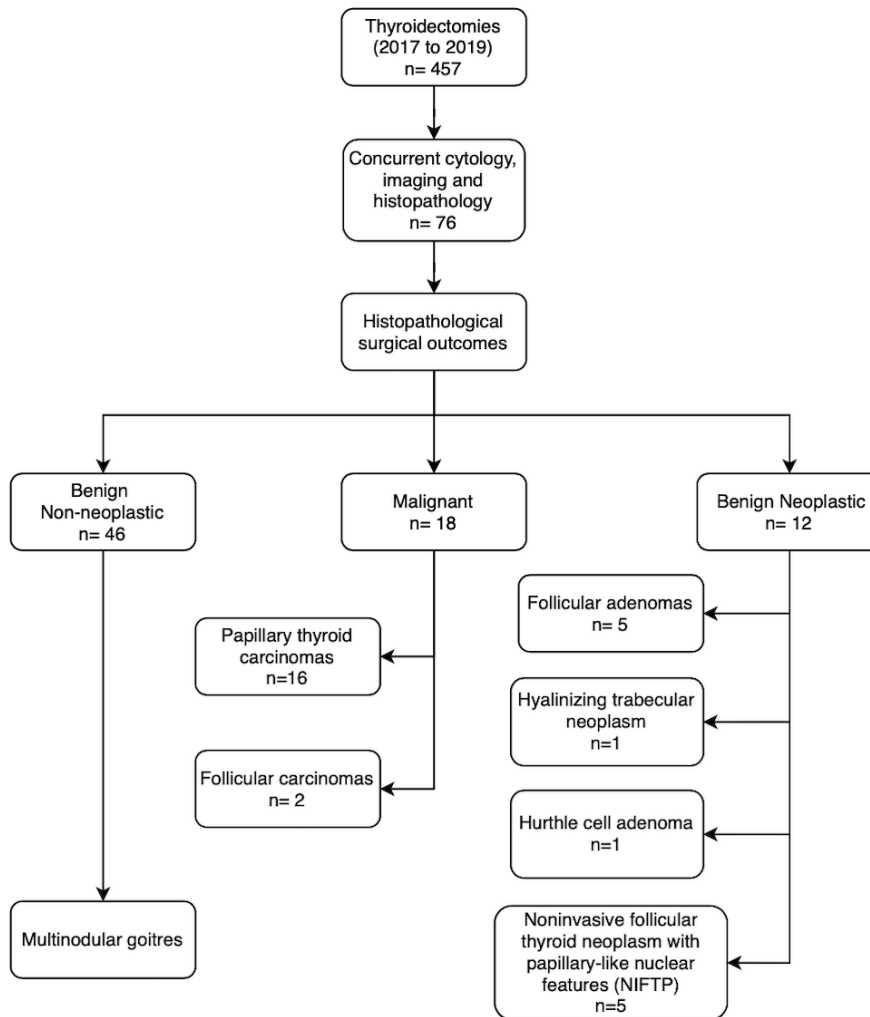


Figure 1: Study design and surgical outcomes

**Conclusions:** Cytology performs better than ACR-TIRADS in predicting malignancy and/or neoplasm of a TN. The role of ultrasound is limited to screening TN that should undergo FNA. A cytologist must not allow ACR-TIRADS score and imaging findings to influence the cytologic interpretation of thyroid FNAs.

**160 A Retrospective Analysis and Size Comparison of Anal and Cervical Pap-Smears at a Large Tertiary Care Teaching Hospital**

Khaled Algashaamy<sup>1</sup>, David Gajzer<sup>2</sup>, Isidro Luna<sup>3</sup>, Yiqin Zuo<sup>4</sup>, Jaylou Velez Torres<sup>5</sup>, Carmen Gomez-Fernandez<sup>5</sup>, Merce Jorda<sup>5</sup>, Monica Garcia-Buitrago<sup>6</sup>

<sup>1</sup>University of Miami/Jackson Memorial Hospital, Miami, <sup>2</sup>University of Miami Miller School of Medicine/Jackson Memorial Hospital, Miami, FL, <sup>3</sup>Jackson Memorial Hospital/University of Miami Hospital, Miami, FL, <sup>4</sup>University of Miami, Miami, FL, <sup>5</sup>University of Miami Miller School of Medicine, Miami, FL, <sup>6</sup>University of Miami Miller School of Medicine/Jackson Health System, Miami

**Disclosures:** Khaled Algashaamy: None; David Gajzer: None; Isidro Luna: None; Yiqin Zuo: None; Jaylou Velez Torres: None; Carmen Gomez-Fernandez: None; Merce Jorda: None; Monica Garcia-Buitrago: None

**Background:** Anal pap smears are increasingly utilized as a screening tool for anal premalignant lesions and cancer, especially in high risk populations. There is a growing body of literature that demonstrates poor concordance rate in the diagnosis of anal squamous intraepithelial lesions (SIL) with a tendency of anal paps to underdiagnose them; this is especially true in cases of high grade squamous intraepithelial lesions (HSIL). We aim to evaluate the size and nuclear cytoplasmic (N/C) ratio of anal and cervical SIL cells.

**Design:** A retrospective search of anal and cervical data from January 2018 to October 2020 was performed using the pathology laboratory information system in our tertiary care teaching hospital. The search was comprised of 337 anal and cervical LSIL and HSIL cases, which were reviewed. The diagnostic cells were analyzed using CellSens image capturing system. The images were blindly reviewed by a cytotechnician and a cytopathology fellow to confirm proper categorization. The nuclear size, cytoplasmic size and N/C ratios were measured. Student's T-test was utilized for statistical analysis.

**Results:** A total of 192 cells were analyzed; including 40 anal HSIL, 72 anal LSIL, 38 cervical HSIL, 32 cervical LSIL and 10 quiescent intermediate cells (5 cervical, 5 anal). The nuclear and cytoplasmic diameter of the anal quiescent intermediate cells ranged from 4.77-8.71 (mean 6.72  $\mu\text{m}$ ) and 18.38-37.74  $\mu\text{m}$  (mean 28.29  $\mu\text{m}$ ), respectively; whereas the nuclear and cytoplasmic diameter of the cervical quiescent intermediate cells ranged from 7.75-9.74  $\mu\text{m}$  (mean 8.95  $\mu\text{m}$ ) and 40.91-48.94  $\mu\text{m}$  (mean 45.55  $\mu\text{m}$ ), respectively (p 0.018 and 0.002). Anal HSIL had a mean nuclear and cytoplasmic diameter of 12.64  $\mu\text{m}$  and 19.68  $\mu\text{m}$ , respectively; and a mean N/C ratio of 0.66. Cervical HSIL showed a mean nuclear and cytoplasmic diameter of 13.75  $\mu\text{m}$  and 18.51  $\mu\text{m}$ , respectively; and an average N/C ratio of 0.74  $\mu\text{m}$ . The difference in N/C ratio between cervical and anal HSIL was statistically significant (p 0.000126). Anal LSIL showed a mean nuclear and cytoplasmic diameter of 12.38  $\mu\text{m}$  and 34.13  $\mu\text{m}$  respectively; with an average N/C ratio of 0.38. Cervical LSIL showed a mean nuclear and cytoplasmic diameter of 14.18  $\mu\text{m}$  and 43.91  $\mu\text{m}$  (p 0.06 and 0.001) and a 0.35  $\mu\text{m}$  N/C ratio.

**Conclusions:** Our cohort showed that cervical SIL cells have a larger nuclear and cytoplasmic size and a higher N/C ratio, compared to their anal counterpart. Quiescent cervical intermediate squamous cells when compared to quiescent anal intermediate cells have a larger nuclear and cytoplasmic size. These findings emphasize the importance of a careful screening of anal samples, as dysplastic cells may appear smaller, leading to misclassification or under diagnosis of dysplasia. Further studies increasing the cohort size are needed to evaluate the need of lowering the threshold for the diagnosis of anal dysplasia honoring the smaller cellular size and to improve the statistical power.



**161 Assessment of Clinical Outcomes of PD-L1 Testing of Non-Small Cell Lung Carcinoma Using Cytology Cellblock Specimens: An Experience of a Large Tertiary Care Institution**

Mohamed Alhamar<sup>1</sup>, Kanika Arora<sup>1</sup>, Oluwayomi Oyedeji<sup>1</sup>, Ziyang Zhang<sup>1</sup>, Daniel Schultz<sup>1</sup>, Chad Stone<sup>1</sup>, Kyle Perry<sup>1</sup>

<sup>1</sup>Henry Ford Health System, Detroit, MI

**Disclosures:** Mohamed Alhamar: None; Kanika Arora: None; Oluwayomi Oyedeji: None; Ziyang Zhang: None; Daniel Schultz: None; Chad Stone: None; Kyle Perry: None

**Background:** Anti-Programmed cell Death-Ligand 1 (PD-L1) immunotherapy treatment of advanced stage non-small cell lung carcinomas (NSCLC) requires prior assessment of PD-L1. Candidates for PD-L1 immunotherapy with advanced disease often have diagnostic material limited to cytologic specimens. This study aims to assess PD-L1 testing on cellblocks by comparing results with clinical response, disease free survival (DFS) & overall survival (OS).

**Design:** We identified 133 cellblocks from NSCLC cases from 2019-2020 tested for PD-L1. Detailed findings including age, gender, specimen source, type of NSCLC, number of PD-L1 tests per case, type of PD-L1, PD-L1 assigned score, clinical stage, anti-PD immunotherapy, chemo- & radiotherapy were recorded. Outcomes studied were clinical response, DFS & OS. Kaplan-Meier curves were generated and compared using log-rank test. Multivariate analysis was performed using Cox hazards models.

**Results:** The median age 70 (range 48-91); 53% male. Tumor type: 77/133 adenocarcinoma, 35/133 squamous cell carcinoma, 21/133 poorly differentiated & other carcinomas. Source of cytology tissue was lung (26/133), mediastinal lymph node (78/133), pleural fluid (24/133), distant metastasis (5/133). 15 cases tested for 2 PD-L1 types while the rest had only one PD-L1 test per case (113=22C3,5=28-2). Tumor proportion score (TPS) category: 50 cases= <1%, 43 cases= Low TPS (1-49%), 40 cases= high TPS (50-100%). Clinical stage: 2=10 cases, 3= 23 cases, 4=100 cases. 66 patients received anti-PD immunotherapy; 84 received chemotherapy; 54 received radiotherapy.

Median follow-up was 120 days (range 2-1002); 20 cases were lost to follow up. 4 cases had complete response while 29 showed partial response. 33 cases showed stable disease while 47 showed progression. 3 patients were alive without disease; 67 alive with disease; 54 died of disease;9 died due to other disease.

Patients who received immunotherapy had longer median survival (p<0.001-Figure 1) & lower hazards of death (Table1/multivariate analysis). However, PD-L1 status assigned on cellblock specimen was not a significant predictor of survival in patients receiving immunotherapy. Complete and partial response showed longest median OS in patients who tested positive for PD-L1 and received immunotherapy (p=0.032-Figure 2).

Prognostic variable	Hazard ratio	Lower .95	Upper .95	p-value
<b>Overall survival</b>				
<b>PD-L1 status &amp; Immunotherapy:</b>				
Positive PD-L1 & Immunotherapy given	0.366	0.000	0.718	0.003
Negative PD-L1 & Immunotherapy NOT given	1.032	0.519	2.051	0.929
Negative PD-L1 & Immunotherapy given	0.433	0.000	0.909	0.027
<b>Clinical Stage</b>				
Stage 3	4.000	0.485	33.003	0.198
Stage 4	10.158	1.387	74.406	0.023
<b>Disease free survival</b>				
<b>PD-L1 status &amp; Immunotherapy</b>				
Positive PD-L1 & Immunotherapy given	0.368	0.000	0.586	<0.0001
Negative PD-L1 & Immunotherapy NOT given	0.688	0.393	1.205	0.191
Negative PD-L1 & Immunotherapy given	0.470	0.000	0.796	0.005
<b>Clinical Stage</b>				
Stage 3	1.150	0.509	2.598	0.736
Stage 4	2.302	1.133	4.675	0.021

Figure 1 - 161

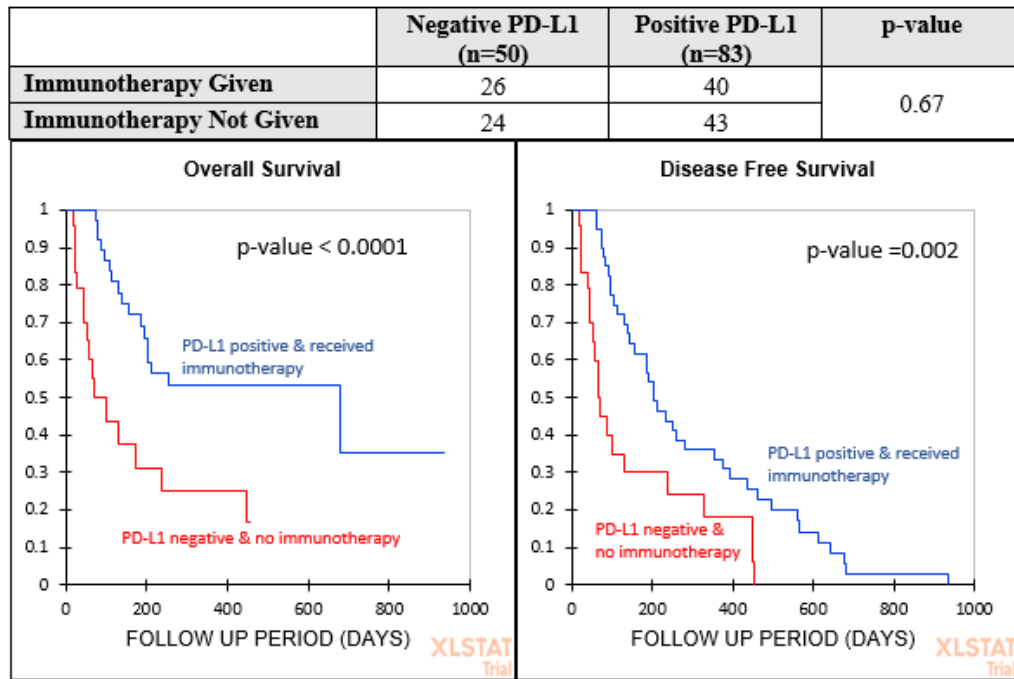
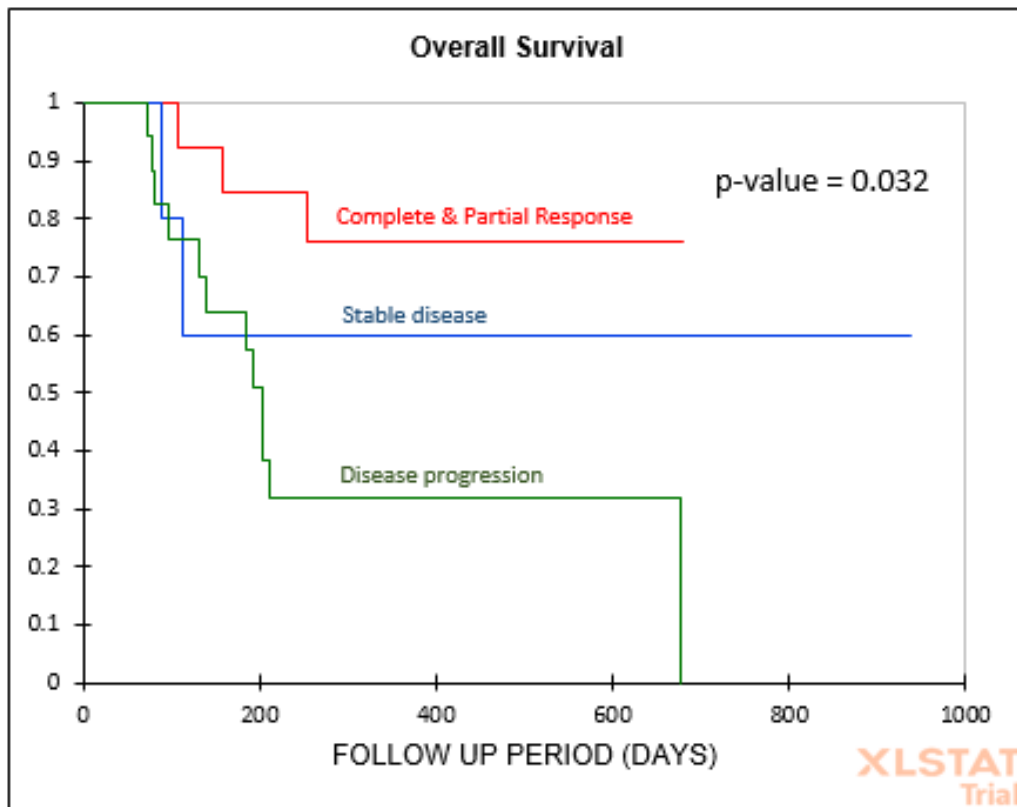


Figure 2 - 161



**Conclusions:** Cytology specimens are a viable choice for PD-L1 testing as reflected in clinical response. However, larger cytology sample sizes may be required to better reflect 'true' PDL1 status in a given patient.



**162 Adapting an Ultra-Rapid Circulating Tumor DNA Assay for Molecular Testing of Cytology Samples: A Proof-of-Concept Study**

Gulsedef Arslan<sup>1</sup>, Roberto Ruiz-Cordero<sup>1</sup>

<sup>1</sup>University of California San Francisco (UCSF), San Francisco, CA

**Disclosures:** Gulsedef Arslan: None; Roberto Ruiz-Cordero: None

**Background:** The Idylla (Biocartis, Belgium) molecular diagnostic platform is an ultra-rapid and fully automated real-time quantitative polymerase chain reaction, cartridge-based platform that can provide mutational results for selected genes in two hours. We evaluated the feasibility of adapting the Idylla circulating tumor (ct) DNA cartridges, designed to detect mutations in plasma samples, for molecular testing using cytology samples.

**Design:** We tested 0.5-1.0 ml of residual material from liquid-based preparations of fine needle aspiration biopsies (FNAB) and cytology fluids from patients whose tumors had been sequenced and shown to harbor mutations in genes for which Idylla cartridges are available. The three different media used for testing included direct fluid, CytoLyt (Hologic, USA), or PreservCyt (Hologic, USA) supernatant.

**Results:** A total of 16 cytology specimens (FNAB n=11, pleural n=3, ascites n=2) with known mutations in *KRAS* (7), *EGFR* (6), *NRAS* (2), and *BRAF* (1) were tested on Idylla. Using 0.5 cc of media as input, we detected expected mutations in 7 (44%) samples, did not detect expected mutations in 2 (12%), and had invalid results in 7 (44%) samples. Most invalid results were due to low DNA input and cartridge malfunction in one case. Using 1.0 cc of input from some invalid samples with available material yielded positive expected results.

**Conclusions:** The Idylla ctDNA cartridges could be adapted and used for ultra-rapid molecular testing using cytology samples; however, appropriate optimization and validation are required and are the focus of ongoing efforts to improve the positive detection rate.

**163 Presence of Single Cells on Diagnostic Fine-Needle Aspiration Smears Is Correlated with Survival in Pancreatic Ductal Adenocarcinoma Independent of Resectability**

Farah Baban<sup>1</sup>, Catherine Hagen<sup>1</sup>, Rondell Graham<sup>1</sup>, Charles Sturgis<sup>1</sup>, Christopher Hartley<sup>1</sup>

<sup>1</sup>Mayo Clinic, Rochester, MN

**Disclosures:** Farah Baban: None; Catherine Hagen: None; Rondell Graham: None; Charles Sturgis: None; Christopher Hartley: None

**Background:** The diagnosis of pancreatic ductal adenocarcinoma (PDAC) is often made via fine-needle aspiration (FNA). FNA smears exert physical strain on tumors -- some resist the strain and others show single cells shedding off of groups. Previously we addressed the prognostic significance of the single cell pattern (SCP) in PDAC in a smaller cohort from one institution. Our aim was to correlate the finding of SCP in FNAs with overall survival in resectable and non-resectable PDAC, with cases from two institutions.

**Design:** Ninety FNAs diagnostic of PDAC were retrieved from the pathology archives from two institutions, and 35 of these tumors were resected. All patients received chemotherapy and/or radiation. The most cellular smears were evaluated for the SCP. SCP was defined as single cells readily visible as separate from clusters at 100x (Figure 1). Presence of SCP was compared to clinicopathologic features gathered from chart review, including ypT and ypN stages (AJCC 8th edition) from 35 resected cases.

**Results:** The majority of FNAs diagnostic of PDAC exhibit SCP (53/62, 85%). SCP is correlated with survival independent of resectability (Table 1, Figure 2). In resected cases, only SCP was correlated with survival, while ypT and ypN stages were not. Resectable cases without SCP showed the best survival, while unresectable cases with SCP showed nearly 10-fold worse median overall survival (Table 1).

Table 1: Overall Survival Univariate and Multivariate Cox Regression Models with Resectability and Single Cell Pattern Median Survival Subtable			
Univariate Models	p-value	Hazard Ratio	95% CI
ypT stage (n=35)	0.68	1.14	0.61-2.12
Tumor size (n=35)	0.29	1.15	0.89-1.5
ypN stage (n=35)	0.06	1.59	0.98-2.59
Unresectable (n=90)	<0.001	3.63	2.17-6.07
Single cells present (n=90)	0.004	2.14	1.27-3.61
Multivariate Model (n=90)			
Unresectable	<0.001	3.88	2.29-6.56
Single cells present	0.002	2.33	1.26-3.98
		# Events/n (median OS months)	
Resectability and Single Cell Pattern Median OS Subtable		SCP Absent	SCP Present
Resectable		10/14 (48.8)	16/21 (23.7)
Unresectable		10/14 (18.7)	37/41 (5.4)
Total		20/28 (23.2)	53/62 (9.8)
Total			
Total		20/28 (23.2)	53/62 (9.8)
Total			

Legend: SCP=Single Cell Pattern; CI=Confidence Interval; OS=Overall Survival

Figure 1 - 163

**Figure 1: Single Cell Pattern Absent (A), Present (B), and Prominent (C), Diff Quik, 100X**

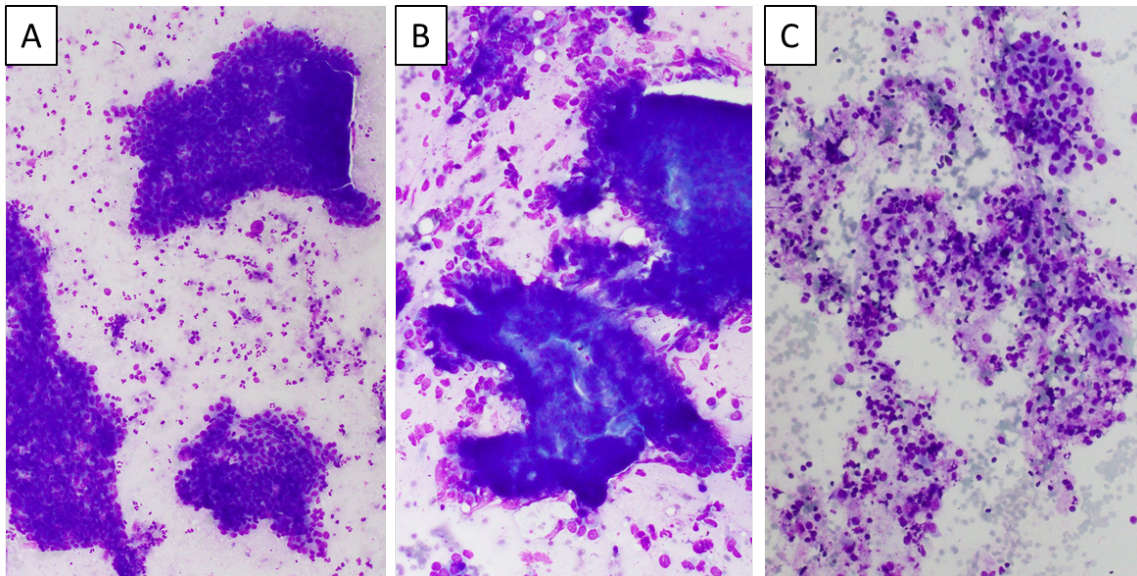
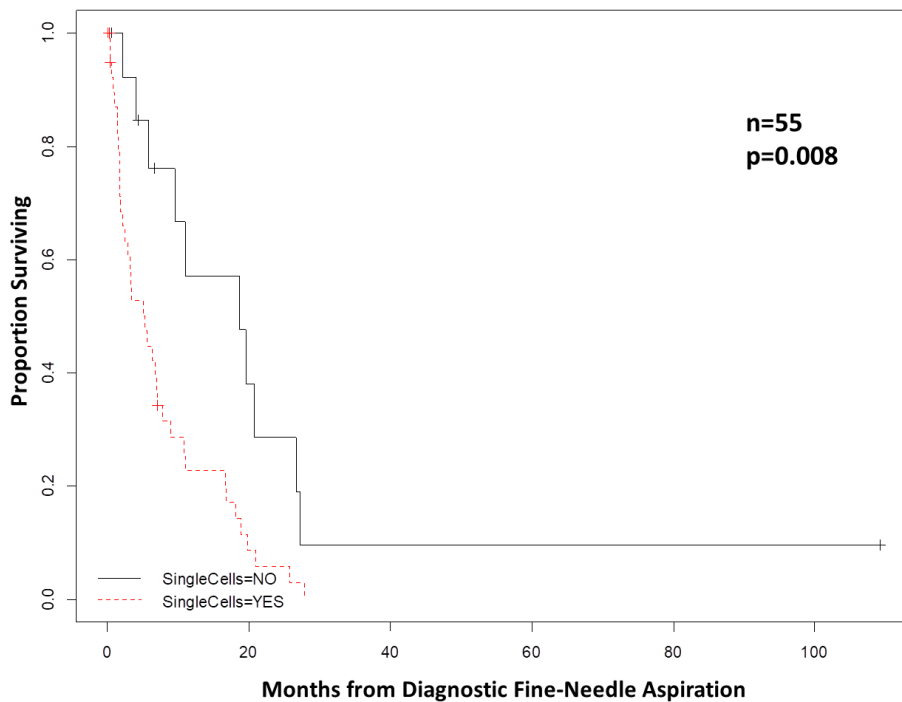




Figure 2 - 163

Figure 2: Overall Survival of Unresectable Pancreatic Ductal Adenocarcinoma Stratified by Presence/Absence of Single Cell Pattern on FNA



**Conclusions:** The presence of single cells shedding off of smears diagnostic of PDAC is a novel prognostic parameter, and may be of unique value in patients with unresectable disease, as no additional tissue is collected in many of these patients. FNAs often represent the only treatment-naive material in resectable PDAC, and SCP appears to prognosticate more effectively than resection parameters.

**164 The Value of Second Opinion Consultation in Non-Gynecologic Cytopathology**

Gabrielle Bailey<sup>1</sup>, Ashleigh Graham<sup>2</sup>, Erika Rodriguez<sup>3</sup>, Zahra Maleki<sup>3</sup>, Christina Adams<sup>4</sup>, Bonnie Williamson<sup>4</sup>, Jessica Kahler<sup>4</sup>

<sup>1</sup>Johns Hopkins Hospital, Baltimore, MD, <sup>2</sup>Johns Hopkins University, Baltimore, MD, <sup>3</sup>Johns Hopkins University School of Medicine, Baltimore, MD, <sup>4</sup>The Johns Hopkins Medical Institutions, Baltimore, MD

**Disclosures:** Gabrielle Bailey: None; Ashleigh Graham: None; Erika Rodriguez: None; Zahra Maleki: None; Christina Adams: None; Bonnie Williamson: None; Jessica Kahler: None

**Background:** The value of consultation in pathology has been well-documented in many subspecialties, including surgical pathology. The purpose of these second-review consultations is to prevent diagnostic errors that could impact patient care and to ensure diagnostic accuracy across institutions. While the use of consultation in surgical pathology is thoroughly studied, the same data for consultation in cytopathology is limited, although the subspecialty is known for a high rate of interobserver variability and cytopathology specimens are often used to direct clinical interventions.

**Design:** We reviewed 928 cytopathology consultation cases (383 men, 545 women, average age of 59 years) signed out at a large academic institution within a 20-month period (February 13, 2019 to October 5, 2020). The contributing institution’s diagnosis was compared to that rendered by the reviewing cytopathologist to assess and quantify diagnostic discrepancies and the characteristics of cases with major discrepancies.

**Results:** The cases were distributed as follows: fine needle aspiration (FNA, n=737, 79.4%), exfoliative non-gynecologic cytology (n=170, 18.3%), and cases with a combination of FNA and non-gynecologic cytology (n=21,

2.3%). There were 379 true consults (40.8%) and 549 confirming consults (59.2%). A total of 170 cases (18.3%) were diagnosed as positive for malignancy in either the original diagnosis or the consultation diagnosis. A total of 455 cases (49.0%) were in agreement with the outside pathologist and 76 cases (8.2%) had a two-step or greater discrepancy (classified as a major discrepancy). The remainder had a one-step discrepancy.

The most common organs and sites with major discrepancies were the pancreas (29 cases), other hepatobiliary sites (7 cases), lymph nodes (9 cases), and parotid glands (6 cases). Of these discrepant cases, 21 had follow-up or concurrent surgical pathology consult specimens and special stains were performed in 11 cases to arrive at the cytopathology diagnosis.

**Conclusions:** Of the 928 cases reviewed in this study, 8.2% had major diagnostic discrepancies reported between the original diagnosis and the second opinion consultation. This rate is consistent with previously reported values in surgical pathology second-opinion review studies. The findings support the importance of second-opinion consultation in cytopathology to guide patient care.

### **165 Identification of Small Cell Lung Carcinoma Subtypes Defined by ASCL1, NEUROD1, YAP1 and POU2F3 in Cytology Specimens**

Marina Baine<sup>1</sup>, Min-Shu Hsieh<sup>2</sup>, Wei-Chu Lai<sup>1</sup>, Jacklynn Egger<sup>1</sup>, Achim Jungbluth<sup>1</sup>, Xiao-Jun Wei<sup>1</sup>, Marc Rosenblum<sup>1</sup>, Oscar Lin<sup>1</sup>, Jennifer Sauter<sup>1</sup>, Jason Chang<sup>1</sup>, Darren Buonocore<sup>1</sup>, William Travis<sup>1</sup>, Triparna Sen<sup>1</sup>, John Poirier<sup>3</sup>, Charles Rudin<sup>1</sup>, Natasha Rekhtman<sup>1</sup>

<sup>1</sup>Memorial Sloan Kettering Cancer Center, New York, NY, <sup>2</sup>National Taiwan University Hospital, Taipei, Taiwan, <sup>3</sup>NYU Langone School of Medicine, New York, NY

**Disclosures:** Marina Baine: None; Min-Shu Hsieh: None; Wei-Chu Lai: None; Jacklynn Egger: None; Achim Jungbluth: None; Xiao-Jun Wei: None; Marc Rosenblum: None; Oscar Lin: *Consultant*, Hologic; *Consultant*, Janssen; Jennifer Sauter: None; Jason Chang: None; Darren Buonocore: None; William Travis: None; Triparna Sen: None; John Poirier: None; Charles Rudin: *Consultant*, Amgen; *Consultant*, AstraZeneca; *Consultant*, Roche; *Consultant*, Ipsen; *Consultant*, Jazz; Natasha Rekhtman: None

**Background:** There has been growing data suggesting that small cell lung carcinoma (SCLC) comprises distinct subtypes defined by expression of transcriptional regulators - ASCL1, NEUROD1, YAP1 and POU2F3. Pre-clinical data suggest distinct therapeutic vulnerabilities of these subtypes, prompting an interest in identifying them in patient samples. We have recently characterized these subtypes immunohistochemically (IHC) and histologically in a large cohort of clinical samples. As cytologic specimens commonly represent sole diagnostic specimen for SCLC patients, here we aimed to determine whether the distribution of subtype-defining markers is equivalent in cytologic and surgical specimens.

**Design:** The expression of ASCL1, NEUROD1, POU2F3 and YAP1 was analyzed by IHC in cytologic specimens (n=26, formalin-fixed blocks) of SCLC, and distribution was compared to that of surgical specimens (n=148). We also compared the distribution of conventional neuroendocrine markers (CNM; synaptophysin, chromogranin, CD56, and INSM1) and their association with novel marker-defined subtypes in cytologic preparations.

**Results:** Cytologic specimens included EBUS-FNA (n=24) and pleural fluid (n=2). ASCL1, NEUROD1, POU2F3 and YAP1 had a similar distribution in cytologic vs surgical specimens both qualitatively and by quantitative H-score analysis (Table 1A, p=0.1-0.9). Distribution of marker defined subtypes based on combined (Table 1B) and relative (Table 1C) expression levels of ASCL1 and NEUROD1 was also similar in the two specimen types (p=0.2-1). POU2F3 was expressed exclusively in ASCL1/NEUROD1 double-negative cases in both specimen types, and was associated with low or minimal expression of CNMs, as defined by lower combined neuroendocrine score (average H-score of 4 CNM), compared to other subtypes (mean 70 vs 177 in cytology specimens, respectively; p<0.01).



**Table 1.** Distribution of novel subtype-defining markers in cytologic and surgical specimens.

(A)	ASCL1		NEUROD1		POU2F3		YAP1		Total N
	% pos	Avg H-score	% pos	Avg H-score	% pos	Avg H-score	% pos	Avg H-score	
Cytology	77	157	46	98	8	240	13	19	26
Surgical	79	179	45	121	7	129	21	34	148
P value	0.81	0.23	0.88	0.46	0.87	0.06	0.33	0.3	

(B)	ASCL1+/NEUROD1+		ASCL1+/NEUROD1-		ASCL1-/NEUROD1+		ASCL1-/NEUROD1-		Total N
	N	%	N	%	N	%	N	%	
Cytology	9	35	11	42	3	12	3	12	26
Surgical	50	38	55	41	9	7	19	14	133
P value	0.64		0.93		0.23		1		

(C)	ASCL1-dominant		NEUROD1-dominant		Double-negative, POU2F3		Double-negative, NOS		Total N
	N	%	N	%	N	%	N	%	
Cytology	17	65	6	23	2	8	1	4	26
Surgical	93	70	21	16	9	7	10	8	133
P value	0.65		0.37		0.86		0.50		

**Conclusions:** Expression of SCLC subtype-defining markers can be reliably assessed by IHC in formalin fixed cytologic preparations and is comparable to that of surgical specimens. Potential utility of POU2F3 as a diagnostic marker in SCLC with minimal or absent CNM expression warrants further study.

**166 Patient-Derived Tumor Organoid Development and Pre-Assessment on Cytology Samples: An Institutional Experience**

Shaham Beg<sup>1</sup>, Kentaro Ohara<sup>2</sup>, Wael Al Zoughbi<sup>2</sup>, Kenneth Eng<sup>3</sup>, Adriana Irizarry<sup>4</sup>, Phoebe Reuben<sup>4</sup>, Michael Sigouros<sup>2</sup>, Jyothi Manohar<sup>2</sup>, Noah Greco<sup>5</sup>, Meagan Ford<sup>2</sup>, Francesca Khani<sup>2</sup>, Brian Robinson<sup>2</sup>, Juan Miguel Mosquera<sup>2</sup>, Olivier Elemento<sup>2</sup>, Andrea Sboner<sup>2</sup>, Maria Laura Martin<sup>4</sup>, Momin Siddiqui<sup>2</sup>  
<sup>1</sup>New York-Presbyterian/Weill Cornell Medical Center, New York, NY, <sup>2</sup>Weill Cornell Medicine, New York, NY, <sup>3</sup>Englander Institute for Precision Medicine, Brooklyn, NY, <sup>4</sup>Englander Institute for Precision Medicine, New York, NY, <sup>5</sup>Weill Cornell Medical Center, New York

**Disclosures:** Shaham Beg: None; Wael Al Zoughbi: None; Adriana Irizarry: None; Phoebe Reuben: None; Jyothi Manohar: None; Noah Greco: None; Meagan Ford: None; Francesca Khani: None; Brian Robinson: None; Juan Miguel Mosquera: None; Olivier Elemento: *Stock Ownership*, Volastra Therapeutics; *Stock Ownership*, OneThree Biotech; Andrea Sboner: None; Maria Laura Martin: None; Momin Siddiqui: None

**Background:** Establishment of patient-derived tumor organoids (PDTOs) and their use in precision oncology is a major development in cancer therapeutics. Improving the success rate to establish PDTOs is a challenge that needs to be overcome in our efforts towards more effective personalized medicine. Here we share our experience of using on-site tumor cellularity assessment through cytology smears and its downstream impact on successful establishment of pan-cancer PDTOs.

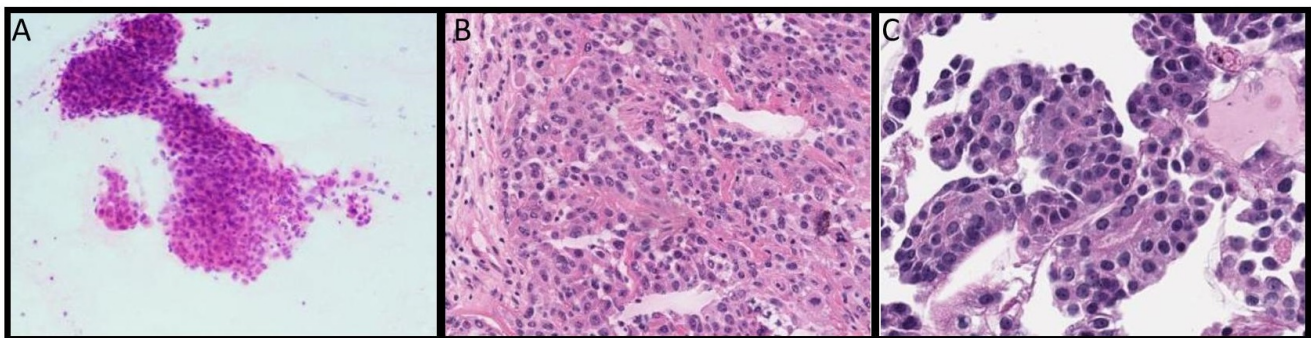
**Design:** In this pilot study, retrospective assessment of samples from 35 patients with various tumor types was performed. Tumor cellularity assessment for adequacy by on-site aspiration cytology smear preparations – prepared before tissue is submitted for organoid development and whole-exome sequencing – was evaluated. The success of tumor organoid growth was compared with tumor cellularity on cytology smears, corresponding tissue biopsy/resection and CLONET (CLONality Estimate in Tumor), a computational algorithm which upon estimation of tumor admixture and ploidy infers the clonal hierarchy of genomic aberrations.

**Results:** Successful PDOs were established in 31.4% (11/35) of tumors, 1 primary (bladder) and 10 metastatic. Colorectal cancers showed highest success rate (63.6%, 7/11) followed by urothelial (50%, 1/2), prostatic (33.3%, 2/6) and pancreatic (16.7%, 1/6). Tumors from breast, upper gastrointestinal tract, kidney and ovary/fallopian tube did not grow as PDOs. 25% (4/16) of cases with high tumor cellularity on smears were established; whereas 37% (7/19) of cases with low cellularity or no tumor cells showed any growth. Mean tumor purity of corresponding tumor tissues with successful organoids, estimated by CLONET was 73.8% vs 59.6% for unsuccessful cases (Table 1).

Primary tumor sites	Total cases	Organoids Growing (smear cellularity)	Organoid Failed (smear cellularity)
Urinary tract	2	1 (low)	1 (low)
Breast	3	0	3 (low 1, no tm 2)
Colorectal	11	7 (2 high, 5 low)	4 (all high)
Upper GI tract	5	0	5 (high 3, low 2)
Kidney	1	0	1 (high)
Ovary/fallopian tube	1	0	1 (high)
Pancreas	6	1 (high)	5 (high 2, low 2, no tm 1)
Prostate	6	2 (high 1, low1)	4 (high 1, low 2, no tm 1)
Cytology smear cellularity	35	11 (high 4, low 7)	24 (high 12, low 8, no tumor 4)
Tumor purity (by CLONET)	35	73.80%	59.60%

Figure 1 - 166

**Figure 1.** Microscopic images of on-site cytology smear (A), tumor tissue (B) and developed organoid (C) obtained from high-grade urothelial carcinoma.



**Conclusions:** Our pilot study suggests that 1) success rate to establish PDOs is higher for certain tumors (e.g. colorectal and urothelial cancers), and 2) establishing PDOs does not necessarily correlate with prior tumor cellularity assessment; although established PDOs have higher tumor cellularity vs unsuccessful ones. Study of our complete PDO biobank and corresponding tissues and CLONET values is ongoing.

**167 Role of Spliced Variant of Actinin-4 (ACTN4va) as a Diagnostic Marker for Pulmonary Neuroendocrine Tumors in Fine-Needle Aspiration Specimens**

Shaham Beg<sup>1</sup>, Alain Borczuk<sup>2</sup>, Momin Siddiqui<sup>2</sup>

<sup>1</sup>New York-Presbyterian/Weill Cornell Medical Center, New York, NY, <sup>2</sup>Weill Cornell Medicine, New York, NY

**Disclosures:** Shaham Beg: None; Alain Borczuk: None; Momin Siddiqui: None

**Background:** ACTN4va is an immunohistochemical (IHC) marker for neuroendocrine differentiation with potentially superior sensitivity and specificity. ACTN4va performance in pulmonary fine needle aspiration (FNA) cell blocks

(CB) has not studied, and large series demonstrating its performance have been few. Reported studies have been limited to surgical specimens and no study exist about its usefulness in FNA CB preparations. In our study, we have reviewed Actinin-4 splice variant IHC expression on FNA of lung neuroendocrine tumors (NT).

**Design:** Eighty nine pulmonary FNA’s including large cell neuroendocrine carcinoma (n=10), typical carcinoid (n=24), small cell carcinoma (n=15), atypical carcinoid (n=18), squamous cell carcinoma (n=12) and adenocarcinoma (n=10) from FNA cell blocks were stained and evaluated for ACTN4va, synaptophysin, chromogranin and CD56.

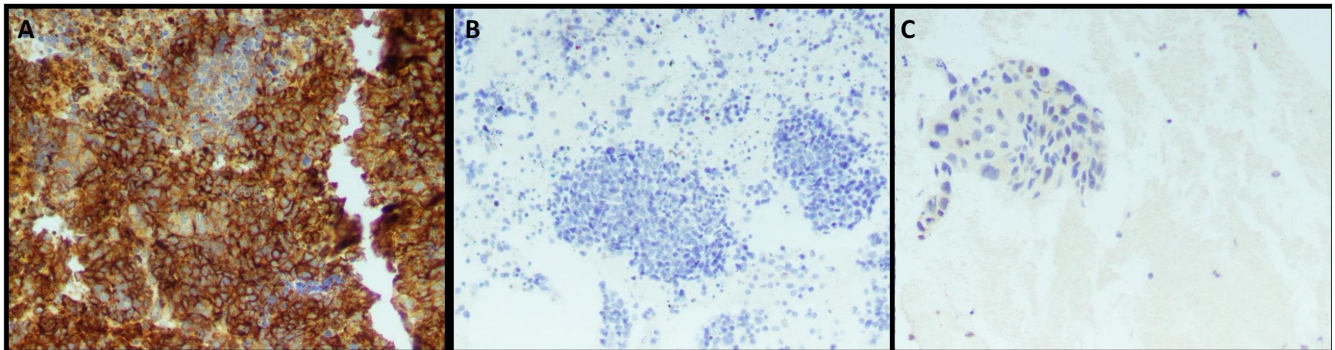
**Results:** Pulmonary NT showed strong cytoplasmic staining for ACTN4va in tumor cells (Table 1).

ACTN4va sensitivity, specificity, positive predictive value, and negative predictive value were 96.4%, 56.25%, 88.5%, and 81.8% in the CB. The sensitivity for the other neuroendocrine markers were 96.7% in the CBs for Synaptophysin; 81.0 % in the CBs for Chromogranin; 100% for CD56 ‘and 85.7% for INSM1. ACTN4va did show cytoplasmic positivity in 6/7 (86%) of pulmonary adenocarcinoma and 1/9 (11%) of squamous cell carcinoma, which decreases its specificity for pulmonary NT (Figure 1). Staining on corresponding resection specimens and additional cases is currently undergoing.

<b>Pulmonary NT</b>	<b>ACTN4va</b>	<b>Synaptophysin</b>	<b>Chromogranin</b>	<b>CD56</b>	<b>INSM1</b>
<b>Large cell neuroendocrine</b>	100% (9/9)	80% (8/10)	37.5% (3/8)	100% (8/8)	NA
<b>Typical carcinoid</b>	95% (19/20)	100% (22/22)	100% (20/20)	100% (8/8)	100% (2/2)
<b>Small cell carcinoma</b>	92% (11/12)	100% (12/12)	43% (3/7)	100% (8/8)	100% (4/4)
<b>Atypical carcinoid</b>	100% (15/15)	100% (16/16)	85% (11/13)	100% (6/6)	0 (0/1)

Figure 1 - 167

**Figure 1:** ACTN4va staining in pulmonary FNA specimens. (A) Strong cytoplasmic staining in pulmonary NT, (B) negative staining in pulmonary NT and (C) pulmonary squamous cell carcinoma.



**Conclusions:** The results of our study have established a high sensitivity of ACTN4va as a diagnostic IHC marker for pulmonary NT’s and it might be new potential marker which can useful in diagnosis of pulmonary NT in FNA samples.



**168 The Role of Nuclear Receptor Subfamily 4 Group A Member 3 (NR4A3) Immunohistochemistry in Distinguishing Acinic Cell Carcinoma from Oncocytic Salivary Gland Neoplasms in Surgical and Limited Cytology Specimens: A Multi-Institutional Experience**

Shaham Beg<sup>1</sup>, Kartik Viswanathan<sup>1</sup>, Bing He<sup>2</sup>, Taotao Zhang<sup>3</sup>, Richard Cantley<sup>4</sup>, Daniel Lubin<sup>5</sup>, Zahra Maleki<sup>6</sup>, Nora Katabi<sup>7</sup>, William Faquin<sup>8</sup>, Peter Sadow<sup>8</sup>, Momin Siddiqui<sup>3</sup>, Theresa Scognamiglio<sup>3</sup>  
<sup>1</sup>New York-Presbyterian/Weill Cornell Medical Center, New York, NY, <sup>2</sup>Cornell University Medical College, <sup>3</sup>Weill Cornell Medicine, New York, NY, <sup>4</sup>University of Michigan, Ann Arbor, MI, <sup>5</sup>Emory University Hospital, Atlanta, GA, <sup>6</sup>Johns Hopkins University School of Medicine, Baltimore, MD, <sup>7</sup>Memorial Sloan Kettering Cancer Center, New York, NY, <sup>8</sup>Massachusetts General Hospital, Harvard Medical School, Boston, MA

**Disclosures:** Shaham Beg: None; Kartik Viswanathan: None; Bing He: None; Taotao Zhang: None; Richard Cantley: None; Daniel Lubin: None; Zahra Maleki: None; Nora Katabi: None; William Faquin: None; Peter Sadow: None; Momin Siddiqui: None; Theresa Scognamiglio: None

**Background:** Acinic cell carcinoma (AciCC) of the salivary gland has a characteristic morphologic appearance. However, other oncocytic neoplastic mimickers (ONCs), such as secretory carcinoma, can pose a diagnostic challenge, and few ancillary tools are available. Recently, AciCCs were reported to harbor a specific driver translocation [t(4;9)(q13;q31)] with increased Nuclear Receptor Subfamily 4 Group A Member 3 (NR4A3) expression on surgical resections (SRs) using immunohistochemistry (IHC). However, data on the utility of NR4A3 IHC for AciCCs in cytologic specimens remains limited. Here, we examined the performance of NR4A3 IHC on cytology cell blocks (CBs) and SRs of AciCCs and its neoplastic mimickers.

**Design:** Our multi-institutional cohort comprised AciCC (16 CB, 9 SR), Warthin tumor (17 CB, 31 SR), Oncocytoma (5 CB, 18 SR), Mucoepidermoid carcinoma (4 CB, 15 SR), Pleomorphic adenoma (2 CB, 10 SR), Secretory carcinoma (2 CB, 7 SR) and Nodular oncocytosis (5 SR) that were immunostained with NR4A3 (Santa Cruz Biotechnology and Origene antibodies). Staining for NR4A3 was quantified from 0 to 3, and extent of tumor staining was expressed as a percentage. NR4A3 IHC was considered positive if staining intensity was >=1+ and in at least >5% of tumor cells.

**Results:** In our multi-institutional tumor cohort, 84% were in the parotid gland, 8.6% were in the submandibular gland, and the remaining were in minor salivary glands. The mean tumor size was 2.6 cm (range 0.3-8.0 cm), median age of patients was 61 years (range 12-89 years), and the male: female ratio was 0.95. Among CBs, nuclear NR4A3 was seen in all AciCCs (16/16, 100%) with diffuse strong positivity, but not in any of the other ONCs. Among SRs, nuclear NR4A3 was seen in 89% AciCCs (8/9), whereas among non-AciCCs SRs (n=86), only one mucoepidermoid carcinoma (1/86, 1.1%) showed focal NR4A3 staining (Table 1). Concordance was noted between the two antibodies.

**Table 1: Summary of NR4A3 staining in salivary gland tumors**

Tumor subtype	Specimen type	NR4A3 Positive	NR4A3 Negative
Acinic cell carcinoma (n=25)	CB (16)	16/16	0
	SR (9)	8/9	0
Warthin tumor (n=48)	CB (17)	0	17/17
	SR (31)	0	31/31
Mucoepidermoid carcinoma (n=19)	CB (4)	0	4/4
	SR (15)	1/15	14/15
Secretory carcinoma (n=9)	CB (2)	0	2/2
	SR (7)	0	7/7
Pleomorphic adenoma (n=12)	CB (2)	0	2/2
	SR (10)	0	10/10
Oncocytoma (n=23)	CB (5)	0	5/5
	SR (18)	0	18/18
Nodular oncocytosis (n=5)	SR (5)	0	5/5

**Conclusions:** NR4A3 IHC is highly sensitive and specific in distinguishing AciCCs from other primary salivary gland ONCs in both cytologic and surgical specimens.

**169 Interpretation of Pap Tests and Follow-Up Histology in Atrophic Cervical Epithelium of Postmenopausal Women: Difficult or Impossible**

Sepideh Besharati<sup>1</sup>, Jonathan Tepp<sup>2</sup>, Xiaowei Chen, Lama Farhat<sup>3</sup>, Patricia Wasserman<sup>4</sup>, Simon Sung<sup>5</sup>, Adela Cimic<sup>4</sup>

<sup>1</sup>Columbia Presbyterian Medical Center, New York, NY, <sup>2</sup>Columbia University Irving Medical Center, New York Presbyterian Hospital, New York, NY, <sup>3</sup>Columbia University Medical Center, New York-Presbyterian, New York, NY, <sup>4</sup>Columbia University Medical Center, <sup>5</sup>Albert Einstein College of Medicine, Montefiore Medical Center, New York, NY

**Disclosures:** Sepideh Besharati: None; Jonathan Tepp: None; Xiaowei Chen: None; Lama Farhat: None; Patricia Wasserman: None; Simon Sung: None; Adela Cimic: None

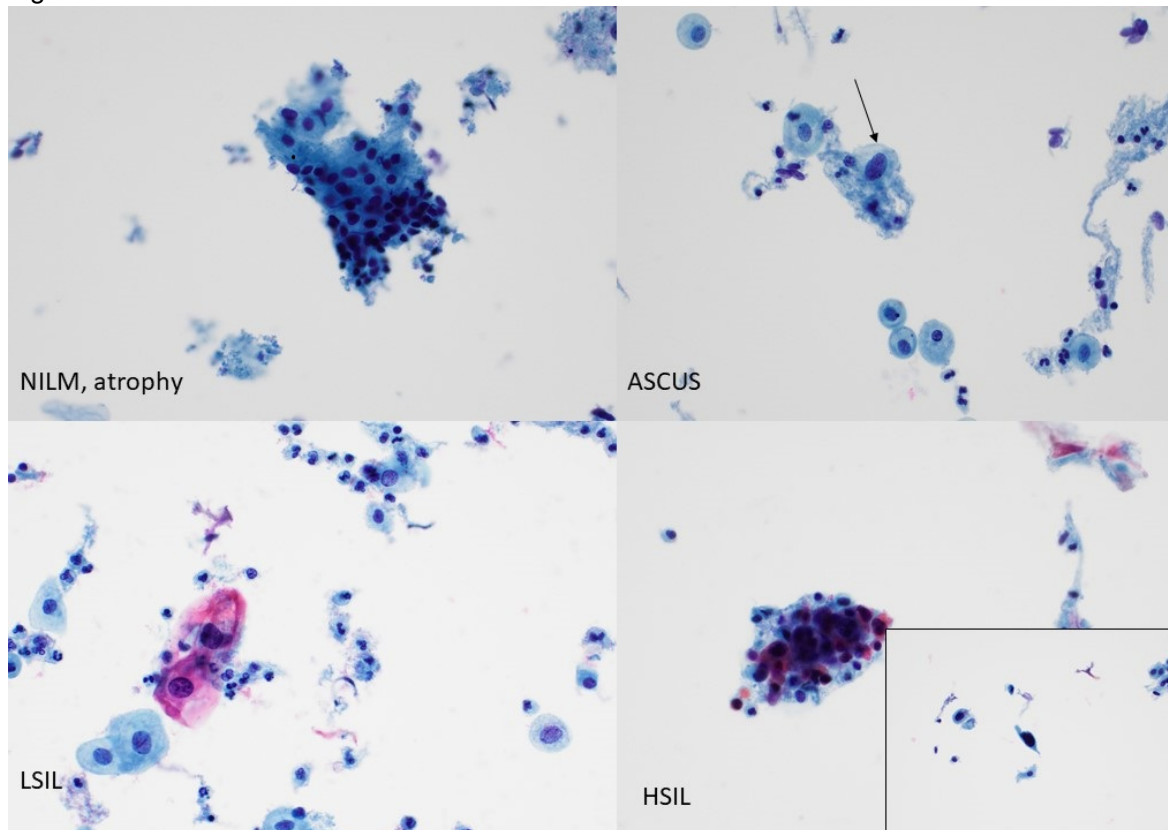
**Background:** Screening tests including Papanicolaou (Pap) and high-risk human papillomavirus (HR-HPV) for early detection of cervical precancerous lesions reduce mortality due to cervical cancer. It is recommended that women over 65 years not be screened if adequate negative prior screening. In postmenopausal women (PMW) cytologic differentiation between atrophy and dysplasia can be challenging. The goal of this study is to examine the accuracy of Pap test and correlation with follow-up histology.

**Design:** A review of 33 cases of PMW (defined by a submitting physician, average age of 62.60 ± 6.74) was performed. Pap test interpretation, HPV co-testing (Roche cobas® HPV) and follow-up cervical histology (within 3 months) on biopsies (n=22) and excisional specimens (n=10) results were reviewed. Cases were independently re-reviewed by two additional cytopathologists and the consensus diagnosis was reached.

**Results:** A review of the Pap tests demonstrated: 30.3% negative for intraepithelial lesion or malignancy (NILM); 3.03% unsatisfactory; 36.3% atypical squamous cells of undetermined significance (ASCUS); 15.1% atypical squamous cells cannot rule out high-grade squamous intraepithelial lesion (ASC-H); 12.1% low-grade squamous intraepithelial lesion (LSIL) and 3.0% high-grade squamous intraepithelial lesion (HSIL) (figure 1). Histologic findings include 63% benign, 6% CIN1, 27% CIN2-3 and 3% invasive squamous carcinoma. One case had atypical glandular cells interpretation in addition to ASC-H that resulted in an adenocarcinoma in situ follow-up. Among 85% of HPV positive cases, 42% were high risk HPV type 16/18. We found 30.3% of cases have agreement between Pap test and histologic diagnosis results. The rates of HR-HPV positive tests were higher in histologic precancerous lesions including CIN1 and CIN2-3 and invasive squamous carcinoma (66.6 %) than benign (28.5%). All high-grade squamous intraepithelial lesions were positive for HR-HPV.

Cytologic interpretation	Number	HPV negative	HPV other	HPV 16/18	Follow-up histologic findings			
					Benign	CIN1	CIN2-3	Invasive carcinoma
NILM	10	1	3	6	7	0	3	0
ASCUS	12	3	5	4	8	1	3	0
ASC-H	5	0	3	2	3	0	1	1
LSIL	4	1	2	2	1	2	1	0
HSIL	1	0	0	1	0	0	1	0
UNSAT	1	0	1	0	1	0	0	0

Figure 1 - 169



**Conclusions:** Pap smear evaluation in atrophic settings is challenging. The transformation zone in PMW tend to be smaller and higher in the cervical canal. This may result in a lower number or no dysplastic cells shedding (sampling error) and very careful screening is necessary particularly in the setting of HPV positivity. Pathologists should be familiar with dysplastic features of HSIL and mild atypia associated with atrophy. Vaginal estrogen could be considered to obtain adequate samples.

**170 Comprehensive Molecular Profiling of Pancreatic Adenocarcinoma in Fine Needle Aspiration and Core Needle Biopsy Specimens**

Soumar Bouza<sup>1</sup>, Patricia Hernandez, Minhua Wang<sup>2</sup>, Dana Razzano<sup>1</sup>, Zenta Walther<sup>2</sup>, Guoping Cai<sup>3</sup>  
<sup>1</sup>Yale School of Medicine, Yale New Haven Hospital, New Haven, CT, <sup>2</sup>Yale School of Medicine, New Haven, CT, <sup>3</sup>Yale University, New Haven, CT

**Disclosures:** Soumar Bouza: None; Patricia Hernandez: None; Minhua Wang: None; Dana Razzano: None; Zenta Walther: None; Guoping Cai: None

**Background:** Molecular testing to identify recurrent molecular alterations in pancreatic adenocarcinoma has been increasingly requested by medical oncologists due to potential therapeutic implications. To date, core needle biopsy (CNB) or resection tissue specimens have been the main sources for molecular analysis although a few recent studies have suggested the feasibility of fine needle aspiration (FNA) material for molecular testing. This study compared the performances of pancreatic adenocarcinoma FNA and CNB specimens for comprehensive molecular analysis.

**Design:** An NGS-based Oncomine Comprehensive Assay (OCA) was used to analyze molecular alterations in FNA cellblock material, CNB or resection specimens, as part of clinical care. The OCA panel examines 161 unique genes and can identify hotspot mutations, copy number variations (CNV) and gene fusions in selected gene subsets. We examined success rates for completion of molecular testing in FNA and CNB specimens and compared these with assay performance in resection specimens.



**Results:** We retrospectively identified 29 FNA, 92 CNB and 23 resection cases in which OCA was requested by the treating oncologist. Hotspot mutation/CNV analysis was successful in 24 (82.8%) FNA and 84 (91.3%) CNB specimens while gene fusion assay was unable to be performed in 11 (37.9%) FNA and 20 (21.7%) CNB specimens, respectively, due to insufficient cellularity or insufficient RNA material. All 23 (100%) resection specimens were adequate for complete OCA molecular profiling including mutation, CNV and gene fusion analysis. There were significant differences in success rates for both hotspot mutation/CNV analysis and complete molecular profiling between resection and FNA or CNB specimens ( $p < 0.01$ ) but not between FNA and CNB samples ( $p > 0.05$ ). The most common molecular alterations identified were mutations in *KRAS* (61.1%) and *TP53* (55.6%) genes.

**Conclusions:** Our study demonstrated similar success rates for comprehensive molecular analysis using FNA and CNB specimens of pancreatic adenocarcinoma, suggesting that FNA material could serve as an alternative source for comprehensive molecular testing.

**171 Cytologic Findings in Patients with SARS-CoV-2 Infection and Body Fluid Effusion**

Richard Cantley<sup>1</sup>, Steven Hrycaj<sup>1</sup>, Kristine Konopka<sup>2</sup>, May Chan<sup>1</sup>, Tao Huang<sup>1</sup>, Liron Pantanowitz<sup>1</sup>  
<sup>1</sup>University of Michigan, Ann Arbor, MI, <sup>2</sup>Michigan Medicine, Ann Arbor, MI

**Disclosures:** Richard Cantley: None; Steven Hrycaj: None; Kristine Konopka: None; May Chan: None; Tao Huang: None; Liron Pantanowitz: None

**Background:** Coronavirus disease 2019 (COVID-19), caused by severe acute respiratory syndrome coronavirus 2 (SARS-CoV-2), is associated with “flu-like” upper respiratory tract symptoms in most cases. However, a significant subset of patients may develop more severe disease, including lower respiratory tract involvement and systemic disease. Body cavity effusions, such as pericardial and pleural effusions have developed in a subset of patients with advanced disease. Further, although this coronavirus is known to be present in certain body fluids (e.g. blood) of COVID patients it remains unclear if body cavity fluids may be a site of infection, potentially harboring viral material. The aim of this study was to characterize the findings in effusions in patients with SARS-CoV-2 infection.

**Design:** Our anatomic pathology archives were searched for all cases of body cavity effusion cytology in SARS-CoV-2 positive patients from 3/1/2020 - 9/1/2020. Clinical history, fluid chemical analysis, cytologic findings, and patient outcomes were recorded. All cytology slides were reviewed. In situ hybridization (ISH) targeting SARS-CoV-2 spike protein transcript (V-nCoV2019-S RNA) was performed on cell block material in all cases.

**Results:** There were 17 effusion cytology cases identified among 15 COVID patients, including 13 pleural, 2 pericardial, and 2 peritoneal effusions (Table 1). 13/15 patients were hospitalized for COVID complications, while 1 was hospitalized for diverticulitis and 1 for management of an adnexal mass. Four patients had a history of malignancy. 8/15 patients died during hospitalization, including 7 from COVID complications. All fluids were transudative by protein criteria. No malignancy was seen in any case. Lymphocytic and/or histiocytic inflammation predominated in 12/17 cases, and 5 exhibited hemophagocytosis (Figure 1). Mesothelial cells ranged from scant and bland to hypercellular and reactive. Absent in all cases were viral cytopathic changes and megakaryocytes. Viral RNA was not detected in any case by ISH.

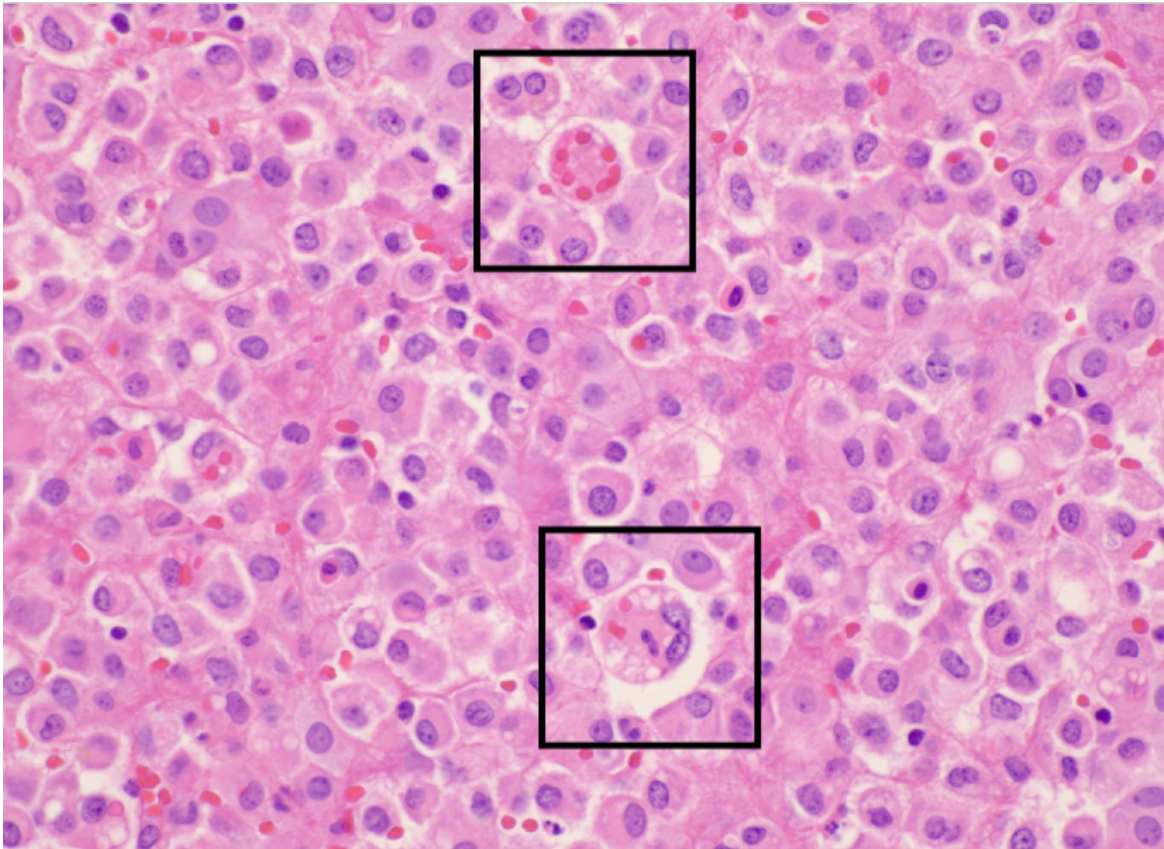
**TABLE 1 - Cytologic and fluid analytic findings in effusions from COVID patient**

Patient	Specimen	Age	Sex	Fluid type	Protein (g/L)	Predominant inflammation	Mesothelial cell findings	Hemophagocytosis?	Clinical outcome
1	1	72	M	Pleural fluid	2.8	Histiocytic	Moderately cellular, reactive change	Absent	Died with COVID
	2			Pleural fluid	3.7	Lymphohistiocytic	Hypercellular, reactive change	Absent	
2	3	70	M	Pleural fluid	0.8	Lymphohistiocytic	Moderately cellular, reactive change	Present (RBCs)	Died of COVID
	4			Pleural fluid	<0.8	Histiocytic	Moderately cellular, reactive change	Present (RBCs)	
3	5	81	F	Pleural fluid	3.5	Lymphohistiocytic	Hypercellular, reactive change	Present (RBCs, lymphocytes, PMNs)	Died of COVID
4	6	67	F	Pleural fluid	1.7	Lymphohistiocytic	Hypercellular, reactive change	Absent	Died of COVID
5	7	59	M	Pleural fluid	4.3	Mixed	Scant	Absent	Died of COVID
6	8	75	M	Pleural fluid	5.1	Mixed	Scant	Absent	Died of COVID
7	9	58	M	Pleural fluid	4.2	Mixed	Scant	Absent	Died of COVID
8	10	42	M	Pleural fluid	NP	Lymphocytic	Scant	Absent	Alive
9	11	49	F	Pleural fluid	5.9	Neutrophilic	Hypercellular, non-reactive	Present (RBCs)	Alive
10	12	76	M	Pleural fluid	3.7	Lymphocytic	Scant	Absent	Alive
11	13	70	M	Pleural fluid	2.3	Lymphocytic	Scant	Absent	Alive
12	14	37	F	Pericardial fluid	2.1	Histiocytic	Moderately cellular, non-reactive	Absent	Died of COVID
13	15	32	F	Pericardial fluid	4.2	Histiocytic	Moderately cellular, non-reactive	Absent	Alive, chest pain
14	16	35	F	Peritoneal fluid	NP	Mixed	Hypercellular, reactive change	Present (PMNs)	Alive
15	17	52	M	Peritoneal fluid	4.6	Lymphohistiocytic	Scant	Absent	Alive

**TABLE 1 - Cytologic and fluid analytic findings in effusions from COVID patients**

\* NP - not performed, RBCs - red blood cells, PMNs - polymorphonuclear neutrophils

Figure 1 - 171



**Conclusions:** The presence of a body cavity effusion is an ominous finding in patients with advanced COVID disease. Such effusions tend to be transudative and are characterized by marked histiocytic and lymphocytic inflammation, and may exhibit hemophagocytosis. No direct infection of mesothelial cells or background inflammatory cells by SARS-CoV-2 was identified by ISH in this series.

**172 HPV Co-testing of Unsatisfactory Papanicolaou Tests: Implications for Follow-up Intervals**

Fei Chen<sup>1</sup>, Issa Hindi<sup>1</sup>, Wei Sun<sup>2</sup>, Negin Shafizadeh<sup>1</sup>, Oliver Szeto<sup>1</sup>, Tamar Brandler<sup>1</sup>, Aylin Simsir<sup>3</sup>  
<sup>1</sup>NYU Langone Health, New York, NY, <sup>2</sup>New York University Langone Medical Center, New York, NY, <sup>3</sup>NYU School of Medicine, New York, NY

**Disclosures:** Fei Chen: None; Issa Hindi: None; Wei Sun: None; Negin Shafizadeh: None; Oliver Szeto: None; Tamar Brandler: None; Aylin Simsir: None

**Background:** The ASCCP management guidelines recommend that women with an unsatisfactory Pap test (UPT) and negative HPV co-test undergo repeat age-based screening in 2 to 4 months. The rationale is that a negative HPV test in the setting of an UPT may reflect an inadequate sample and therefore should not be interpreted as truly “negative”. For patients 25 years and older who are co-tested, if HPV is positive for the 16 or 18 genotypes, direct referral for colposcopy is recommended.

Our study aimed to determine if a negative HPV co-test result is predictive of the absence of a high grade squamous intraepithelial lesion (HGSIL) and whether these patients may be called back for repeat testing at an interval longer than 2-4 months.

**Design:** Follow up cervical cytology and biopsy results in women with UPT and HPV co-tests between 2017-2019 were collected. Original UPT and HPV co-test results were correlated with follow up Pap and biopsy results.



**Results:** There were 708 UPT cases out of 30,647 total Pap tests (2.3%). Among the 708 UPT cases, 407 had HPV co-testing (57%); 260 (37%) were followed by repeat Pap or biopsy within 2-4 months and 317 (45%) within 12 months. The total follow-up rate was 81%, with a range of 10 days to 18 months. Table 1 depicts follow up information for women with UPT and HPV co-testing. Negative predict values of HPV co-testing for LGSIL and HGSIL detection were 98% and 100%, respectively, while positive predictive values were 43% and 4.7%.

**Table 1. Follow Up Pap Test and Biopsy Results for Unsatisfactory Cases with HPV Co-testing**

HPV status	Follow up (pap and/or biopsy)						total
	Unsat pap	Negative	ASCUS	LGSIL	HGSIL	No follow up	
HPV +	0 (0%)	7 (24%)	4 (14%)	<b>9 (31%)**</b>	1* (3%)	8 (28%)	29
HPV -	21 (6%)	158 (42%)	10 (3%)	3 (0.7%)	0 (0%)	186 (49%)	378
total	21 (5%)	165 (41%)	14 (3%)	12 (3%)**	1 (0.2%)	194 (47%)	407

HPV, human papillomavirus; Unsat pap, unsatisfactory Papanicolaou test; ASCUS, atypical squamous cells of undetermined significance; LGSIL, low grade squamous intraepithelial lesion; HGSIL, high grade squamous intraepithelial lesion

\* HPV 16 positive

**\*\*5 (56%) HPV 16 positive, and 4 (44%) HPV high-risk other 16 and 18 positive**

**Conclusions:** A negative HPV co-test in women with an UPT predicted the lack of HGSIL in our study. Compliance with the recommended follow up time of 2-4 months for women with UPT was low at 37%. This may be due to multiple factors, one presumably being the women's reluctance to undergo a repeat pelvic exam due to its uncomfortable nature. Even with a longer follow up time of up to 12 months, there were no HGSILs in the HPV negative group. Our study suggests that women with an UPT and a negative HPV co-test may be safely called back at an interval longer than 2-4 months.

**173 Breast Fine Needle Aspiration as an Initial Diagnostic Tool: Cytologic, Histologic and Radiologic Correlations in a Large County Hospital**

Zhengshan (Allen) Chen<sup>1</sup>, Christine Salibay<sup>2</sup>, Wafaa Elatre<sup>1</sup>, Wesley Naritoku<sup>2</sup>, Yanling Ma<sup>1</sup>, Sue Martin<sup>2</sup>, Tiannan Wang<sup>3</sup>

<sup>1</sup>LAC+USC Medical Center, Los Angeles, CA, <sup>2</sup>Keck School of Medicine of USC, Los Angeles, CA, <sup>3</sup>University of Southern California, Keck School of Medicine of USC, LAC+USC Medical Center, Los Angeles, CA

**Disclosures:** Zhengshan (Allen) Chen: None; Christine Salibay: None; Wafaa Elatre: None; Wesley Naritoku: None; Yanling Ma: None; Sue Martin: None; Tiannan Wang: None

**Background:** While both fine needle aspiration biopsy (FNAB) and core needle biopsy (CNB) are acceptable for evaluation of breast masses, CNB is used more frequently. In the COVID-19 pandemic, however, many procedures such as CNB were delayed. FNAB is a simple, rapid, and cost-effective diagnostic tool. The Yokohama system for breast FNAB report has been proposed for years; however, its clinical application remains uncertain. In this study, we evaluated breast FNAB by the Yokohama system and correlated cytologic, histologic, and radiologic findings.

**Design:** A retrospective study of 318 breast FNAB cases from 2015 to 2020 was performed. All breast FNAB samples were classified by the Yokohama system. The patients' Breast Imaging-Reporting and Data System (BIRADS) scores were recorded. The cytologic, histologic and radiologic findings were analyzed.

**Results:** Overall 83/318 FNAB cases had a subsequent histological diagnosis. Of these, the cytology was insufficient in 12 (14.5%) cases, benign in 55 (66.3%) cases, and malignant in 14 (16.9%) cases (Table 1). Of the 12 insufficient cases, 10 were benign, 1 was atypical ductal hyperplasia (ADH) and 1 was invasive ductal carcinoma (IDCA) by follow-up histology. Of the 55 cases that were benign by FNAB, 34 (61.8%) were fibroadenoma including

one case with focal ADH on resection, and 9 (16.4%) were fibrocystic changes. 2 cases (2.4%) were diagnosed as atypical by FNAB, and CNB showed both to be benign. No cases were classified as suspicious. All malignant cases by FNAB were confirmed malignant by histology, including IDCA (78.6%), invasive lobular carcinoma (14.3%) and malignant phyllodes tumors (7.1%). In addition, all 27 radiologic BIRADS 2 or 3 lesions were benign and all 12 BIRADS 5 lesions were malignant. In BIRADS 4 category, 92.9% (39) cases were benign and 7.1% (3) cases were confirmed atypical or malignant.

**Table 1. Clinicopathologic Correlation of Patients with Breast Fine Needle Aspiration**

Yokohama System categories	No. (%)	Biopsy or Resection No. (%)			Radiology BIRADS score No. (%)				
		Benign	Atypical	Malignant	N/A	2	3	4	5
<b>Insufficient</b>	12 (14.5)	10 (83.3)	1 (8.3)	1 (8.3)	0	2 (16.7)	6 (50.0)	3 (25.0)	1 (8.3)
<b>Benign</b>	55 (66.3)	54 (98.2)	1 (1.8)	0	0	10 (18.2)	9 (16.4)	36 (65.5)	0
<b>Atypical</b>	2 (2.4)	2 (100.0)	0	0	0	0	0	2 (100.0)	0
<b>Suspicious</b>	0	0	0	0	0	0	0	0	0
<b>Malignant</b>	14 (16.9)	0	0	14 (100.0)	2 (14.3)	0	0	1 (7.0)	11 (78.6)
<b>Total</b>	83	66 (79.5)	2 (2.4)	15 (18.1)	2 (2.4)	12 (14.5)	15 (18.1)	42 (50.6)	12 (14.5)

BIRADS score (Breast Imaging-Reporting and Data System): N/A-not available; 2-benign; 3-probably benign; 4-suspicious abnormality; 5-highly suggestive of malignancy.

**Conclusions:** Using histological diagnosis as the gold standard, breast FNAB had a sensitivity of 93.3%, a specificity of 100.0%, a positive predictive value of 100.0% and a negative predictive value of 98.2%. Therefore, FNAB proved to be a rapid and reliable diagnostic tool for breast lesions. Radiologically, BIRADS 2 or 3 correlated well with benign lesions, BIRADS 5 correlated well with malignant lesions, but the majority of BIRADS 4 lesions were benign.

**174 Comparison of Cervical Screen Results on Female-to-Male Transgender Patients to Female Patients**

Katelynn Davis<sup>1</sup>, Regina Kwon<sup>1</sup>, Christopher Morris<sup>2</sup>, Zahra Maleki<sup>1</sup>, Marissa White<sup>1</sup>, Erika Rodriguez<sup>1</sup>  
<sup>1</sup>Johns Hopkins University School of Medicine, Baltimore, MD, <sup>2</sup>Johns Hopkins Medical Institutions, Baltimore, MD

**Disclosures:** Katelynn Davis: None; Zahra Maleki: None; Marissa White: None; Erika Rodriguez: None

**Background:** There is limited data on cervical screen results on female-to-male (FTM) transgender patients. A consequence of the well-established barriers to transitioning and transgender patient healthcare is decreased cervical cancer screening in FTM patients. This combined with other factors such higher prevalence of smoking results in a disparity in cervical cancer risk. Herein, we compiled cervical screen test and HPV vaccination status on FTM patients and compared these results with age appropriate controls.

**Design:** A search on our previous and current databases was performed for Pap tests obtained from patients with a diagnosis of gender identity disorder, transsexualism, transvestism, or variations of those diagnoses. The pathology reports, demographics, and recent clinical notes were reviewed. Relative risks of abnormal Pap smear (other than ASCUS), or HPV infection, were calculated against age matched controls using the relative risk calculator available at medcalc ([https://www.medcalc.org/calc/relative\\_risk.php](https://www.medcalc.org/calc/relative_risk.php)). Age-matched controls were obtained by using the R package Matchit (method = "exact") on a database of patients who had Pap smears performed from 2017-2018.

**Results:** A total of 89 Pap tests from FTM individuals were identified with an average age of 31.3 years, ranging from 21 to 60 years. The Pap test diagnoses were distributed as follows: Negative for intraepithelial lesion (NIEL) (n=84, 94.4%), ASCUS (n=0), LSIL (n=4, 4.5%), HSIL (n=1, 1.1%). 50 of the 89 patients received concurrent HPV

testing, which was distributed as follows: overall HR HPV positive (n=4, 8%), HPV 16 (n=1, 2%), HPV 18 (n=0), HPV non 16-18 or unspecified (n=3, 6%). Of note, a total of 40 patients (44.9%) received the HPV vaccine. 74 patients (83.1%) did not have a previous Pap test reported. A total of 73 (82.0%) had been treated with testosterone, and 42 (47.2%) had reconstructive surgery. The FTM population was compared using age match controls. The mean, median and standard deviation (SD) of age of the control group were (33.4, 33.0, 9.7), and for the case group was (31.5, 30.0, 8.8), respectively. Relative risk of abnormal Pap test was 1.26(95% CI: 0.54-2.95), P value 0.60, and for HPV was 0.456(95% CI 0.17-1.17), P value 0.10.

**Conclusions:** The majority of FTM individuals did not have a Pap test documented on our system despite the average age of 31 years old at current testing. There was no statistically significant difference on the relative risk of abnormal Pap test or HPV infection on the study population when compared with the control group.

**175 Machine Learning/Convolutional Neural Network in Fluid Cytology for Predicting Malignancy**

Simona De Michele<sup>1</sup>, Patricia Wasserman<sup>2</sup>, Simon Sung<sup>3</sup>

<sup>1</sup>Columbia University Irving Medical Center, New York Presbyterian Hospital, New York, NY, <sup>2</sup>Columbia University Medical Center, <sup>3</sup>Albert Einstein College of Medicine, Montefiore Medical Center, New York, NY

**Disclosures:** Simona De Michele: None; Patricia Wasserman: None; Simon Sung: None

**Background:** Effusion cytology has been shown to have high specificity but suboptimal sensitivity, ranging from 50% to 70%. The false negative rate is even higher for first cytological analysis of pleural effusions of unknown cause. Furthermore, the distinction between mesothelioma and metastatic tumor can be very challenging. Advances in machine learning algorithms in medicine may improve diagnostic accuracy while minimizing subjectivity. We propose to evaluate two convolutional neural networks (CNNs) for predicting benign, adenocarcinoma (ADCA), and mesothelioma in pleural and peritoneal effusion cytology from ThinPrep slides.

**Design:** We searched our data base for pleural and ascites effusions with diagnosis of benign/reactive, metastatic ADCA, and mesothelioma. All cytologic diagnosis were confirmed with correlating surgical pathology or clinical follow-up. All cases were de-identified and prepared with ThinPrep slides. The slides were scanned with Leica Aperio AT2 scanner. Representative images were obtained at 40x magnification with Aperio Image scope (v12.4.0.7018) and saved as JPEG images. We divided the images in 8:1:1 ratio of training:validation:testing sets, respectively. We used two popular pre-trained CNNs, VGG19 and Inception V3, trained with 30 epochs, implemented on pytorch 1.5.1 in python 3.8.3. Accuracy, sensitivity, and specificity were calculated.

**Results:** We collected a total of 39 pleural and peritoneal fluid samples; 12 benign, 27 malignant (16 ADCAs, 11 mesotheliomas). We extracted a total of 4110 images, and divided into a training set of 3288 samples (743 ADCA, 580 benign, 1965 mesothelioma), a validation set of 412 (111 ADCA, 71 benign, 230 mesothelioma), and a test set of 410 samples (113 ADCA, 73 benign, 224 mesothelioma). The CNN algorithm predicted benign, ADCA, and mesothelioma with accuracy of 98.8%, and 99.2% for Inception V3 and VGG19, respectively. Sensitivity and specificity were, 100% and 97.3% for Inception V3, and 99.7% and 98.65% for VGG-19, respectively. All mesotheliomas were predicted correctly. Two benign lesions were predicted as ADCA in Inception V3. One ADCA was predicted as benign, and one benign as ADCA in VGG19.

**Conclusions:** In our proof of concept study, we demonstrate the potential utility of machine learning algorithms for differentiating between benign and malignant lesions in fluid cytology. As machine learning in medicine rapidly improves, it can have a meaningful impact in practical clinical application.

**176 A Decade of Change: Trends in the Practice of Cytopathology at a Tertiary Cancer Center**

Peyman Dinarvand<sup>1</sup>, Chinhua Liu<sup>1</sup>, Sinchita Roy-Chowdhuri<sup>1</sup>

<sup>1</sup>The University of Texas MD Anderson Cancer Center, Houston, TX

**Disclosures:** Peyman Dinarvand: None; Chinhua Liu: None; Sinchita Roy-Chowdhuri: None

**Background:** The practice of cytopathology has evolved over the past decade. Significant advances in minimally invasive procedures and tumor sampling techniques, discovery of new biomarkers, and novel ancillary tests, have played an important role in changing our practice. Cytopathology has evolved from a primarily morphology-based diagnostic modality to one where it provides predictive and prognostic information that impact therapeutic decisions. In this study, we evaluated the changing trends in cytopathology practice at our institution over the past decade.

**Design:** A retrospective review of our institutional database was performed for cytopathology cases from the years 2009 and 2019. Cases were stratified by the type of procedure and additional ancillary studies that were performed.

**Results:** The overall number of exfoliative cases between 2009 and 2019 decreased 12% (n=18338 versus n=16087, respectively), primarily due to a decrease in gynecologic Pap testing (64%); however, the numbers of serous fluids and CSF specimens saw increases of 125% and 44%, respectively (Figure 1A). The number of fine needle aspiration (FNA) cases increased by 23% from 2009 to 2019 (n=11628 versus n=14322, respectively), driven primarily by a 180% increase in endobronchial ultrasound guided transbronchial aspirations (EBUS TBNA) (Figure 1B). While the number of FNA cases increased across most body sites, with lymph node (40%), soft tissue (40%) and liver (96%) aspirations showing the largest increases, the number of breast FNAs decreased by 43% (n=1364 versus n=784) (Figure 1B). The number of FNA cases with immunostains performed increased 476% from 247 cases in 2009 to 1422 cases in 2019; while the number of cases with molecular testing increased 250% from 284 cases in 2009 to 993 cases in 2019 (Figure 2).

Figure 1 - 176

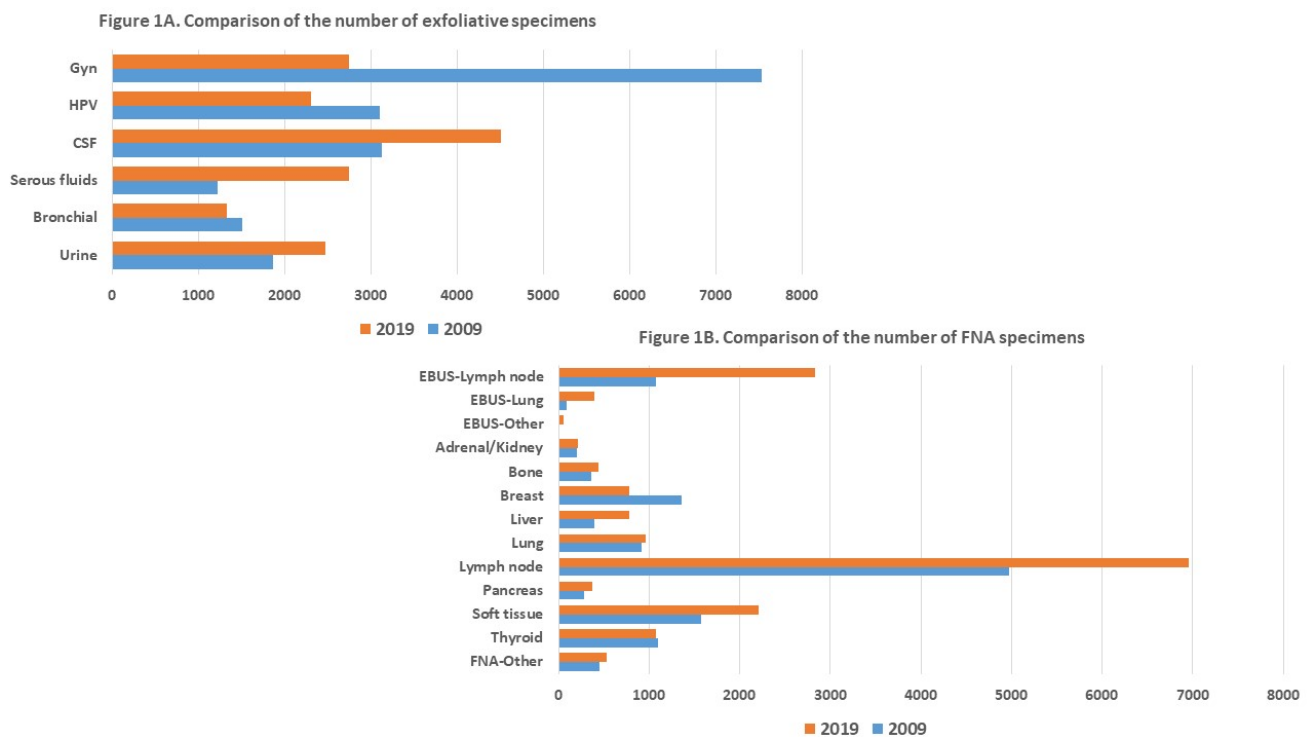
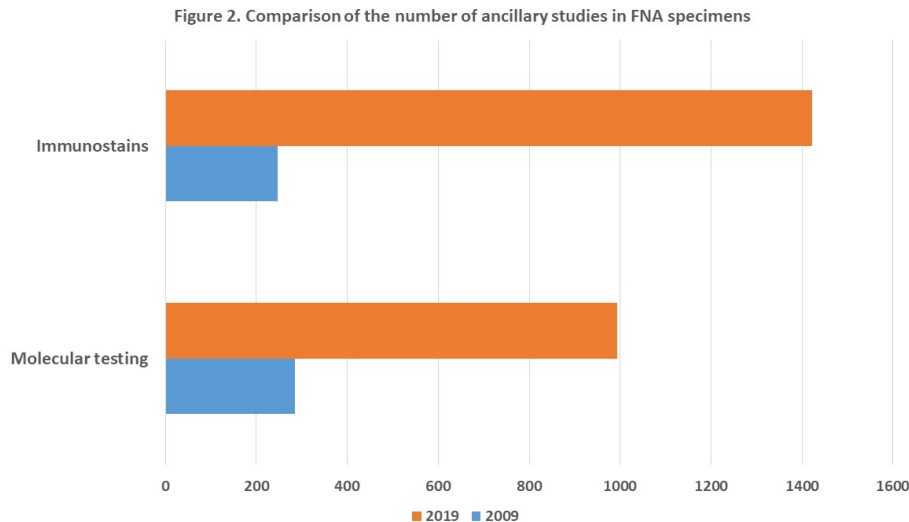




Figure 2 - 176



**Conclusions:** The trend in our cytopathology practice shows an uptick in the number of FNA cases, primarily driven by a significant increase in EBUS TBNA procedures. While the number of exfoliative specimens showed an increase for most sites, the volume of gynecologic Pap testing showed a significant decrease, in keeping with current trends in gynecologic screening practices. Our study also demonstrates a dramatic increase in the number of FNA cases used for immunostains and molecular testing, suggesting an increasing need for doing ancillary studies in the cytopathology practice.

**177 Utility of SOX11 as a Diagnostic Marker for Solid Pseudopapillary Neoplasm of Pancreas Using Cytologic Smear Preparations**

Peyman Dinarvand<sup>1</sup>, Wei-Lien (Billy) Wang<sup>1</sup>, Sinchita Roy-Chowdhuri<sup>1</sup>  
<sup>1</sup>The University of Texas MD Anderson Cancer Center, Houston, TX

**Disclosures:** Peyman Dinarvand: None; Wei-Lien (Billy) Wang: None; Sinchita Roy-Chowdhuri: None

**Background:** Solid pseudopapillary neoplasm (SPN) of the pancreas is a rare, low-grade tumor generally associated with a good prognosis. The diagnosis can sometimes be challenging on fine needle aspiration (FNA) specimens, which can be the only diagnostic source available. The differential diagnosis can include neuroendocrine tumor (NET) and acinar cell carcinoma. Nuclear staining for beta-catenin, is often used as a diagnostic marker for SPN but can also be seen in a subset of other pancreatic tumors. Recent studies have indicated that SRY-related high-mobility group box 11 (SOX11) is a highly sensitive and specific marker for SPN. We evaluated the utility of SOX11 for the diagnosis of SPN using cytologic smears and cell blocks.

**Design:** A retrospective review of our institutional pathology database from 2005 to 2020 was performed to identify endoscopic ultrasound (EUS) guided FNA cases where SPN was in the differential diagnosis based on the cytomorphology. SOX11 immunocytochemistry was performed on alcohol-fixed Papanicolaou stained smears and the corresponding cell blocks (CB), when available. Additional immunostains (e.g. beta-catenin, synaptophysin, chromogranin) that had been performed as part of the clinical work-up were also reviewed. All cases, but one, had surgical follow-up with histologic diagnoses which were also reviewed.

**Results:** Of the 18 cases included in this study, 8 cases had a final diagnosis of SPN and 10 cases were NET. SOX11 showed strong nuclear staining in all 8 SPN cases (smears; n= 8 and CB; n=7) (Figure 1). One SPN case did not have an available CB for immunostaining. Five of these cases had nuclear beta-catenin expression in the tumor cells and 7 cases had surgical follow-up that confirmed the diagnosis. The remaining 10 cases were negative for SOX11 on both smears and CB. All 10 cases had follow-up histologic diagnoses of NET and beta-catenin was

negative in all 10 cases. Sensitivity, specificity, positive predictive value, negative predictive value, and accuracy of SOX11 for diagnosis of SPN in cytology smears and cell block sections were 100%.

Figure 1 - 177

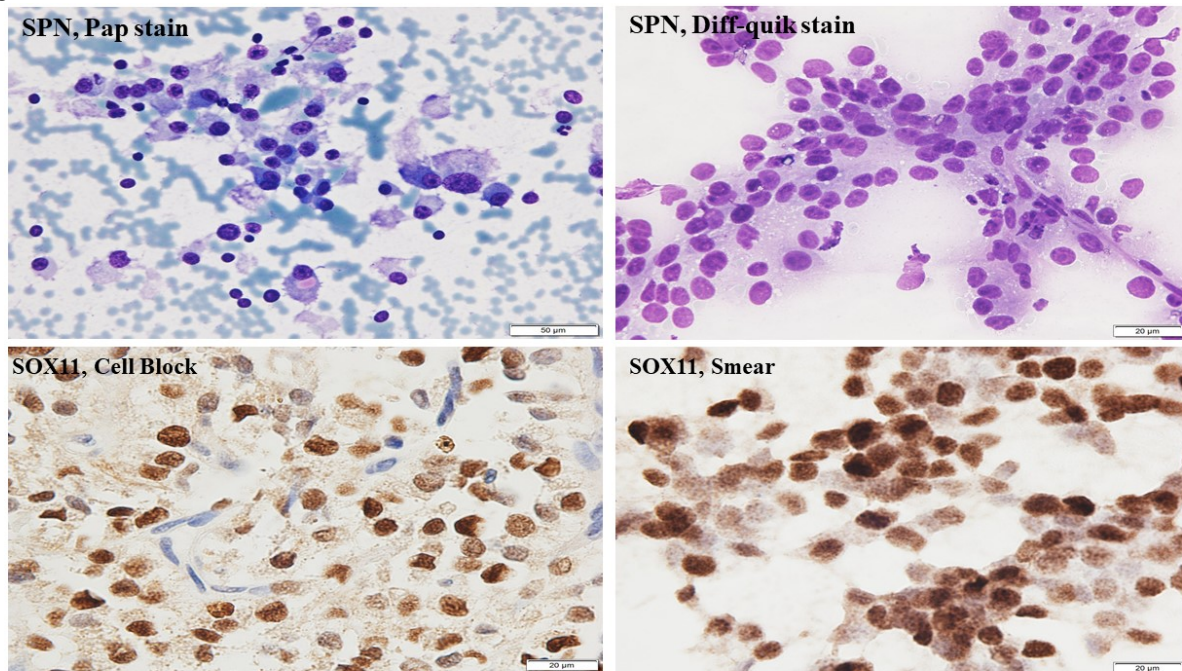


Figure 1

**Conclusions:** In challenging cytology cases with scant cellularity, SOX11 immunostain can serve as a highly sensitive and specific marker for the diagnosis of SPN. Our study demonstrates the utility of SOX11 in cytologic smears, especially in cases where the lack of a cell block for immunostains precludes a definitive diagnosis.

### 178 Evaluation of Bronchoalveolar Lavage Cytology in COVID-19 Patients

Peyman Dinarvand<sup>1</sup>, Qiong Gan<sup>1</sup>

<sup>1</sup>The University of Texas MD Anderson Cancer Center, Houston, TX

**Disclosures:** Peyman Dinarvand: None; Qiong Gan: None

**Background:** COVID-19 is a predominantly respiratory and sometimes multiorgan disease which is caused by SARS-CoV-2. Similar to other coronaviruses SARS-CoV, SARS-CoV-2 is an exceptionally infectious virus that has spread quickly in the world after its initial discovery. Changes in bronchoalveolar lavage (BAL) fluid and cells mirror the pathological processes in the respiratory system. The cytology of BAL fluid is the assessment of the cellular and non-cellular components of the fluid. In this study, for the first time, we evaluated cytomorphological changes observed on smears prepared from BAL in COVID-19 patients.

**Design:** There are thirteen COVID-19 patients (group 1) with PCR-confirmed SARS-CoV-2-positivity (nasopharyngeal swab tests) in our database who had BAL procedure performed during a time period of two weeks after the initial positive tests. Ten SARS-CoV-2-negative patients with acute inflammation on BAL (group 2) and ten SARS-CoV-2-negative patients without acute inflammation (group 3) on BAL were evaluated as controls in this study (totally 33 patients in entire study). All evaluations were blindly performed by two cytopathologists.

**Results:** In 11 (out of 13) BAL cases of COVID-19-positive patients, significantly enlarged, multi-vacuolated macrophages are seen that are not present on the control groups (Figure 1). The macrophages have a twice-larger size of the macrophages we see in our control groups (Figure 1). Moreover, in all these 11 cases, variable amount of thick, fragmented mucin in the background was identified, which was not present in the control groups (Figure 2).

Finally, the percentage of hemosiderin-laden macrophages as highlighted by Iron staining was significantly higher (50%) in COVID-19 patients in comparison to control groups (30% and 20% for groups 2 and 3, respectively).

Figure 1 - 178

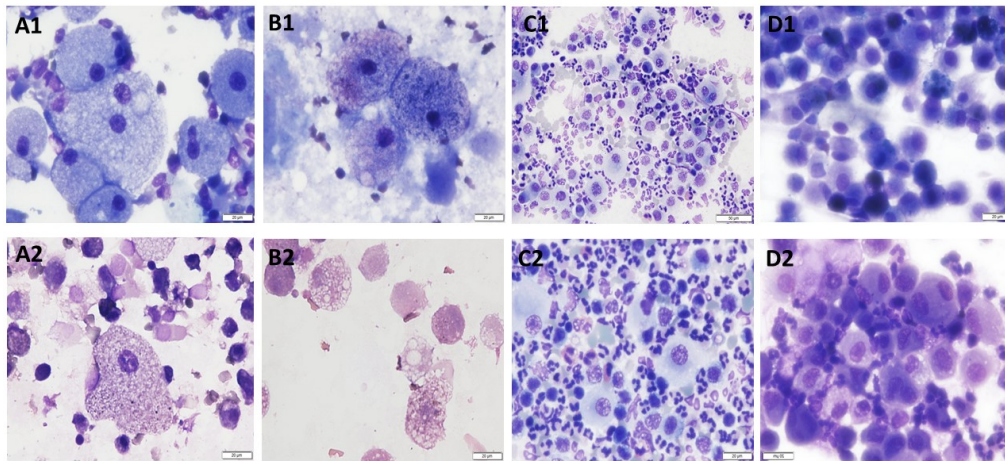


Figure 1. Examples of macrophages in BAL of COVID-19 positive cases (A and B), in Pneumonia due to non-COVID-19 reasons (C), and in cases without Pneumonia (D).

Figure 2 - 178

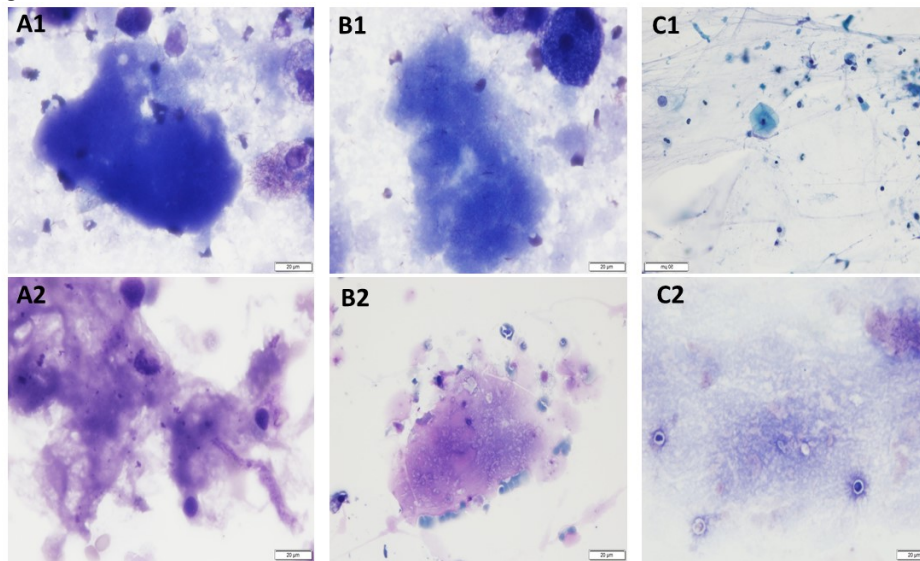


Figure 2. Presence of fragmented, thick mucin in the background of BAL of COVID-19 positive cases (A and B) and their absence in COVID-19 negative cases (C).

**Conclusions:** Although the clinical significance is unknown, the observation of significantly enlarged macrophages with numerous different-sized cytoplasmic vacuoles and thick mucin in BAL is unique in COVID-19 patients, which might be correlated with the severity of patient's respiratory symptoms. Further studies will be needed to determine whether the higher percentage of hemosiderin-laden macrophages in COVID-19 patients is related to alveolar damage or is just a co-incidence.



**179 CD44 Expression in Malignant Pleural Effusion (MPE) is Associated with Worse Overall Survival in Patients with Advanced Breast Carcinoma**

Darin Dolezal<sup>1</sup>, Dana Razzano<sup>2</sup>, Padmini Manrai<sup>3</sup>, Malini Harigopal<sup>1</sup>

<sup>1</sup>Yale School of Medicine, New Haven, CT, <sup>2</sup>Yale School of Medicine, Yale New Haven Hospital, New Haven, CT, <sup>3</sup>Yale University, New Haven, CT

**Disclosures:** Darin Dolezal: None; Dana Razzano: None; Padmini Manrai: None; Malini Harigopal: None

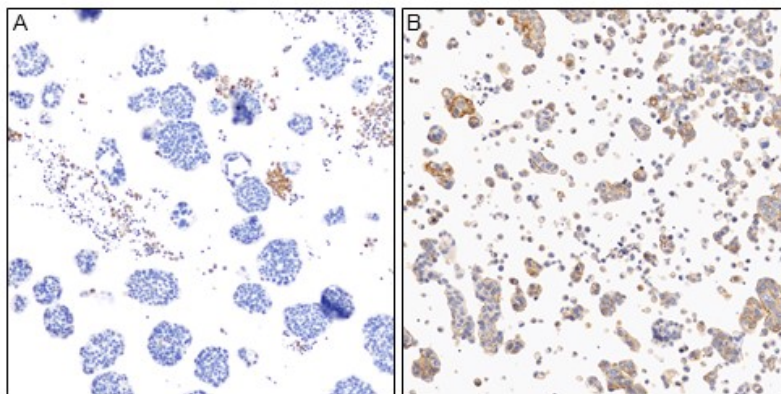
**Background:** MPE is a complication of breast cancer generally associated with advanced disease. However, as treatment options expand, more accurate prognostication at time of MPE may help guide patient management. Prior studies have shown that patients displaying spheroid formations on MPE have improved outcomes. CD44 (surface adhesion molecule and receptor for hyaluronic acid) is a well-established breast stem cell marker that is also enriched in breast circulating tumor cells. We hypothesized that CD44 expression in MPE could identify patients with worse outcomes and CD44 immunostaining of MPE could be used a potential predictive biomarker for patient survival.

**Design:** We assessed CD44 expression by IHC in 40 MPEs collected 2016-2017 from 36 patients with metastatic breast carcinoma. MPEs were categorized into two tumor patterns: small clusters with spheroid formation (hollow, or morula-like, n=15), or single cells and solid sheets (i.e. no spheroids, n=25). CD44 expression in neoplastic cells was assigned an H-score; CD44-positivity was set as H-score >20 (score range 0-300). Overall survival (OS) from time of MPE cytologic diagnosis was assessed by Kaplan-Meier test.

**Results:** CD44 expression (CD44+) was observed in 22/40 (55%) cases (H avg=65, range=0-240). CD44+ MPE was associated with poorly differentiated grade of primary tumor (7/15 (47%) of the tumors associated with CD44+ MPE had poorly differentiated grade vs. 1/13 (8%) associated with CD44- MPE; p<.05), and triple-negative hormone receptor status (5/17 (29%) of CD44+ MPEs were triple-negative status vs. 1/17 (6%) of CD44- MPEs). MPEs displaying spheroids were generally CD44- (H avg 27.5, range 0-140, n=16), whereas MPEs displaying single cells or solid sheets had increased CD44+ staining (H avg 90.6, range 0-240, n=24, p=.005) (Figure 1A-B). Patients with CD44+ MPE had significantly worse median OS (29 months) compared to patients with CD44- MPEs (median OS undefined at 39 month median follow up; p=.047, Figure 2). Patients with single cells and solid sheets on MPE had poor median OS (8 months) compared to those with spheroids (median OS undefined at 41 month median follow-up, p=.01). CD44+ combined with single cells or solid sheets on MPE portended the poorest outcome (median OS= 3 months vs. median OS= 40 months in all MPEs, p=.021, Figure 2).

Figure 1 - 179

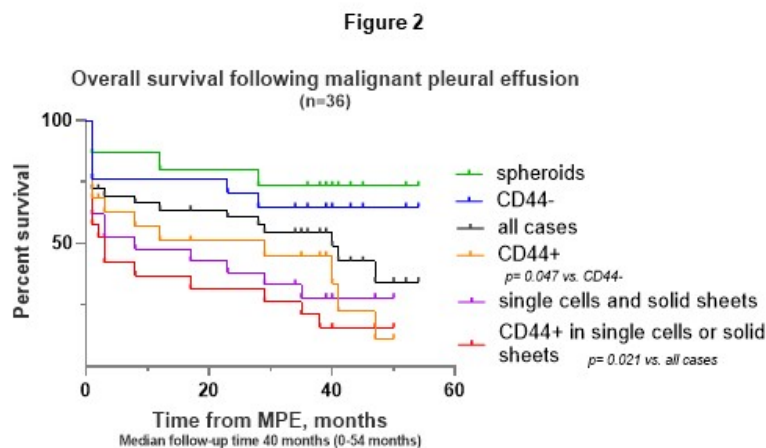
Figure 1



Representative CD44 immunostaining in different cytologic patterns of breast MPE. CD44 expression is absent/minimal in spheroid formations (A) and robust in single cells and solid fragments (B). CD44 stains 'dot-like' in benign mesothelial cells.



Figure 2 - 179



**Conclusions:** In our study, CD44 positivity in breast MPE with single tumor cells was associated with an aggressive clinical course and worse outcomes in patients with metastatic breast carcinoma.

**180 When It Comes to Urethral Washings, Does the Paris System Hold Water?**

Liz Edmund<sup>1</sup>, Darren Buonocore<sup>1</sup>  
<sup>1</sup>Memorial Sloan Kettering Cancer Center, New York, NY

**Disclosures:** Liz Edmund: None; Darren Buonocore: None

**Background:** The Paris system defines urine cytology as positive for high grade urothelial carcinoma (HGUC) if a specimen contains at least 5-10 viable malignant cells that demonstrate N/C ratio equal to or > 0.7, nuclear hyperchromasia, coarse chromatin and irregular nuclear membranes. This definition establishes no distinction between different types of urinary cytology specimens. We will demonstrate that some criteria hold more strictly for urine cytology specimens (UC, voided and instrumented urine) than for urethral washings (UW).

**Design:** From 2013 to 2018, we collected cytology specimens for 20 patients who had a cytologic diagnosis of suspicious or positive for HGUC in urine, underwent cystectomy and subsequently had a diagnosis of positive or suspicious for HGUC on a UW. The average length of time to recurrence post-surgery was 2 years. The pre- and post-cystectomy specimens were reviewed by two pathologists and the following cytomorphologic criteria were assessed: cellularity, nuclear membrane irregularity, nuclear to cytoplasmic (N/C) ratio, hyperchromasia, chromatin quality, and nucleoli. Fisher’s exact test was implemented to compare the cytomorphologic features of UC and UW (n=40), voided urine only (VU) and UW (n=24), and instrumented urine only (IU) and UW (n=16).

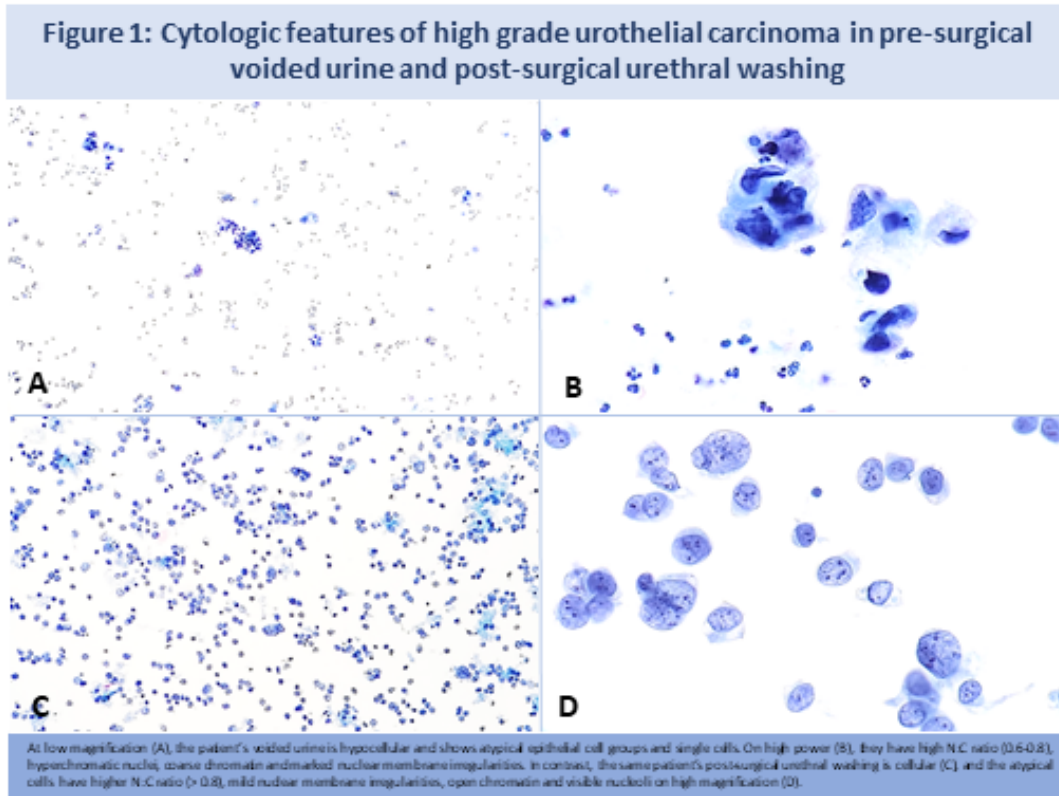
**Results:** In comparison with the original tumor in the UC, the recurrent HGUC in the UW exhibits significant morphologic differences including higher N/C ratio, vesicular chromatin with conspicuous nucleoli, and less hyperchromasia and degeneration (Table 1). Similar findings were seen when the tumors in the UW was compared with VU specimens only (Table 1). Interestingly, when comparing the recurrent HGUC in the UW to the original tumor in urine collected during or post-cystoscopy (IU), there were no statistically significant differences in cytomorphologic criteria, except for nuclear hyperchromasia. Hyperchromasia was seen in 100% of IU tumors and only 37% of UW tumors, with a p-value of 0.026.

**Table 1: Cytomorphologic features of paired post-surgical urethral washings and pre-surgical urine cytology specimens**

	Paired post-surgical urethral washings and urine cytology (voided/instrumented)		Paired post-surgical urethral washings and voided urine only	
	UW (n=20)	UC (n=20)	UW (n=12)	VU (n=12)
<b>Cellularity</b>				
2-3+	15 (75%)	18 (90%)	8 (66.6%)	10 (83.3%)
1+	5 (25%)	2 (10%)	4 (33.3%)	2 (16.7%)
<b>P-value</b>	<b>0.406</b>		<b>0.64</b>	
<b>Nuclear Membrane irregularity</b>				
Mod-marked	16 (80%)	17 (85%)	10 (83.3%)	12 (100%)
Mild	4 (20%)	3 (15%)	2 (16.7%)	0 (0%)
<b>P-value</b>	<b>1.000</b>		<b>0.478</b>	
<b>N/C ratio</b>				
>0.8	16 (80%)	5 (25%)	10 (83.3%)	4 (33.3%)
0.6-0.8	4 (20%)	15 (75%)	2 (16.7%)	8 (66.7%)
<b>P-value</b>	<b>0.0012</b>		<b>0.036</b>	
<b>Mitosis</b>				
Present	8 (40%)	1 (5%)	3 (25%)	0 (0%)
Absent	12 (60%)	19 (95%)	9 (75%)	12 (100%)
<b>P-value</b>	<b>0.020</b>		<b>0.217</b>	
<b>Hyperchromasia</b>				
Mod-marked	7 (35%)	20 (100%)	4 (33.3%)	12 (100%)
Mild	13 (65%)	0 (0%)	8 (66.7%)	0 (0%)
<b>P-value</b>	<b>0.001</b>		<b>0.0013</b>	
<b>Degeneration</b>				
Mod-marked	8 (40%)	2 (10%)	4 (33.3%)	12 (100%)
None-mild	12 (60%)	18 (90%)	8 (66.7%)	0 (0%)
<b>P-value</b>	<b>0.0648</b>		<b>0.0013</b>	
<b>Chromatin</b>				
Vesicular	14 (70%)	3 (15%)	8 (66.7%)	0 (0%)
Coarse	6 (30%)	17 (85%)	4 (33.3%)	12 (100%)
<b>P-value</b>	<b>0.0011</b>		<b>0.0013</b>	
<b>Nucleoli (x 10 objective)</b>				
Visible	17 (85%)	10 (50%)	10 (83.3%)	4 (33.3%)
Not visible	3 (15%)	10 (50%)	2 (16.7%)	8 (66.7%)
<b>P-value</b>	<b>0.0407</b>		<b>0.036</b>	

Abbreviations: N/C- nuclear to cytoplasmic

Figure 1 - 180



**Conclusions:** Although the Paris system establishes cytologic guidelines for diagnosing HGUC in urine cytology specimens, it does not distinguish between the different urinary cytologic specimens. In our practice, we notice that the recurrent tumors in the UW are more hypochromatic and have more vesicular chromatin and conspicuous nucleoli than the tumors in the patients' original urine cytology. We hypothesize that these differences in morphology may be due better preservation and reduced exposure to urine in UW as compared to UC.

**181 Cytologic Features of Sex-Cord Stromal Tumors in Women**

Liz Edmund<sup>1</sup>, Abeer Salama<sup>1</sup>, Rajmohan Murali<sup>1</sup>  
<sup>1</sup>Memorial Sloan Kettering Cancer Center, New York, NY

**Disclosures:** Liz Edmund: None; Abeer Salama: None; Rajmohan Murali: None

**Background:** Gynecologic sex cord-stromal tumors (SCSTs) arise from the sex cords of the embryonic gonad. They represent 5% of primary neoplasms that arise in the ovary, and may display malignant behavior, with peritoneal and distant metastasis, and recurrences in body fluids. In this study, we describe the cytomorphologic features of SCSTs in females, including adult and juvenile granulosa cell tumors (AGCTs and JGCTs), Sertoli-Leydig cell tumors (SLCTs) and steroid cell tumor (SCT).

**Design:** Available cytology slides from females with a histologic diagnosis of sex-cord stromal tumor between 2009 and 2020 were retrieved from institutional archives and were reviewed with respect to cytoarchitectural features (Table).

**Results:** The study cohort comprised 30 cytology specimens from 24 females (aged 7-90 years, median 57 years), including 25, 2, 2 and 1 specimens from 19, 2, 2 and 1 patients with AGCT, JGCT, SLCT and SCT, respectively. The cytologic findings are detailed in the Table. Features common to both AGCTs and other SCSTs included 3-

dimensional groups, small loose clusters, abundant single cells and naked nuclei, while rosettes and a streaming appearance of cell groups were only seen in AGCTs (Table). Less common features included rare papillary fragments seen in AGCTs and other SCSTs, and metachromatic stroma in one AGCT. AGCTs predominantly exhibited high nuclear: cytoplasmic (N/C) ratios, with mild nuclear pleomorphism, round-oval nuclei, with finely granular chromatin, prominent nuclear grooves and small nucleoli, while other SCSTs showed lower N/C ratios, mild to moderate nuclear pleomorphism, round to oval occasionally binucleated nuclei, with finely to coarsely granular chromatin, small nucleoli, and moderate to abundant granular or vacuolated cytoplasm. Mitotic figures, necrosis and inflammation were rarely identified (Table).

**Table: Cytologic features of sex-cord stromal tumors**

Patient no. (age at diagnosis)	Specimen site/type	Cellularity	Cellular arrangements*	N:C ratio	Nuclear shape	Nuclear grooves	Nuclear pleomorphism	Chromatin pattern	Naked nuclei	Comments/Mutations
<b>Granulosa cell tumors, adult type</b>										
1 (53 y)	Pelvic lymph node (FNA)	I	3D clusters, papillary fragments	H	Oval/angulated	+	Moderate	Finely granular	-	
1 (53 y)	External iliac lymph node, (FNA)	H	3D clusters, papillary fragments, stromal fragments, rare rosettes	H	Oval	+	Mild	Finely granular	+	
2 (57 y)	Pelvis subcutaneous nodule (FNA)	I	3D clusters with streaming	H	Oval	+	Mild	Finely granular	+	
2 (57 y)	Peritoneum (TP)	I	3D clusters with streaming, rare rosettes	H	Oval	+	Mild	Finely granular	+	
2 (57 y)	Abdominal nodule (TP)	H	3D clusters with streaming + rosettes	H	Round/oval	+	Mild	Finely granular	+	FOXL2 TERT
3 (78 y)	Ureter (brushing)	L	3D clusters with streaming	H	Oval	+	Mild	Finely granular	-	FOXL2 TERT
4 (74 y)	Abdominal nodule (FNA)	H	Large syncytial sheets, 3D clusters and small loose clusters, rare rosettes	H	Round/oval	+	Mild	Finely granular	+	Nuclear inclusions
5 (59 y)	Omental nodule (TP)	H	Large syncytial sheets, small loose clusters, rare rosettes	H	Round/oval	+	Mild	Finely granular	+	Nuclear inclusions
6 (43 y)	Pelvis (TP)	H	Large 3D clusters with streaming, rare rosettes	H	Round/oval	+	Mild	Finely granular	+	
7 (56 y)	Abdomen (TP)	I	3D clusters	H	Round/oval	+, rare	Mild	Finely granular	+	FOXL2 TERT
	Pleura (TP)	I	Large syncytial sheets, papillae and 3D and loose clusters, rare rosettes	H	Round/oval	+	Mild	Finely granular	+	
8 (63 y)	Abdomen (TP)	H	3D clusters and small	H	Oval	+	Mild	Finely granular	+	FOXL2



			loose clusters							<i>TERT</i>
8 (64 y)	Abdomen (TP)	H	Large 3D groups and smaller loose clusters	H	Round/oval	+	Mild	Vesicular	+	
9 (90 y)	Pelvis (TP)	I	Rare loose clusters; one possible rosette-like structure	H	Oval	+	Mild	Vesicular	+	
10 (54 y)	Peritoneal washing	H	Small sheets and 3D clusters, rosettes	H	Round/oval	+	Mild	Finely granular	-	Inflammation
11 (26 y)	Ascitic fluid	L	small loose clusters	H	Round/oval/ angulated	+, rare	Moderate	Finely granular	-	Inflammation
12 (47 y)	Peritoneum (FNA)	H	Large syncytial sheets, 3D clusters, small loose clusters, rare rosettes	H	Oval	+	Moderate	Finely granular	+	<i>FOXL2</i> <i>TERT</i>
13 (50 y)	Peritoneal washing	L	Small 3D clusters*	I-H	Oval/ angulated	+	Moderate	Finely granular	-	
14 (71 y)	Iliac bone (TP)	I	3D clusters	H	Round/oval	+	Moderate	Finely granular	+	Mitotic figures identified; Necrosis and inflammation
14 (71 y)	Sacral soft tissue (TP)	I	3D clusters with streaming	H	Round/oval	+	Moderate	Finely granular	+	
15 (65 y)	Subcutaneous nodule (TP)	I	Small, loose clusters	I	Round/oval	+	Mild	Finely granular	+	
16 (66 y)	Abdomen (TP)	H	3D clusters, rosettes, eosinophilic globules	H	Round/oval	+	Mild	Finely granular	+	
17 (57 y)	Retroperitoneal lymph node (TP)	H	Syncytial sheets, small loose clusters, rosettes; associated metachromatic stroma	L	Round/oval	+	Mild	Finely granular	+	<i>FOXL2</i> <i>TERT</i>
18 (66 y)	Peritoneal nodule (TP)	H	3D clusters, some papilliform, rare rosettes	H	Round/oval	+	Mild	Finely granular	+	
19 (32 y)	Ascitic fluid	L	Small, loose clusters	H	Oval	+	Mild	Finely granular	-	<i>FOXL2</i>
<b>Juvenile granulosa cell tumors</b>										
20 (7 y)	Peritoneal washing	I	Small, loose clusters	I-H	Round/oval; bizarre and multinucleated cells	-	Marked	Coarsely granular	+	Mitotic figures, including atypical forms; <i>TP53</i> <i>AKT1</i>

21 (66 y)	Peritoneal washing	L	Loose clusters	I	Round/oval/angulated	-	Moderate	Vesicular	-	
<b>Poorly differentiated Sertoli-Leydig cell tumors</b>										
22 (22 y)	Pelvis (TP)	I	Small 3D clusters	I-H	Oval/angulated	-	Moderate	Coarsely granular	+	
23 (36 y)	Ascitic fluid	I	Small clusters	I	Round/oval; Binucleation present	-	Mild	Finely granular	-	
<b>Steroid cell tumor</b>										
24 (81 y)	Abdominal mass (FNA)	H	Sheets, 3D clusters and papillary groups (with fibrovascular cores)	L	Round	-	Moderate	Speckled and open/granular	+	
<p>Abbreviations:</p> <p>3D – three dimensional; TP- touch preparation; FNA- fine needle aspiration; H-high; I- intermediate; L-low</p> <p>* singly dispersed tumor cells also seen</p> <p>+ present</p> <p>- not present</p>										

**Conclusions:** AGCTs are characterized by the presence of 3-dimensional cell groups, small loose clusters, rosettes and rare papillae, and were comprised of neoplastic cells with often high N/C ratio, round-oval nuclei, finely granular chromatin and prominent nuclear grooves, while other SCSTs lacked rosettes and nuclear grooves, and had generally lower N/C ratios, greater nuclear pleomorphism, and moderate to abundant granular to vacuolated cytoplasm. Ancillary studies (e.g. immunochemistry for FOXL2, inhibin and calretinin or sequencing for FOXL2 mutations) can aid in the diagnosis of these tumors.

**182 The Optimal Approach of EBUS-FNA Rapid On-site Evaluation (ROSE): A Five-Year Experience from a Large Academic Medical Center**

Shaimaa Elzamy<sup>1</sup>, Ali Al-Habib<sup>1</sup>, Jaiyeola Thomas-Ogunniyi<sup>2</sup>, Jing Liu<sup>3</sup>, Hui Zhu<sup>2</sup>, Jamie Buryanek<sup>2</sup>, Pushan Jani<sup>1</sup>, Songlin Zhang<sup>2</sup>

<sup>1</sup>McGovern Medical School at UTHealth, The University of Texas Health Science Center at Houston, Houston, TX, <sup>2</sup>The University of Texas Health Science Center at Houston, Houston, TX, <sup>3</sup>The University of Texas at Houston, Houston, TX

**Disclosures:** Shaimaa Elzamy: None; Ali Al-Habib: None; Jaiyeola Thomas-Ogunniyi: None; Jing Liu: None; Hui Zhu: None; Jamie Buryanek: None; Pushan Jani: None; Songlin Zhang: None

**Background:** Endobronchial ultrasound-guided fine needle aspiration (EBUS-FNA) is a widely used procedure for diagnosing and staging of mediastinal and lung lesions. Rapid on-site evaluation (ROSE) has shown significant value for both triaging and diagnosing those lesions. The most recent CAP guidelines (2019) recommend using ROSE when EBUS-FNA is performed. However, ROSE may not be available for some pulmonary centers. Performing ROSE could be challenging and stressful during the procedure because most pulmonologists use 2-3 separate needles to save time since patients are deeply sedated. The aim of the present study is to investigate the optimal ROSE procedure.

**Design:** A retrospective cytology report review of EBUS-FNA procedures performed between October 2014 and May 2019 revealed 516 cases that were included in the study. The number of passes for each procedure was documented. The adequacy of both the final ROSE and the final cytology results were reviewed and classified as adequate and inadequate. We also studied the adequacy if only the first 3 passes, the first 5 passes, the odd

passes or the even passes were evaluated. The results were either adequate, inadequate, or not applicable. We then compared the adequacy result of each category to the final ROSE adequacy.

**Results:** The final ROSE interpretation was adequate in 370 (71.7%) and inadequate in 146 (28.3%) cases. After reviewing the pap stained slides and cellblocks, the final cytology results were adequate in 473 (91.7%) and inadequate in 43 (8.3%) of the cases. The number of passes per procedure ranged from 1 to 17 (median 4, IQR 2). The number of passes evaluated were  $\leq 3$  in 274 (53.1%) and  $> 3$  in 242 (46.9%) of the cases. While the number of passes evaluated were  $\leq 5$  in 433 (83.9%) and  $> 5$  in 83 (16%) of the cases. The adequacy results for the first 3, 5, odd, and even passes were 63.4%, 70.3%, 57.5% and 52.9% respectively. By comparing to the final ROSE adequacy results, the differences of adequacy results for each category was -8.5%, -1.4%, -14.2%, and -18.8% respectively.

**Conclusions:** Our results showed that ROSE evaluation of the first 5 passes during the EBUS-FNA procedure could achieve the similar adequacy rate compared to the final ROSE evaluation of all the passes. This coincide with the recent CAP guidelines to perform 5 passes during EBUS-FNA if ROSE is not available. To reduce the procedure time for EBUS-FNA, we recommend performing ROSE for the first 5 passes, and save all additional passes for cellblock preparation if more than 5 passes are attempted.

**183 Probability of Malignancy as Determined by ThyroSeq v3 GC Varies According to the Subtype of Atypia of Undetermined Significance**

David Gajzer<sup>1</sup>, Khaled Algashaamy<sup>2</sup>, Yiqin Zuo<sup>3</sup>, Merce Jorda<sup>4</sup>, Monica Garcia-Buitrago<sup>5</sup>, Carmen Gomez-Fernandez<sup>4</sup>, Jaylou Velez Torres<sup>4</sup>

<sup>1</sup>University of Miami Miller School of Medicine/Jackson Memorial Hospital, Miami, FL, <sup>2</sup>University of Miami/Jackson Memorial Hospital, Miami, <sup>3</sup>University of Miami, Miami, FL, <sup>4</sup>University of Miami Miller School of Medicine, Miami, FL <sup>5</sup>University of Miami Miller School of Medicine/Jackson Health System, Miami

**Disclosures:** David Gajzer: None; Khaled Algashaamy: None; Yiqin Zuo: None; Merce Jorda: None; Monica Garcia-Buitrago: None; Carmen Gomez-Fernandez: None; Jaylou Velez Torres: None

**Background:** Thyroid fine-needle aspiration cytology (FNAC) is a well-established technique that plays a critical role in the preoperative diagnosis of thyroid nodules. Determining the risk of malignancy for aspirates diagnosed as atypia of undetermined significance (AUS) can present a challenge. ThyroSeq molecular testing has become a standard tool to assess probability of malignancy (POM) in these specimens, as it carries important implications for clinical management. We aimed to investigate whether defined AUS subcategories are associated with specific POM and genetic alterations.

**Design:** FNAC from 2019 with final diagnosis of AUS and subcategorized as follicular cells with either cytologic (FC-C), architectural (FC-A), or cytologic and architectural atypia (FC-CA), or predominance of Hurthle cells (PHC) and associated ThyroSeq reports were retrieved from the pathology files of our institution. The percentages of specimens with positive ThyroSeq by subcategory and average POM were computed, and the frequency of individual mutations or genetic alterations analyzed.  $P < 0.05$  was considered significant.

**Results:** 316 cases of AUS including 122 FC-A, 67 FC-C, 69 FC-CA, and 51 PHC were analyzed. ThyroSeq results were positive in 45% of FC-CA, 31% of FC-C, 21% of FC-A, and 14% of PHC. Specimens with both cytologic and architectural atypia were significantly more often positive than those with architectural atypia only ( $p = 0.0009$ ), but not those with cytologic atypia only ( $p = 0.1$ ). No significant difference in positivity was observed between specimens demonstrating either cytologic or architectural atypia only. The reported probability of cancer or NIFTP averaged by subcategory were as follows: 67% - FC-CA, 63% - FC-A, 60% - FC-C; 59% - PHC). High positive POM results were most frequently seen in cases with both cytologic and architectural atypia. RAS mutations were predominant in all subcategories (16 - FC-A), (12 - FC-C), (16 - FC-CA), (4- PHC), while BRAF mutations were most frequent in FC-CA (6).

**Conclusions:** Thyroid FNA specimens exhibiting both cytologic and architectural atypia (FC-CA) are associated with the highest POM, are most frequently associated with genetic alterations and most commonly carry BRAF mutations. RAS mutations are most frequent among all subcategories. Cytologic atypia is associated with a higher

frequency of genetic alterations than architectural atypia. Awareness of variable cancer probability by AUS subcategory allows for more tailored management.

**184 Performance of Rapid Onsite Evaluation Using Touch Preparations of Core Needle Biopsies in the Diagnosis of Renal Masses: A 415 Case Experience**

Ian Gelarden, Bonnie Choy<sup>1</sup>

<sup>1</sup>Northwestern Memorial Hospital, Chicago, IL

**Disclosures:** Ian Gelarden: None; Bonnie Choy: None

**Background:** Touch preparations (TPs) of core needle biopsies (CNBs) are utilized to ensure sample adequacy and appropriate specimen triage. Percutaneous CNBs are becoming more commonly performed to evaluate renal masses. However, rapid onsite evaluation (ROSE) using TPs can be challenging due to broad differential diagnoses and subtypes of renal tumors. Our study examines the concordance of TPs and corresponding CNBs in adequacy and diagnostic interpretations of renal masses.

**Design:** Our pathology database was searched for all renal mass CNBs with ROSE using TPs between 07/2011 and 10/2020. Concordance was considered when: 1) inadequate at ROSE with nondiagnostic CNB, 2) benign impression at ROSE with negative diagnosis on CNB, and 3) any abnormal impression (atypical, neoplasm, suspicious, or malignant) at ROSE with abnormal diagnosis (atypical, neoplasm, suspicious, or malignant) on CNB.

**Results:** 415 total CNBs of renal masses from 380 patients (152 female, 228 male; age range: 20-91 years, median 65 years) were identified. Size of renal masses ranged from 0.9-15 cm (median 2.85 cm). ROSE was performed on all cases. Number of passes per case ranged from 1-9 (median 3 passes), and number of TPs per case ranged from 1-10 (median 3 TPs).

In addition to assessment of adequacy, ROSE impression of TPs was available in 386 (93%) cases and classified as: inadequate (n=73, 19%), benign (n=8, 2%), atypical (n=27, 15%), neoplasm (n=63, 16%), suspicious for malignancy (n=27, 7%), positive for malignancy (n=158, 41%). 336 (81%) TPs were deemed adequate during ROSE, of which 320 (95%) CNBs were satisfactory for evaluation. 79 (19%) TPs were inadequate, but subsequently 51 (65%) CNBs were found to have sufficient material for diagnosis. Overall, the concordant rate between ROSE impression on TPs and final diagnosis on CNBs is 82% (Table 1). Reasons for discordance include: 1) absent or scant lesional material on TPs but sufficient lesional cells on CNBs, and 2) over interpretation of renal parenchyma as lesional cells at ROSE.

**Table 1. Concordance between ROSE impression using TP and final diagnosis on CNB**

TP Impression at ROSE	Final Diagnosis on CNB						Total
	Nondiagnostic	Negative	Atypical	Neoplasm	Suspicious	Malignant	
Inadequate	26	9	2	10	-	26	73 (18.9%)
Benign	-	5	-	-	-	3	8 (2.1%)
Atypical / Lesional	6	5	3	20	-	23	57 (14.8%)
Neoplasm	2	-	-	26	-	35	63 (16.3%)
Suspicious	3	-	-	1	1	22	27 (7.0%)
Malignant	3	-	1	12	-	142	158 (40.9%)
<b>Total</b>	<b>40 (10.4%)</b>	<b>19 (4.9%)</b>	<b>6 (1.6%)</b>	<b>69 (17.9%)</b>	<b>1 (0.3%)</b>	<b>251 (65.0%)</b>	<b>386</b>

**Conclusions:** Our study demonstrated that ROSE using TPs ensures adequate diagnostic material on CNBs and has a high concordance rate with the final diagnosis. ROSE of renal masses can be difficult and discordance in interpretation infrequently occurs. However, recognition of common pitfalls can further improve the ROSE performance of renal masses.



**185 RAS Mutation and Associated Risk of Thyroid Malignancy: A Fine Needle Aspiration Study with Cytology-Histology Correlation**

Syed Gilani<sup>1</sup>, Guoping Cai<sup>2</sup>, Manju Prasad<sup>1</sup>, Adebowale Adeniran<sup>1</sup>

<sup>1</sup>Yale School of Medicine, New Haven, CT, <sup>2</sup>Yale University, New Haven, CT

**Disclosures:** Syed Gilani: None; Guoping Cai: None; Manju Prasad: None; Adebowale Adeniran: None

**Background:** Activating point mutations of the *RAS* gene (*NRAS*, *HRAS* and *KRAS*) can be seen in benign and malignant thyroid tumors and among these, *NRAS* are more commonly seen. This study was conducted to evaluate risk of thyroid malignancy (ROM) associated with *RAS* mutations at our institution.

**Design:** We searched our electronic database system between January 2015 and March 2020 for thyroid fine needle aspiration (FNA) cases with any type of *RAS* mutation. Molecular alterations were identified by using either ThyroSeq GC (genomic classifier) or ThyGeNEXT (thyroid oncogene panel)/ThyraMIR (miRNA classifier).

**Results:** A total of 84 (age: 48+15, F=66 and M=18) cases were identified and of those 52 had histologic follow-up with the more than half (n=27) had undergone total thyroidectomy. The overall ROM associated with *RAS* mutations (with or without any other molecular alteration) was 32% while the ROM was lower (22%) with *RAS* mutations only. Specific *NRAS*, *HRAS* and *KRAS* mutation-associated ROMs (with or without any other molecular alteration) were 36%, 42% and 10%, respectively. Among these *RAS*-mutated cases, the cases with Bethesda category IV cytologic diagnosis had a higher ROM than the cases with category III diagnosis (42% versus 19%, respectively). Seventeen histologically confirmed malignant cases were mostly classified as category IV lesions (n=12, 71%) and reminder were either category III (n=4) or V lesions (n=1).

**Table: Correlation of *RAS* mutations with histologic follow-up**

Molecular tests		Histologic Diagnosis		
		Nonneoplastic	Neoplastic	Malignant
NRAS (n=30)	NRAS only (n=15)	n=9	n=3 (2 NIFTP & 1 FA)	n=3 (PTC)
	NRAS & other alterations* (n=15)	n=3	n=1 (HCA)	n=8 (2 HCC, 3 PTC, 3 FC)
HRAS (n=12)	HRAS only (n=6)	n=2	n=2 (FA and NIFTP)	n=2 (PTC, FV)
	HRAS & other alterations* (n=6)	n=1	n=2 (FA and NIFTP)	n=3 (PTC, FV)
KRAS (n=10)	KRAS only (n=6)	n=4	n=1 (NIFTP)	n=1 (FC)
	KRAS & other alterations* (n=4)	n=2	n=2 (FA, HCA)	-

Other alterations include positive gene expression profile, positive gene fusion, positive MIR, EIF1AX, PTEN mutations and copy number alterations. NIFTP: Non-invasive follicular thyroid neoplasm with papillary-like nuclear features, FA: follicular adenoma, HCA: Hurthle cell adenoma, PTC: Papillary thyroid carcinoma, FV: Follicular variant, HCC: Hurthle cell carcinoma, FC: Follicular carcinoma.

**Conclusions:** Our study demonstrated that the overall ROM in thyroid FNA with associated *RAS* mutation was intermediate (32%) and *NRAS* and *HRAS* mutations appeared to have higher ROM than *KRAS* mutation. Most malignant cases associated with *RAS* mutations were cytologically classified as follicular/Hurthle cell neoplasms (Bethesda category IV).

**186 Using the Rate of RAS and RAF Mutations Identified in Thyroid Fine Needle Aspirations Together with the Bethesda Category III:VI Ratio: Metrics for Evaluating the Diagnostic Performance of Cytopathologists**

Hamza Gokozan<sup>1</sup>, Thomas Dilcher<sup>2</sup>, Susan Alperstein<sup>3</sup>, Maria Mostyka<sup>1</sup>, Theresa Scognamiglio<sup>3</sup>, Hanna Rennert<sup>3</sup>, Wei Song<sup>4</sup>, James Solomon<sup>1</sup>, Hyeon Jin Park<sup>3</sup>, Shaham Beg<sup>1</sup>, Evan Stern<sup>1</sup>, Momin Siddiqui<sup>3</sup>, Jonas Heymann<sup>3</sup>

<sup>1</sup>New York-Presbyterian/Weill Cornell Medical Center, New York, NY, <sup>2</sup>New York-Presbyterian Hospital, New York, NY, <sup>3</sup>Weill Cornell Medicine, New York, NY, <sup>4</sup>Weill Cornell Medical College, New York, NY

**Disclosures:** Hamza Gokozan: None; Thomas Dilcher: None; Susan Alperstein: None; Maria Mostyka: None; Theresa Scognamiglio: None; Hanna Rennert: None; Wei Song: None; James Solomon: None; Hyeon Jin Park: None; Shaham Beg: None; Evan Stern: None; Momin Siddiqui: None; Jonas Heymann: None

**Background:** Molecular testing (MT) of thyroid fine needle aspiration biopsy (FNA) derived genetic material is commonly used to assess malignancy risk for indeterminate cases, particularly those in category III (AUS) per The Bethesda System for Reporting Thyroid Cytopathology (TBS). Although quality assurance metrics have been proposed, TBS provides little guidance for the appropriate use of AUS, resulting in significant interobserver variability. Herein, we combine MT with cytomorphology to monitor individual practices in rendering AUS diagnoses.

**Design:** Clinician-requested MT was used to evaluate pre-operative FNAs, including reflexive evaluation of all cases in TBS categories III and IV. MT was also reflexively employed to evaluate resected malignancies (Table). Neoplasia-associated genetic alterations (NGA) were categorized as “*BRAF* V600E”, “*RAS*-like” (*HRAS*, *NRAS*, or *KRAS* or non-V600E *BRAF* mutation), or “other”. We also performed blinded, retrospective review of a subset of FNA cases with *BRAF* V600E mutation initially categorized as AUS.

**Results:** Cytopathologists (CP) evaluated 7382 thyroid FNAs over a 54-month period. AUS rate was 9.3% overall with ranges of 5.4-12.4% over any 6-month increment and 4.3-24.2% among 6 CPs who evaluated >150 cases over the study period. AUS rate tracked closely with TBS category III:VI ratio, which was 2.4 overall and 1.1-8.1 among the 6 CPs. MT was performed on 588 cases from 560 patients (79% women) of median age 56 years (range, 8-89); *RAS*-like and *BRAF* V600E mutations were evaluated in 437 (AUS, n=238) and 460 (AUS, n=260) cases, respectively. *BRAF* V600E and *RAS*-like mutations represented a majority of NGAs (Figure 1). *BRAF* V600E was most common (76% of cases) in TBS category VI and rare (3%) in category III. *RAS*-like mutations were most common in TBS categories III (13%), IV (25%), and V (17.5%). NGA rate in AUS cases for each of the 6 CPs did not correlate with TBS category III:VI ratio (Figure 2). Review of 4/9 total FNA cases initially categorized as AUS and with *BRAF* V600E mutation demonstrated low cellularity and/or poor cellular preservation. Interobserver variability was similar to that in cases with other mutations.

Characteristics of molecular tests utilized to sequence selected target genes.					
Test	Test Utilization		Sequencing Targets		
	Pre-Operative	Post-Operative	<i>HRAS</i> , <i>NRAS</i> , and <i>KRAS</i> exons 2 and 3	<i>BRAF</i> exon 15 (including V600)	Other
Afirma Gene Expression Classifier <sup>1</sup>	X				
Afirma Gene Sequencing Classifier <sup>1</sup>	X			X	<i>RET</i> (fusion)
ThyGenX <sup>2</sup>	X		X	X	<i>PIK3CA</i> , <i>RET</i> (fusion), Other (fusion)
ThyGeNEXT <sup>2</sup>	X		X	X	<i>PTEN</i> , <i>PIK3CA</i> , <i>GNAS</i> , <i>pTERT</i> , <i>RET</i> (fusion), Other (fusion)
ThyroSeq v3 <sup>3</sup>	X		X	X	<i>PTEN</i> , <i>TP53</i> , <i>CDKN2A</i> , <i>PIK3CA</i> , <i>GNAS</i> , <i>pTERT</i> , CNA, <i>RET</i> (fusion), Other (fusion)
Oncomine Comprehensive Assay v2 <sup>4</sup>	X	X	X	X	<i>PTEN</i> , <i>TP53</i> , <i>CDKN2A</i> , <i>PIK3CA</i> , <i>GNAS</i> , <i>RET</i> (fusion), Other (fusion)
Ion AmpliSeq Cancer Hotspot Panel v2 <sup>4</sup>		X	X	X	<i>PTEN</i> , <i>TP53</i> , <i>CDKN2A</i> , <i>PIK3CA</i> , <i>GNAS</i>

<sup>1</sup>Veracyte, South San Francisco, CA; <sup>2</sup>Interpace Biosciences, Parsippany, NJ; <sup>3</sup>Joint partnership between UPMC, Pittsburgh, PA and Sonic Healthcare, Austin, TX; <sup>4</sup>ThermoFisher Scientific, Waltham, MA

Abbreviations: FNA - Fine needle aspiration biopsy; FFPE - formalin-fixed, paraffin-embedded tissue; CNA - copy number alterations

Figure 1 - 186

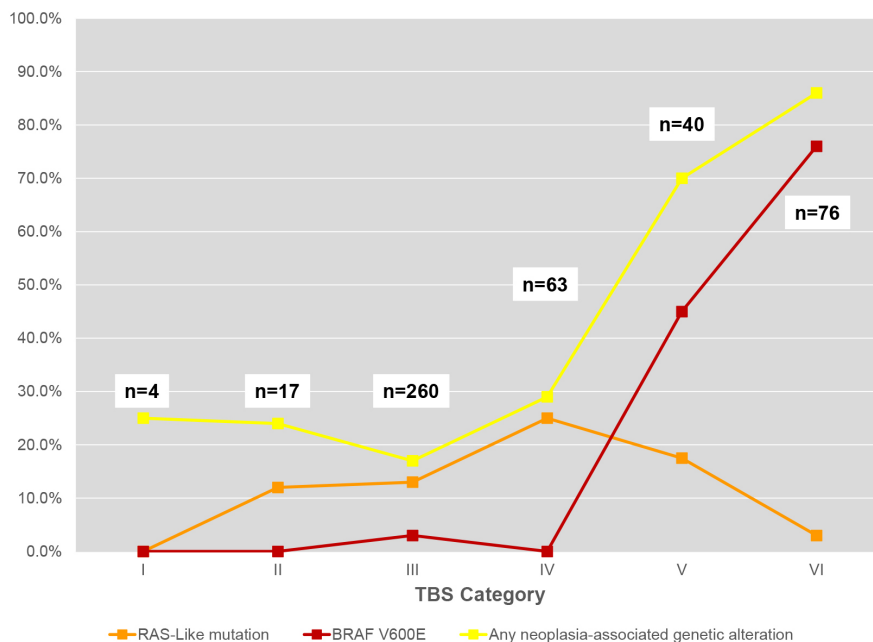
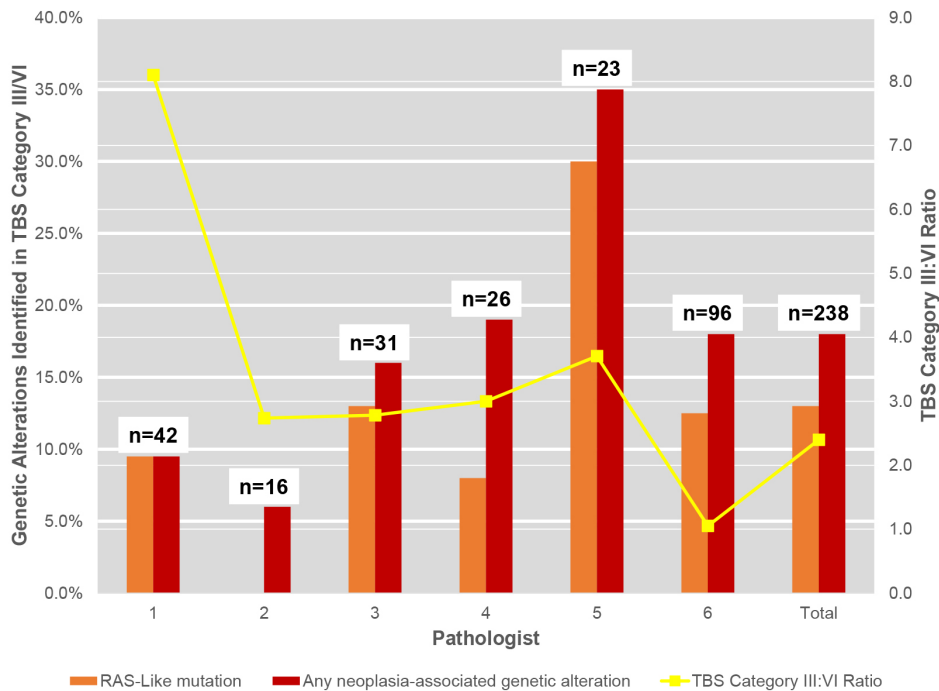


Figure 2 - 186



**Conclusions:** Calculation of both NGA rate among AUS cases and TBS category III:VI ratio enables individual CPs to calibrate diagnostic thyroid FNA thresholds as follows. CPs with elevated TBS category III:VI ratio (e.g. study pathologist #1) may reference NGA rates to determine if a rise or fall in diagnostic threshold is warranted. Inversely, anomalous NGA rates may indicate low or high diagnostic thresholds, even for CPs with typical TBS category III:VI ratio (e.g. study pathologists #5 and 2, respectively). The desirable NGA rate appears to be 5-20%, and it can be determined through targeted MT in a small number of genes.

**187 Anal Dysplasia Screening in High-Risk Patients: A Tertiary Care Center Experience**

Maria Gonzalez<sup>1</sup>, Ammar Karo<sup>1</sup>, Osama Elfituri<sup>1</sup>, Odile David<sup>1</sup>  
<sup>1</sup>University of Illinois at Chicago, Chicago, IL

**Disclosures:** Maria Gonzalez: None; Ammar Karo: None; Osama Elfituri: None; Odile David: None

**Background:** Although anal cancer accounts for only 0.5% of all carcinomas in the United States, the number of cases and deaths has increased each year for the past 10 years. However, the screening and surveillance guidelines are not well established. The current recommendations are to perform anal pap smears in high-risk patients with Human papillomavirus genotyping and to follow up any abnormal results with a clinical exam and high-resolution anoscopy within a year. Due to the ambiguity of these surveillance guidelines, the primary aim of this study was to determine the correlation between anal Pap smears, high-resolution anoscopies, and biopsy at our institution.

**Design:** A retrospective chart review was performed for all anal Pap smear results from 2014 to 2019. Data collected included demographics, risk factors, Human Immunodeficiency Virus status, time to follow up, anal Pap smears, Human papillomavirus status, and genotyping, and biopsy results. Clinical follow-up and concordance between cytology and histology were assessed.

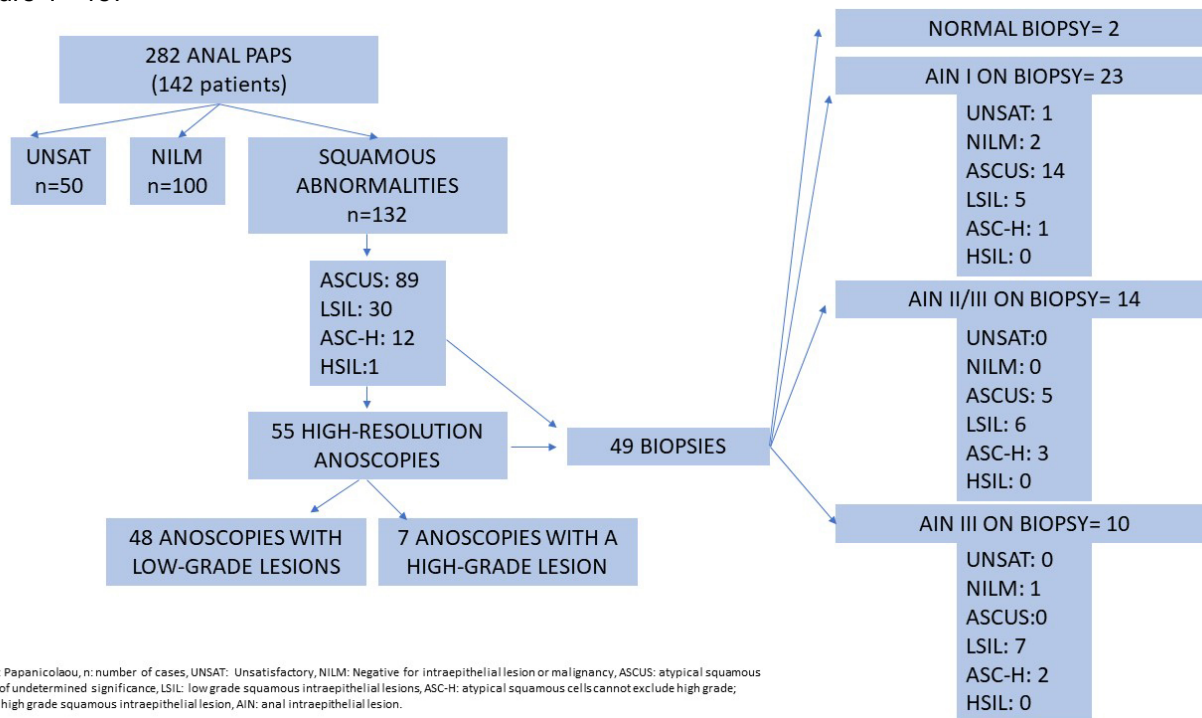
**Results:** A total of 282 anal pap smears were performed on 142 individual patients (median age 48 years, range 22-69 years). Of these, 46.8% showed squamous cell abnormalities (32.5% showed dysplasia), and 17.7% were unsatisfactory specimens. In our cohort of patients, 88% were male, 47.8% were African American, 27.4% had high-risk Human papillomavirus, 66.2% had Human Immunodeficiency Virus, and 2.8% had syphilis.



Of the 132 high-risk patients with abnormal cytology, 41.6% subsequently underwent high-resolution anoscopy. Only 37.1% had biopsies performed. Of the 23 cases diagnosed as high-grade dysplasia (anal intraepithelial lesion grade II/III) on biopsy, 4.3 % (n=1) had normal cytology, 56.5% (n=13) had low-grade squamous intraepithelial lesion, 21.7% (n=5) had atypical squamous cells cannot exclude high-grade, and 4.3% (n=1) had high-grade squamous intraepithelial lesion.

	HIGH-RESOLUTION ANOSCOPY	ANAL CYTOLOGY (PAP SMEARS)
<b>SENSITIVITY</b>	<b>13%</b>	<b>95%</b>
<b>SPECIFICITY</b>	<b>88%</b>	<b>0%</b>
<b>POSITIVE PREDICTIVE VALUE</b>	<b>85%</b>	<b>91%</b>
<b>NEGATIVE PREDICTIVE VALUE</b>	<b>16%</b>	<b>0%</b>
<b>ACCURACY</b>	<b>25%</b>	<b>87%</b>

Figure 1 - 187



PAPs: Papanicolaou, n: number of cases, UNSAT: Unsatisfactory, NILM: Negative for intraepithelial lesion or malignancy, ASCUS: atypical squamous cells of undetermined significance, LSIL: low grade squamous intraepithelial lesions, ASC-H: atypical squamous cells cannot exclude high grade, HSIL: high grade squamous intraepithelial lesion, AIN: anal intraepithelial lesion.

**Conclusions:** Cytology was superior to high-resolution anoscopy with respect to sensitivity, positive predictive value, and accuracy rates. These findings reinforce the value of cytology in screening algorithms of high-risk patients. At our institution, patients with abnormal anal Paps have a low-rate of follow-up with high-resolution anoscopy, emphasizing the need for adequate anal Pap testing and follow-up of high-risk patients. Efforts to improve education about adequate sampling and follow up will help ensure appropriate screening and secondary prevention.

**188 Association of High-Risk HPV Strains other than 16 And 18 with Abnormal Cervicovaginal Cytology Progression over 3-Year Period: Results from a Single Academic Institution**

Abhinav Grover<sup>1</sup>, Mariam Ratiani<sup>2</sup>, Sally Sniedze<sup>3</sup>, Bryan Hunt<sup>2</sup>, Tamar Giorgadze<sup>2</sup>  
<sup>1</sup>Medical College of Wisconsin Affiliated Hospitals, Milwaukee, WI, <sup>2</sup>Medical College of Wisconsin, Milwaukee, WI, <sup>3</sup>Wisconsin Diagnostic Laboratories, Wauwatosa, WI

**Disclosures:** Abhinav Grover: None; Mariam Ratiani: None; Sally Sniedze: None; Bryan Hunt: None; Tamar Giorgadze: None

**Background:** Worldwide, cervical cancer is the fourth most common cancer among women. Evidence linking human papillomavirus (HPV) to cervical cancer is extensive. HPV has over 200 strains, approximately 40 infect the genital area. Of these, 13-15 are high risk (HR) and are known to be carcinogenic. The most virulent HPV 16 and 18 have a bivalent vaccine available since 2006. More recently, in 2015, a nonavalent vaccine against HPV 6,11,16,18,31,33,45,52 and 58 was made available however it remains under-utilized. Our previous study has shown that HR-HPV strains other than 16 and 18 are seen much more frequently than HPV16 and HPV18 in our patient population, suggesting a shift in dominant HR-HPV strains. The aim of our current study was to perform a preliminary assessment of association of HR-HPV strains (other than 16 and 18) with risk of progression towards abnormal cervicovaginal cytology.

**Design:** We conducted a retrospective review of our healthcare database from 2015 through 2017 to identify 122 consecutive patients with negative for intraepithelial lesion or malignancy (NILM) Papanicolaou (PAP) test (ThinPrep) and positive HR-HPV strains (other than 16 and 18) co-test (Roche Cobas, HR-HPV types 31,33,35,39,42,43,45,51,53,54,55,57). In this cohort we assessed PAP test result progression from NILM to abnormal cervicovaginal cytology, including atypical squamous cells of undetermined significance (ASCUS), low grade squamous intraepithelial lesion (LSIL), atypical squamous cell high grade (ASC-H), high grade intraepithelial lesion (HSIL) or invasive cancer.

**Results:** A total of 122 female patients who were infected with HR-HPV strains (other than 16 and 18) were included. In a follow up period ranging from 6 months to 3 years, cervicovaginal cytology of 64 out of the 122 patients remained NILM with no progression, 18 progressed to ASCUS, 19 had LSIL, 7 had HSIL and 14 had abnormal glandular cytology on any subsequent PAP smear. The cumulative rate of progression from NILM to abnormal cervicovaginal cytology was 47.5% (Table 1).

**Table 1: Rate of association of high-risk HPV strains (other than 16 and 18) with cervicovaginal cytology progression (n=122)**

Progression within 3 years	Cervical cytology findings	Number of patients (%)	Overall number (%)
No progression documented	NILM	64 (52.5)	64(52.5)
Progression documented	ASC-US	18 (14.8)	58 (47.5)
	LSIL	19 (15.5)	
	HSIL	7 (5.7)	
	Abnormal glandular cytology	14 (11.5)	

NILM: Negative for intraepithelial lesion or malignancy; ASC-US: Atypical squamous cells of undetermined significance; LSIL: Low grade squamous intraepithelial lesion; HSIL: High grade intraepithelial lesion

**Conclusions:** Our preliminary findings indicate a high association of HR-HPV strains other than 16 and 18 and progression to abnormal cervicovaginal cytology. We will explore these associations in larger population datasets to confirm our findings and encourage better utilization of the more comprehensive nonavalent HPV vaccine.

**189 The Utility of High-Risk Human Papilloma Virus in Situ Hybridization (hrHPV ISH) in Cytology Cell Block Material from Cystic Head and Neck Lesions**

Lucy Han<sup>1</sup>, Tara Saunders<sup>1</sup>, Sarah Calkins<sup>1</sup>

<sup>1</sup>University of California, San Francisco, San Francisco, CA

**Disclosures:** Lucy Han: None; Tara Saunders: None; Sarah Calkins: None

**Background:** Human papilloma virus-related oropharyngeal squamous cell carcinoma (HPV-OSCC) presents frequently as metastasis in a neck lymph node which is often cystic/necrotic. Fine needle aspiration biopsies (FNA) are often first line diagnostic procedures for these lymph nodes. p16 immunohistochemistry (IHC) is utilized as a surrogate marker for hrHPV association but can be challenging to interpret in the context of cystic/necrotic tissue. Our study evaluated the utility of hrHPV ISH in cytology cell blocks of cystic head and neck lesions.

**Design:** Twenty four cystic head and neck FNA cases with cytology cell blocks and surgical pathology correlates were evaluated. p16 IHC and hrHPV ISH were assessed on all cell blocks (C-p16 and C-hrHPV ISH) and hrHPV ISH on all surgical samples (S-hrHPV ISH). All results were interpreted under blind review by 3 cytopathologists and classified as negative, positive or equivocal; discrepant cases and unusual staining patterns were re-reviewed to achieve consensus.

**Results:** Two cases were excluded due to insufficient tissue in the cell block on recut. Based on C-hrHPV ISH, 12 cases were positive, 5 cases were negative, and 5 cases were equivocal (Table 1). Of the 12 positive C-hrHPV ISH cases, all had concordant S-hrHPV ISH results with no false positives. Of the 5 negative C-hrHPV ISH cases, 4 cases had concordant S-hrHPV ISH results and 1 case had a discordant S-hrHPV ISH result. Of the 5 equivocal C-hrHPV ISH cases, S-hrHPV ISH were both positive and negative. Fourteen cases were equivocal by C-p16; among these cases, 9 cases were reliably classified by C-hrHPV ISH (5 positive, 4 negative; 64%).

Table 1: hrHPV ISH and p16 IHC interpretations on cell blocks and surgical correlates.

Case	Cell block hrHPV (C-hrHPV)	Surgical hrHPV (S-hrHPV)	Cell block p16 (C-p16)
1	Positive	Positive	Positive
2	Positive	Positive	Positive
3	Positive	Positive	Positive
4	Positive	Positive	Positive
5	Positive	Positive	Positive
6	Positive	Positive	Positive
7	Positive	Positive	Positive
8	Positive	Positive	Equivocal
9	Positive	Positive	Equivocal
10	Positive	Positive	Equivocal
11	Positive	Positive	Equivocal
12	Positive	Positive	Equivocal
13	Negative	Positive	Equivocal
14	Negative	Negative	Equivocal
15	Negative	Negative	Equivocal
16	Negative	Negative	Equivocal
17	Negative	Negative	Equivocal
18	Equivocal	Positive	Equivocal
19	Equivocal	Positive	Equivocal
20	Equivocal	Positive	Equivocal
21	Equivocal	Negative	Equivocal
22	Equivocal	Negative	Negative

**Conclusions:** hrHPV ISH testing in cell blocks can be reliably utilized to evaluate for HPV status, especially when the results are positive. A definitive negative interpretation of C-hrHPV ISH should be used with caution, especially in cases without intact fragments of tumor cells, and an equivocal category may be most appropriate when a definitive result cannot be rendered. Compared to p16, hrHPV ISH is more frequently diagnostic in cytology cell blocks and could be a helpful tool in HPV-OSCC diagnosis and management.

**190 Implementation of the Milan System for Reporting Salivary Gland Cytopathology (MSRSGC): An Interobserver Reproducibility Study from a Large Academic Medical Center**

Issa Hindi<sup>1</sup>, Aylin Simsir<sup>2</sup>, Tamar Brandler<sup>1</sup>, Wei Sun<sup>3</sup>, Oliver Szeto<sup>1</sup>, Fang Zhou<sup>2</sup>, Osvaldo Hernandez<sup>1</sup>  
<sup>1</sup>NYU Langone Health, New York, NY, <sup>2</sup>NYU School of Medicine, New York, NY, <sup>3</sup>New York University Langone Medical Center, New York, NY

**Disclosures:** Issa Hindi: None; Aylin Simsir: None; Tamar Brandler: None; Wei Sun: None; Oliver Szeto: None; Fang Zhou: None; Osvaldo Hernandez: None

**Background:** Fine needle aspiration (FNA) of salivary gland lesions is a fast, minimally invasive and cost-effective procedure that aids in early patient management decisions. Recently, the Milan System for reporting Salivary Gland cytopathology (MSRSGC) was published in order to establish diagnostic categories with implied malignancy risks and recommended clinical follow-up. Our study aims to assess the interobserver reproducibility of salivary gland cytology diagnoses using the MSRSGC.

**Design:** Salivary gland cytology slides from 101 cases with surgical pathology follow-up from 11/2016-06/2019 were blindly and independently reviewed and classified according to the MSRSGC by four cytopathologists. Unweighted and linearly weighted percent agreement and Gwet's AC1 coefficients were calculated in AgreeStat 2015.6/Windows (AgreeStat Analytics).

**Results:** Unweighted percent agreement was 0.69 (substantial agreement) and weighted percent agreement was 0.92 (almost perfect agreement). Unweighted Gwet's AC<sub>1</sub> was 0.64 (substantial agreement), and weighted Gwet's AC<sub>1</sub> was 0.84 (almost perfect agreement) (Table 1).

50 of 101 (49%) cases had complete agreement among all 4 observers, 77 (76%) had at least 3 observers agreeing on the same diagnosis, and 99 (98%) had at least 2 observers agreeing on the same diagnosis. Category IVA (benign neoplasm) was the most likely to show interobserver agreement: among the 51 cases in which at least 2 cytopathologists agreed on a diagnosis of category IVA, 34 (67%) showed complete agreement among all 4 cytopathologists.

Two cases showed no agreement among any observers. One low-grade mucoepidermoid carcinoma had MSRSGC diagnoses ranging from I to IVB, and one secretory carcinoma had MSRSGC diagnoses ranging from III to VI. Low-grade mucoepidermoid carcinoma is reportedly the most common malignant salivary gland tumor associated with false-negative diagnoses on cytology and is often misdiagnosed as a pleomorphic adenoma, due to the presence of bland-appearing intermediate cells as well as confusion between mucin and chondromyxoid stroma (Figure 1). The case of secretory carcinoma showed scant cellularity on cytology, confounding an accurate diagnosis (Figure 2).

**Table 1: Results of interobserver agreement analyses**

Agreement Coefficient	Coefficient	95% Confidence Interval (CI)	Agreement Interpretation*
Unweighted Gwet's AC <sub>1</sub>	0.64	0.57-0.72	Substantial
Unweighted percent agreement	0.69	0.62-0.75	Substantial
Weighted Gwet's AC <sub>1</sub>	0.84	0.78-0.89	Almost perfect
Weighted percent agreement	0.92	0.90-0.94	Almost perfect

\*Interpretation criteria: <0.00: poor; 0.00–0.20: slight; 0.21–0.40: fair; 0.41–0.60: moderate; 0.61–0.80: substantial, and 0.81–1.00: almost perfect.



Figure 1 - 190

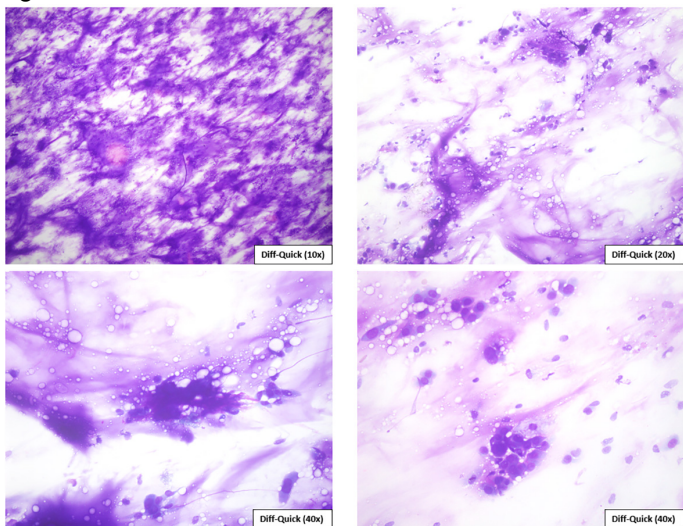
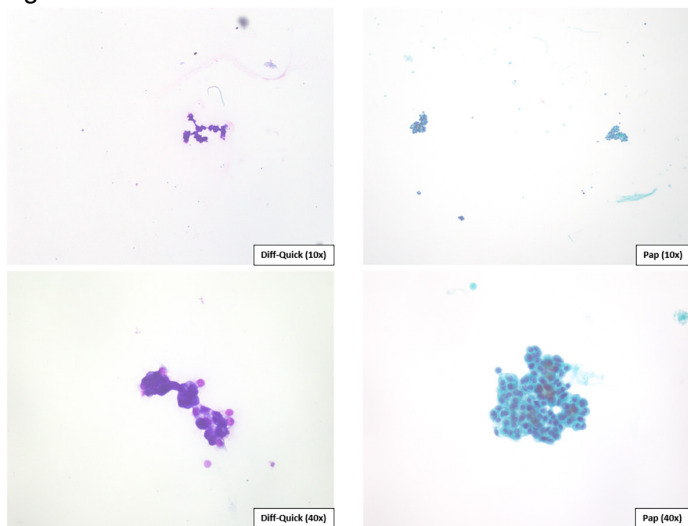


Figure 2 - 190



**Conclusions:** Interobserver reliability analyses using the MSRSGC showed substantial to almost perfect agreement among the four observers in our study. Only two cases showed no agreement. Category IVA (benign neoplasm) is the most likely to show complete agreement among all observers.

## 191 Cytologic Features of Gynecologic Tract Germ Cell Tumors and Carcinomas Exhibiting Germ Cell Differentiation

Anjelica Hodgson<sup>1</sup>, Veronica Kim<sup>1</sup>, Rajmohan Murali<sup>1</sup>

<sup>1</sup>Memorial Sloan Kettering Cancer Center, New York, NY

**Disclosures:** Anjelica Hodgson: None; Veronica Kim: None; Rajmohan Murali: None

**Background:** Ovarian germ cell tumors are among the most heterogenous group of neoplasms occurring in the gynecological tract. In addition to tumors arising from germ cells, somatic neoplasms, particularly carcinomas, may also exhibit germ cell tumor differentiation. The morphologic features of these neoplasms in cytologic preparations are not well described. We sought to describe the cytologic features of gynecologic tumors exhibiting germ cell differentiation.

**Design:** A search of our institutional database was done in order to identify histologically-confirmed ovarian germ cell tumors and gynecologic carcinomas with germ cell tumor differentiation. Available cytologic material was reviewed by a cytotechnologist, a gynecologic pathology fellow and a cytopathologist/gynecologic pathologist with respect to the features depicted in the Table.

**Results:** A total of 15 cytologic specimens from 12 women (aged 19 to 82 years) were identified and included touch preparations of core biopsies from various sites (n=6), fine needle aspiration (n=2), pelvic washing (n=1), ascitic fluid (n=4), pelvic cyst fluid (n=1), and endometrial aspirate (n=1). Of the 12 patients, 7 had primary gynecologic germ cell tumors while 4 had gynecologic (ovarian and endometrial) tumors exhibiting somatic yolk sac tumor differentiation; the remaining patient had an intestinal-type adenocarcinoma arising within an ovarian teratoma. Specimen cellularity was variable. Most cases showed at least small clusters/groups of cells with a minority showing only single cells. Cytoplasmic volume was moderate to minimal in all cases. Nuclear outlines and chromatin patterns were also variable and, at times, differed among specimens from the same case. Mitotic activity and necrosis was not evident in any case.

Patient (age at diagnosis)	Histologic diagnosis	Primary tumor site	Cytologic specimen and location	Cellularity	Cellular arrangement	Nuclear pleomorphism	Nuclear outlines	Chromatin pattern / Conspicuous nucleoli	Cytoplasm
Germ cell tumors									
1 (19 years)	Yolk sac tumor	Vulva	Touch prep, needle rinse; Inguinal lymph node	Moderate	Cohesive clusters	Marked	Irregular	Dispersed / +	Moderate; fine vacuoles
2 (30 years)	Mixed germ cell tumor (dysgerminoma and yolk sac tumor)	Ovary	Touch prep, needle rinse, Peritoneum	Moderate-high; 'tigroid' background	3-dimensional groups	Marked	Irregular	Coarsely granular / +	Scant-moderate; focal fine vacuolation
2 (30 years)	Mixed germ cell tumor (dysgerminoma and yolk sac tumor)	Ovary	Touch prep, needle rinse; Liver mass	Low	3-dimensional groups	Moderate	Oval	Coarsely granular / -	Scant-moderate; very focal fine vacuolation
3 (27 years)	Immature teratoma	Ovary	Fine needle aspiration; Abdominal wall mass	Low	Large groups with overlapping	Mild	Oval	Variable / -	Abundant; dense, squamoid
4 (55 years))	Yolk sac tumor	Ovary	Washing; Pelvis	Low	Small clusters	Moderate	Round to oval	Dispersed / +	Scant-moderate; granular
5 (23 years)	Yolk sac tumor	Ovary	Touch prep, needle rinse; Peritoneum	Moderate	3-dimensional groups	Marked	Irregular	Coarsely granular / -	Moderate; focal fine vacuolation
5 (23 years)	Yolk sac tumor	Ovary	Effusion; Peritoneal cavity	Low	Small clusters	Moderate	Round to oval	Dispersed / +	Moderate; granular
6 (27 years)	Immature teratoma	Ovary	Effusion; Peritoneal cavity	Moderate	Single cells	Mild	Round	Coarsely granular / -	Moderate-abundant; dense/squamoid or foamy
7 (22 years)	Mixed germ cell tumor (mature teratoma and yolk sac tumor)	Ovary	Effusion; Peritoneal cavity	Low	Single cells and small clusters	Moderate	Round to oval	Vesicular / +	Scant-moderate; granular
Carcinomas with germ cell tumor differentiation									
8 (44 years)	Endometrioid borderline tumor with undifferentiated	Ovary	Effusion; Peritoneal cavity	Moderate-high	3-dimenisonal groups (rounded, ball-like)	Marked	Irregular	Variable / +	Scant

	carcinoma and yolk sac tumor component								
9 (65 years)	High grade serous carcinoma with yolk sac tumor differentiation	Ovary	Cyst fluid; Pelvis	Low	Single cells and small clusters	Moderate	Oval	Coarsely granular / +	Scant
10 (82 years)	High grade endometrial carcinoma with yolk sac tumor differentiation	Endometrium	Aspirate; Endometrium	Low	Small groups with overlapping	Marked	Round to oval	Coarsely granular / +	Moderate; granular
11 (58 years)	Endometrial carcinoma with yolk sac tumor differentiation	Endometrium	Touch prep, needle rinse; Lung mass	Moderate	Cohesive clusters	Marked	Oval	Coarsely granular / -	Moderate; granular or finely vacuolated
11 (58 years)	Endometrial carcinoma with yolk sac tumor differentiation	Endometrium	Touch prep, needle rinse; external iliac lymph node	Moderate	Cohesive clusters	Marked	Oval	Coarsely granular / -	Moderate; fine vacuolation
Somatic carcinoma in a teratoma									
12 (53 years)	Intestinal type adenocarcinoma arising in mature teratoma	Ovary	Fine needle aspiration; Abdominal wall mass	High; mucin in background	3-dimensional groups	Moderate	Irregular	Coarsely granular / -	Scant-moderate; mucinous in some cells

**Conclusions:** Germ cell tumors and somatic neoplasms exhibiting germ cell tumor differentiation share a number of cytologic features and may be difficult to distinguish from one another without knowledge of a prior history. In addition, recognition of a germ cell derivation or component may be difficult without the use of immunocytochemistry. As would be expected, primary germ cell tumors tend to occur in younger patients compared to carcinomas exhibiting somatic germ cell tumor differentiation.

**192 Anaplasia and Multinucleation in Metastases of Oropharyngeal Squamous Cell Carcinoma is Associated with Poorer Outcomes**

Lucy Jager<sup>1</sup>, Daniel Johnson<sup>2</sup>, Brian Finkelman<sup>2</sup>, Borislav Alexiev<sup>3</sup>

<sup>1</sup>Feinberg School of Medicine/Northwestern University, Chicago, IL, <sup>2</sup>Northwestern University Feinberg School of Medicine, Chicago, IL, <sup>3</sup>Northwestern Memorial Hospital, Chicago, IL

**Disclosures:** Lucy Jager: None; Daniel Johnson: None; Brian Finkelman: None; Borislav Alexiev: None

**Background:** The presence of tumor cell anaplasia or multinucleation (A/M) in oropharyngeal squamous cell carcinoma (OPSCC) has recently been found to be associated with increased disease recurrence and poorer disease-specific survival, regardless of HPV status. Thus it has been suggested that A/M could serve as a critical marker of higher risk and poorer prognosis. We aim to see if A/M is reliably detectable in cytology specimens of metastatic OPSCC and how it relates to disease-specific mortality.

**Design:** Our pathology files were searched from 2013 to 2020 for surgical specimens diagnosed as OPSCC with associated cytology specimens of metastatic sites. Surgical cases were reviewed for A/M in the primary tumor. The entire associated cytology specimen (smears, touch preps, cell block, core biopsy slides) was reviewed for the same criteria without knowledge of the histology. A/M was defined as any 400x magnification field (area = 0.2 mm<sup>2</sup>) with ≥ 3 tumor cells with nuclei with diameter equal to or wider than 5 lymphocyte nuclei (approximately 25µm) or having multiple nuclei.

**Results:** 174 unique patients with both surgical and cytology specimens were found in our records, of which 87 had cytology specimens available for review. Review of the corresponding cytology cases from metastatic sites, showed 22 (25%) with some degree of A/M [Table, Figures 1 and 2]. Of these, 11 had A/M on histology and 11 did not have A/M on histology. Five of the 22 patients (22.7%) with A/M on cytology died of disease while 4 of 62 patients without A/M on cytology or histology died of disease (6.5%). This finding was statistically significant ( $p=0.034$  by Chi-square test). Three patients had A/M on histology but not on cytology; 0 of the 3 died. Comparing the disease-specific mortality of patients with A/M to those without on cytology showed an even greater significance ( $p=0.027$ ).

	n	Age, Mean (Years)	Recurrence (n)	Distant Metastases (n)	Mortality (n)	Disease Specific Mortality (n, %)	Follow Up Time, Mean (Days)
Cytologic A/M + Surgical A/M +	11	51	3	1	2	2 (18%)	782
Cytologic A/M + Surgical A/M -	11	61	3	1	3	3 (27%)	1030
Cytologic A/M - Surgical A/M +	3	64	1	1	0	0 (0%)	1747
Cytologic A/M - Surgical A/M -	62	62	12	3	6	4 (6%)	968

Figure 1 - 192

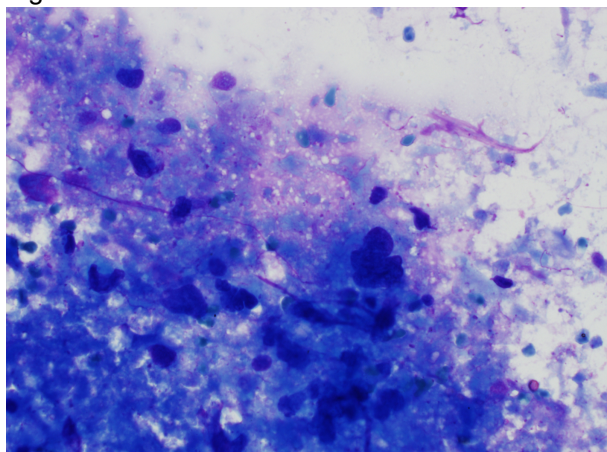
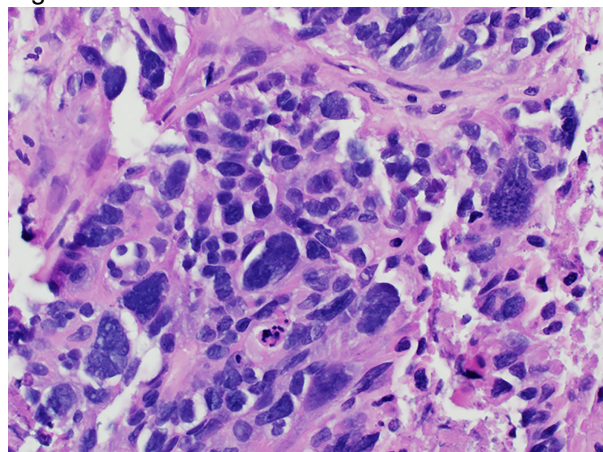


Figure 2 - 192



**Conclusions:** In OPSCC A/M can be identified in corresponding cytology cases of metastatic sites, regardless of primary tumor histology. Our study identified A/M on cytology in 11 of 14 (79%) cases with A/M on histology and in 11 of 73 (15.1%) cases without A/M on histology. In addition, patients with A/M on cytologic specimens of metastatic sites had increased disease-specific mortality. These findings suggest that metastases can acquire A/M, and the presence of A/M in metastases is a marker of aggressive behavior. Identification of A/M on cytology specimens may be important to indicate a more aggressive course and help guide patient management.



**193 Anal ASCUS in HIV-Positive Patients: An Interpretation with Frequent HSIL on Biopsy**

Taylor Jenkins<sup>1</sup>, Edward Stelow<sup>1</sup>

<sup>1</sup>University of Virginia Health System, Charlottesville, VA

**Disclosures:** Taylor Jenkins: None; Edward Stelow: None

**Background:** HPV-related anal neoplasia is a significant cause of morbidity in patients with HIV infection. Anal cytology (Pap) and HPV testing have increased detection rates of anal squamous intraepithelial lesions (SIL). Despite screening these at-risk populations, anal squamous cell carcinoma is increasing. Cytologic interpretation of anal SIL has more interobserver variability as compared to SIL in gynecologic locations, leading to higher rates of anal ASCUS. We herein evaluate the percentage of anal ASCUS with subsequent high-grade SIL (HSIL) on biopsy.

**Design:** A three-year retrospective database search was performed for anal Pap ASCUS cases. For comparison, a one-year retrospective search for gynecologic Pap ASCUS cases was performed. HIV status, HPV results, and follow-up biopsy diagnoses were recorded.

**Results:** 56 of 60 anal ASCUS Paps with available follow-up had HPV testing performed at the time of Pap. 49 of the 56 (88%) had positive high-risk HPV results. 31 of the 49 (63%) HPV-positive cases had HSIL diagnoses on biopsy. HPV 16 was detected in 68% and HPV 18 in 19% of the HPV-positive cases. Two of the seven (29%) HPV-negative cases had HSIL on biopsy. Three of four cases (75%) that did not have HPV testing done at the time of Pap had HSIL on biopsy. 97% of these patients have HIV diagnoses and 58% are male.

110 of 242 gynecologic ASCUS Paps had follow up biopsy results, 18 (16%) of which had HSIL diagnoses. Of these, 16 (89%) were positive for high-risk HPV at the time of Pap. HPV 16 was detected in 25% and HPV 18 in 6% of the HPV-positive cases. <1% of these patients have HIV diagnoses.

**Conclusions:** The detection of HSIL on biopsy following an ASCUS diagnosis is significantly higher in anal cytology ( $p = <.0001$ ). The vast majority of these patients are HIV positive and have high-risk HPV detected at the time of Pap, with a propensity for HPV 16 positivity ( $p=.007$ ). Additionally, in our population the majority of the patients are male. The discrepancy between ASCUS Paps and subsequent HSIL diagnoses may be attributed to altered cytology due to patient sex and the location in the anal canal. Decreased estrogen exposure and increased keratinization may produce a different morphology than squamous epithelium from gynecologic mucosal sites, causing difficulty in interpretation. Correlation with HPV results and anoscopy examination should be strongly considered in anal ASCUS cases.

**194 PD-L1 Immunohistochemistry in Cytological Specimens of Head and Neck Squamous Cell Carcinoma: An Imprecise Approach for Selecting Patients Likely to Benefit from Checkpoint Inhibitor Therapy**

Avi Kandel<sup>1</sup>, William Westra<sup>1</sup>, Marshall Posner<sup>1</sup>, Qiusheng Si<sup>1</sup>

<sup>1</sup>Icahn School of Medicine at Mount Sinai, New York, NY

**Disclosures:** Avi Kandel: None; William Westra: None; Marshall Posner: None; Qiusheng Si: None

**Background:** Programmed death ligand-1 (PD-L1) is a regulatory molecule expressed in T cells which dampens the immune response when bound to one of its complementary ligands (e.g. PD-1). Some carcinomas evade the immune response by expressing PD-L1 on their cell surfaces. To date, PD-L1 immunohistochemistry (IHC) is the best way to identify those patients with head and neck squamous cell carcinomas (HNSCC) most likely to benefit from monoclonal antibody therapies targeting the PD-1/PD-L1 pathway, but interpretation can be confounded by heterogeneous PD-L1 expression. The purpose of this study was to determine if a tumor's PD-L1 status could be influenced by limited tumor sampling as afforded by fine needle aspiration (FNA).

**Design:** The pathology files between 2017 and 2020 were reviewed to identify patients with available FNA cell blocks (FNACB) and matching resections of HNSCCs. IHC staining was performed using the DAKO 22C3 antibody probe. PD-L1 combined proportion scores (CPS) were recorded independently by two pathologists using a two-tiered scoring system (<1 = negative, ≥1 = positive). PD-L1 status for the paired specimens was compared.

**Results:** 31 patients with matching samples were identified. There was only a 41.9% correlation for PD-L1 status when comparing the paired samples. 28 (90.3%) of the resections were PD-L1 positive, but only 12 (38.7%) of the FNACBs were positive. A HNSCC was much more likely to be scored as positive if IHC was performed on the resection compared to the matched FNACB ( $p < 0.05$ , Fischer exact). Of 19 FNACBs that were PD-L1 negative, 17 (89.5%) were positive in the paired resections. Cellularity of the FNACBs and HPV status had no impact on PD-L1 correlation. Using the resections as the standard for PD-L1 status, use of FNACBs as a testing substrate has a sensitivity of 39.3% and a specificity of 66.7%.

**Conclusions:** Interpretation of PD-L1 IHC is challenging but critical. A false positive reading runs the risk of subjecting a patient with HNSCC to ineffective therapy that is costly and associated with side effects; and a false negative reading may deny a patient access to potentially life-saving therapy. Our study suggests that FNAs of HNSCC is not be a reliable substrate for PD-L1 determination.

**195 Cytologic Features of Gestational Trophoblastic Neoplasms and Somatic Neoplasms Exhibiting Trophoblastic Differentiation**

Veronica Kim<sup>1</sup>, Anjelica Hodgson<sup>1</sup>, Rajmohan Murali<sup>1</sup>  
<sup>1</sup>Memorial Sloan Kettering Cancer Center, New York, NY

**Disclosures:** Veronica Kim: None; Anjelica Hodgson: None; Rajmohan Murali: None

**Background:** Trophoblastic neoplasms of the gynecologic tract may arise in association with a gestation (and are thus chimeric) or may be non-gestational. Somatic neoplasms (particularly carcinomas) arising in various anatomic sites may also exhibit trophoblastic differentiation. Both groups of tumors are rare. In this study, we sought to describe the cytologic features of these neoplasms, which have not been well described to date.

**Design:** Cytologic specimens from patients with histologically confirmed gynecological trophoblastic neoplasms or other neoplasms exhibiting trophoblastic differentiation were retrieved from our departmental archives. All available cytologic material was reviewed by a cytotechnologist, a gynecologic pathology fellow, and a cytopathologist/gynecologic pathologist and consensus was achieved for the features depicted in the Table.

**Results:** From 7 women aged 32-74 years, we evaluated 8 cytologic specimens: touch preparations of core biopsies from various sites (n=4); fine needle aspiration (n=1); pelvic washing (n=1); ascitic fluid (n=1); and pleural fluid (n=1). Three specimens were of gestational origin, 4 (from 3 women) were somatic neoplasms exhibiting trophoblastic differentiation, while the origin (uterine vs. lung) and nature of the remaining case was not clear. The cytologic features are detailed in the Table. Cellularity was variable. Tumor cells most commonly formed 3-dimensional groups or were singly dispersed, and cytoplasmic volume was at most moderate. Nuclear outlines were typically irregular, although some rounding was seen specifically in tumors with chorionic-type differentiation. Nuclear contours were usually irregular although one tumor (seen in 2 specimens) exhibited mostly smooth contours. Coarsely granular chromatin was ubiquitous and evident mitotic activity was not a feature in any case. Five cases exhibited marked nuclear pleomorphism, and rare multinucleated or giant cells were seen in 4 cases.

Patient (age at diagnosis)	Histological diagnosis	Primary tumor site	Cytologic specimen and location	Cellular arrangement	Cytoplasmic volume	Nuclear outlines	Nuclear size variation	Nuclear contours	Multinucleated/giant cells
<b>Gestational trophoblastic tumors</b>									
1 (53 years)	Malignant neoplasm with extensive trophoblastic differentiation, difficult to classify	Uterus	Touch prep and needle rinse; Liver mass	Cohesive flat groups	Moderate to scant	Irregular	High	Irregular	Yes, rare
2 (33 years)	Choriocarcinoma	Uterus	Touch prep and needle rinse; Lung mass	3-dimensional groups	Moderate to scant	Irregular	High	Irregular	Yes, rare

3 (34 years)	Atypical trophoblastic proliferation, suspicious for epithelioid trophoblastic tumor	Uterus	Washing; Pelvis	Single cells	Moderate	Round to irregular	Unable to assess	Irregular	No
<b>Somatic tumors with trophoblastic differentiation</b>									
4 (60 years)	High grade serous carcinoma with chorionic-type intermediate trophoblastic differentiation	Ovary	Thin Prep; Peritoneal effusion	3-dimensional groups	Moderate	Round to oval	Moderate	Mostly smooth	Yes, rare
4 (60 years)	High grade serous carcinoma with chorionic-type intermediate trophoblastic differentiation	Ovary	Thin Prep; Pleural effusion	3-dimensional groups, single cells	Moderate	Round to oval	Moderate	Mostly smooth	No
5 (64 years)	Poorly differentiated carcinoma with syncytiotrophoblastic differentiation	Lung	Fine needle aspiration; Lung mass	Single cells	Moderate-scant	Irregular	High	Highly irregular	No
6 (32 years)	Poorly differentiated carcinoma with trophoblastic differentiation	Bile duct	Touch prep; Lung mass	3-dimensional groups	Scant	Irregular	High	Irregular	Yes, rare
<b>Unclear if gestational or somatic origin</b>									
7 (74 years)	Malignant epithelioid neoplasm with trophoblastic differentiation	Lung vs. uterus	Touch prep and needle rinse; Pleural mass	3-dimensional groups	Scant	Irregular	High	Irregular	No

**Conclusions:** Trophoblastic neoplasms of gestational origin and somatic neoplasms exhibiting trophoblastic differentiation share a number of cytologic features. Especially in the context of a suggestive history of antecedent gestation or gestational trophoblastic disease (or elevated serum markers eg HCG), trophoblastic differentiation should be considered in a cytologic specimen exhibiting marked nuclear pleomorphism, including multinucleate or giant cells, and should be evaluated using immunocytochemistry.

**196 Pathologist-Performed Ultrasound-Guided Fine Needle Aspirations: Beyond the Thyroid**

Evelyna Kliassov<sup>1</sup>, David McKenzie<sup>2</sup>, Raj Dash<sup>3</sup>, Wen-Chi Foo<sup>3</sup>, Xiaoyin “Sara” Jiang<sup>1</sup>, Claudia Jones<sup>3</sup>  
<sup>1</sup>Duke University, Durham, NC, <sup>2</sup>Duke University Health System, Durham, NC, <sup>3</sup>Duke University Medical Center, Durham, NC

**Disclosures:** Evelyna Kliassov: None; David McKenzie: None; Raj Dash: None; Wen-Chi Foo: None; Xiaoyin “Sara” Jiang: None

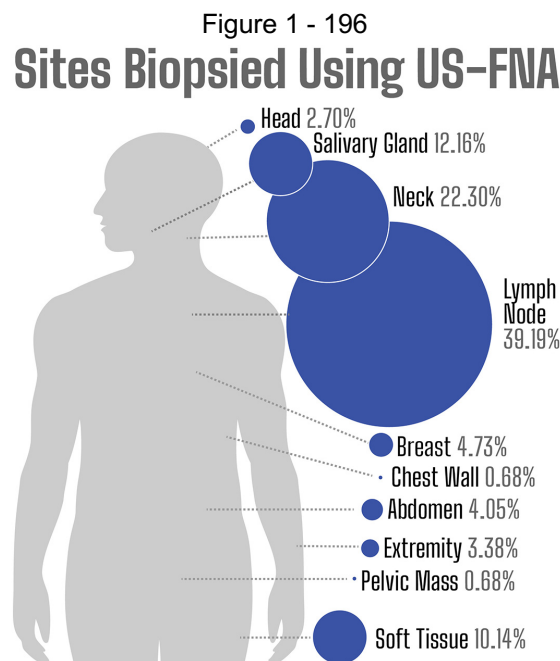
**Background:** Due to ease of use and accessibility, ultrasound-guidance has increasingly been used by cytopathologists when performing fine needle aspiration (FNA) biopsies. While thyroid nodules make up the bulk of lesions sampled using ultrasound-guided FNA (USFNA) in pathology-based clinics, USFNA has utility in non-thyroid sites as well. Characterization of major nodule locations, as well as diagnostic performance, is crucial to understanding the role of pathologist-performed USFNA in patient care.

**Design:** We performed a retrospective study of pathologist performed USFNA cases in non-thyroid sites over a 10-year period, and identified site, patient characteristics, and diagnostic categories.

**Results:** Over the study period, 148 USFNAs of non-thyroid sites were performed by pathologists. The majority of biopsies were performed on lymph nodes (n= 58, 39%) and neck, NOS (n=33, 22%). Salivary gland (n=18, 12%) and soft tissue (n=15, 10%) represented other common sites where ultrasound guidance was used. (Figure 1: Distribution of sites of USFNA biopsies) The majority of cases were definitively benign (n=54, 36%) or malignant (n=39, 26%). There were 13 cases (9%) that were nondiagnostic; these consisted of blood, scanty cellular samples, or cystic fluid only.

Table 1. Distribution of diagnostic categories (N=148)

Diagnostic Category	Cases (N)	Cases (%)
Negative. No evidence of malignancy.	54	36.49%
Benign Neoplasm	7	4.73%
Descriptive Diagnosis	14	9.46%
Atypical/Inconclusive	14	9.46%
Suspicious for malignancy	7	4.73 %
Diagnostic of Malignancy	39	26.35%
Non – diagnostic	13	8.78%



**Conclusions:** Over the study period at our institution, the majority of non-thyroid nodules that underwent ultrasound guided fine needle aspiration biopsy were located in the lymph nodes and neck, with a variety of other sites sampled, including salivary gland, abdominal, and soft tissue sites. Interestingly, while salivary tumors are a common site for our clinic overall, they made up a smaller proportion of the USFNA cases, likely due to ease of palpation for most salivary lesions. Most diagnoses were definitively either benign or malignant. In our practice, the choice of use of whether to use ultrasound is at the discretion of the attending pathologist; often, USFNA is chosen for non-palpable, deep-seated nodules, small lesions and lesions in close proximity to vascular structures. This context explains the non-diagnostic rate of 9%, which is higher than for palpable lesions. Overall, the technique of USFNA in sites other than thyroid has allowed better visualization of nodule characteristics, allowed for sampling of non-palpable superficial lesions, and avoiding important adjacent structures, with good diagnostic yield.

**197 Lymphoid Cell Rich Fine Needle Aspirations of the Salivary Gland: What is the Risk of Malignancy?**

Vimal Krishnan<sup>1</sup>, Shikha Bose<sup>2</sup>, Rania Bakkar<sup>1</sup>

<sup>1</sup>Cedars-Sinai Medical Center, Los Angeles, CA, <sup>2</sup>Cedars-Sinai Medical Center, West Hollywood, CA



**Disclosures:** Vimal Krishnan: None; Shikha Bose: None

**Background:** Lymphoid cell rich fine needle aspirations (FNAs) of the salivary glands pose a diagnostic dilemma, with a wide range of differential diagnoses that include several benign and malignant entities. There is limited literature regarding the entities that are commonly encountered in this situation. Our goal was to characterize the surgical outcome in these cases and to evaluate the risk of malignancy.

**Design:** This is a retrospective study at a tertiary care institution. Our database was queried over a 10-year period. FNAs yielding a prominent population of well-visualized lymphoid cells were included. Only cases with surgical follow-up were evaluated. FNAs with epithelial cells, diagnostic features of any entity (such as granulomas or chondromyxoid stroma), history of metastatic malignancy, or scant cellularity were excluded. Lymphoid cells were classified as atypical if monomorphic, with hyperchromatic nuclei and/or irregular nuclear contours. Statistical analysis was performed.

**Results:** Of the 105 cases that met the inclusion criteria, 29 (28%) had surgical follow-up. 22 were from the parotid and 7 from the submandibular gland. 34% of cases were non-neoplastic (benign lymphoepithelial cyst (n=4), reactive lymph node (n=5) and chronic sialadenitis (n=1)). A benign epithelial neoplasm (pleomorphic adenoma (n=2) and Warthin’s tumor (n=1)) was identified in 10% of the cases. One case with non-atypical lymphocytes proved to be a mucoepidermoid carcinoma (n=1). Lymphomas were detected in 52% (n=15). 8/15 were low-grade and 7/15 were high-grade lymphoma (Figure 1). Most of these cases (11/15) had atypical lymphocytes on FNA (Figure 2). Flow cytometry or clonality PCR was only performed in 4/15, and was suspicious for lymphoma in 3/4. Overall, the risk of malignancy, epithelial and lymphoid, was 55% (16/29). Morphology on FNA had a sensitivity of 69% and a specificity of 92% for malignancy. The positive predictive value on FNA of atypical lymphocytes for malignancy was 92%. In cases with non-atypical lymphocytes, five cases were malignant on surgical excision (5/17).

Figure 1 - 197

**Figure 1:** Cases with lymphoproliferative disease (n=15) on follow-up. Most high-grade lymphomas were DLBCL (n=6), with one case of grade 3 follicular lymphoma. Among low-grade lymphomas, follicular lymphoma grade 1 or 2 (n=4), marginal zone lymphoma (n=2) and mantle zone lymphoma (n=1) were found. One case was indeterminate and classified as atypical lymphoid proliferation, favor low-grade lymphoma.

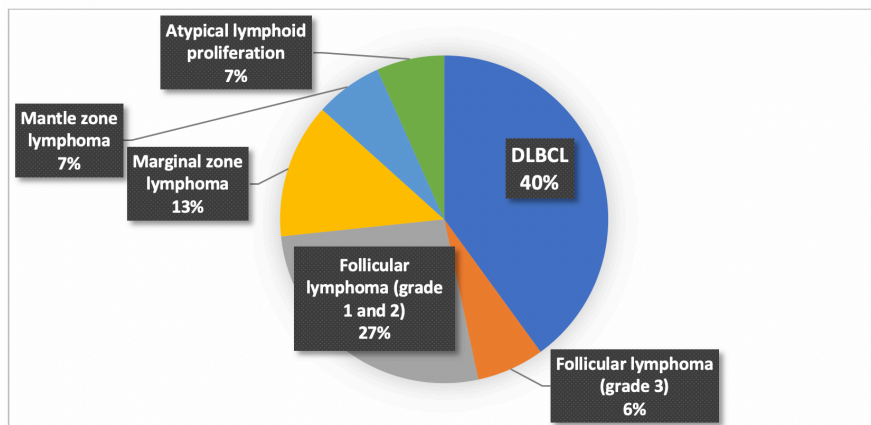
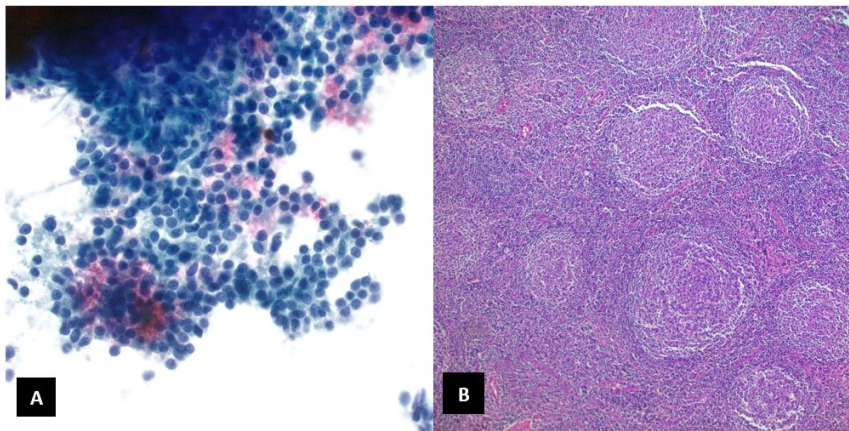


Figure 2 - 197

**Figure 2:** Example of a case with atypical lymphocytes on FNA (panel A), with follicular lymphoma on follow-up (panel B).



**Conclusions:** Lymphoid cell rich FNAs carry a 55% overall risk of malignancy, of which lymphomas comprise the major component. Specificity of FNA for malignancy is high (92%) and lymphocyte atypia is a strong predictor of malignancy. Ancillary studies may be of added value in FNAs with non-atypical lymphoid cells. FNA has a valuable role in triaging lymphoid lesions of the salivary glands.

**198 NOR-1 (NR4A3) Immunostaining Can Be Reliably Performed on Cytologic Preparations for the Preoperative Diagnosis of Acinic Cell Carcinoma of the Salivary Gland**

Vimal Krishnan<sup>1</sup>, Luan Nguyen<sup>1</sup>, Mariza De Peralta-Venturina<sup>1</sup>, Xuemo Fan<sup>1</sup>

<sup>1</sup>Cedars-Sinai Medical Center, Los Angeles, CA

**Disclosures:** Vimal Krishnan: None; Mariza De Peralta-Venturina: None; Xuemo Fan: None

**Background:** Acinic cell carcinoma of the salivary gland (ACC-SG) is characterized by recurrent rearrangements in the nuclear receptor subfamily 4 group A member 3 (NR4A3). NR4A3 immunostaining using NOR-1 antibody has been shown to be highly specific and sensitive for the diagnosis of ACC-SG on surgical specimens and cell block material of fine needle aspirates (FNAs). However, salivary gland aspirates often have low cellularity and preparation of a cell block is not always possible. Our goal was to evaluate whether NR4A3 immunostaining can be reliably performed on conventional or liquid-based cytologic preparations to diagnose ACC-SG.

**Design:** A retrospective search from a single institution over a 10 year period revealed 7 cases with at least one adequate cytologic preparation (defined as having at least 2 well-preserved cellular clusters) and ACC-SG diagnosis confirmed on surgical resection. The previously stained conventional smear and/or liquid-based preparation (SurePath) were destained and then immunostained with NOR-1 antibody (sc-393902 [H-7], Santa Cruz Biotechnology Inc) at a titer of 1:30. Twenty-four mimicker lesions were included: normal acini (3), chronic sialadenitis (3), oncocytoma (1), pleomorphic adenoma (6), Warthin's tumor (8), mucoepidermoid carcinoma (1), secretory carcinoma (1) and salivary duct carcinoma (1). When available, surgical resections were also stained for comparison.

**Results:** All seven cases of ACC-SG showed distinct nuclear staining for NOR-1 (4 diffuse and strong, and 3 with more heterogeneous staining) on either conventional smear or liquid-based preparation (Surepath). Staining was more evident on single cells and cells in small clusters, in contrast to rare thick tissue fragments which showed staining only in the periphery of the clusters. None of the twenty-four mimicker lesions showed nuclear staining. Rare cases showed focal nonspecific cytoplasmic staining in macrophages.

**Conclusions:** NOR-1 immunohistochemical staining can be reliably performed on cytologic smears and liquid-based preparations of salivary gland tumors. This provides a valuable tool for distinguishing ACC-SG from its cytologic mimics on preoperative cytology with excellent sensitivity and specificity to optimize patient management.

**199 Machine Learning Approach to Bethesda System for Reporting Thyroid Cytopathology**

Sara Kwong<sup>1</sup>, John Paul Graff<sup>2</sup>, Kurt Schaberg<sup>2</sup>, Alaa Afify<sup>3</sup>

<sup>1</sup>UC Davis Health, Davis, CA, <sup>2</sup>University of California, Davis, Sacramento, CA, <sup>3</sup>University of California, Davis, Davis, CA

**Disclosures:** Sara Kwong: None; John Paul Graff: None; Kurt Schaberg: None; Alaa Afify: None

**Background:** Recent studies have shown that the implementation of artificial intelligence may aid and improve the diagnostic accuracy in cytopathology. The goal of this study is to determine whether a machine learning algorithm(s) can improve the diagnostic accuracy of thyroid fine needle aspirations, by comparing the diagnostic accuracy from a trained model created with IBM Watson to that of cytopathologists.

**Design:** This is a retrospective study in which we reviewed electronic medical records and identified all the patients who underwent thyroid fine needle aspirations. We retrieved and reviewed a total of 85 cases, and then captured the areas of interests at 10x and 40x magnification. The images were separated into 4 sub-categories: benign, atypia of undetermined significance (AUS), suspicious for papillary thyroid carcinoma (Suspicious), and papillary thyroid carcinoma (PTC). All the captured images are separated into two different datasets: a training dataset and a validation dataset. The training dataset was trained using convolutional neural networks (CNN) from IBM Watson PowerVision AI. The finalized model was tested with the validation dataset. The validation dataset was also evaluated by two cytopathologists, a senior cytopathologist and a junior cytopathologist. The interpretation accuracies of the cytopathologists were compared to that of the machine learning model.

**Results:** A cut-off of 0.5 was selected for the machine learning model accuracy, and interpretations above 0.5 were considered as the model's final interpretation. The trained model showed highest accuracy in the categories of PTC (95%) and lower accuracies in Benign (72%), AUS (70%) and Suspicious (75%) categories; which reflects the subjectivity in interpretation.

The overall validation dataset accuracy of the trained model was very similar to that of a senior cytopathologist (Table 1). The accuracies were compared using a student T test (two tailed test, two sample equal variance test), using alpha of 0.05. The p-value for the senior cytopathologist and the trained model was 0.57 and the p-value for the junior cytopathologist and the trained model was 0.068. Our findings show a significant difference between the model and a junior cytopathologist.

Categories	Cytopathologist 1	Cytopathologist 2	Trained Model
Overall accuracy	0.75	0.47	0.78
Benign	0.76	0.96	0.72
AUS	0.7	0.05	0.7
Suspicious	0.75	0.25	0.75
PTC	0.8	0.5	0.95

**Conclusions:** Machine learning algorithm(s) can be used to accurately diagnose thyroid fine needle aspiration.

The trained model shows accuracies similar or superior to that of a senior cytopathologist. Therefore, it may be a great tool to a junior cytopathologist or a non-cytopathology trained pathologist as a supplementary diagnostic tool.

**200 Long Term Follow Up of Patients With Negative Initial Anal Cytology With HPV Co-Testing**

Hansen Lam<sup>1</sup>, Xintong Wang<sup>1</sup>, Volha Lenskaya<sup>2</sup>, Baidarbhi Chakraborty<sup>2</sup>, Dan Lu<sup>1</sup>, Arnold Szporn<sup>2</sup>, Maureen Zakowski<sup>2</sup>, Qiusheng Si<sup>2</sup>

<sup>1</sup>Mount Sinai Hospital, New York, NY, <sup>2</sup>Icahn School of Medicine at Mount Sinai, New York, NY

**Disclosures:** Hansen Lam: None; Xintong Wang: None; Baidarbhi Chakraborty: None; Dan Lu: None; Arnold Szporn: None; Maureen Zakowski: None; Qiusheng Si: None

**Background:** Anal squamous carcinoma in high risk patients has increased in 30 years. Anal cytology and HPV testing has been proposed. Patient management with negative anal cytology is unclear. We studied long term outcomes of patients to provide management information.

**Design:** Electronic medical records were searched 2008-2020 for patients whose earliest anal cytology was negative and had concurrent HPV genotyping (co-test). Information included: earliest co-test, earliest LSIL, earliest HSIL, last diagnostic anal specimen. Demographics included age, sex and HIV status. Anal HPV genotyping was performed by RT-PCR (Cobas® HPV Test, Roche). HPV+ results reported as 16, 18 or Other High Risk (HPVO). Coinfection was defined as any combination of 16, 18 and HPVO.

**Results:** 249 patients (21-72 years, 239M, 10F, 1-12 year follow up), had negative initial anal co-test cytology. Concurrent genotyping found 74.9% (179/249) HPV+ patients, with 68.1% (122/179), 17.8% (14/179), 2.2% (4/179), and 21.7% (39/179) HPVO, 16, 18, and HPV coinfection. HIV status was available in 50.2% (125/249) patients (HIV+ 80%, 100/125). Biopsy concurrent co-test was negative with no previous lesion diagnosed in 62.6% (156/249) patients, who we considered a baseline negative group; 37.3% (93/249) patients had LSIL previous to, or concurrent with earliest co-test; 7.6% (19/249) patients had falsely negative cytology. In the baseline negative group, 63.4% (99/156) showed no progression. LSIL was the earliest lesion in 26.9% (42/156), and HSIL in 9.6% (15/156). HIV+ status was significantly associated with progression to any lesion ( $p < 0.05$ ). Single HPV infections, particularly HPVO and 16, and coinfections were associated with progression to LSIL and HSIL ( $p < 0.05$ ). In all patients who progressed, HPVO contributed to coinfection. Mean months to progression in HPV- patients was 33. Mean months to progression in patients with HPVO or coinfection was 22. In patients with a previous or concurrent LSIL, co-test showed 83.8% (78/93) HPV+, and progression to HSIL occurred in 27.9% (26/93), with mean months to progression of 36. Patients with HPV coinfection experienced significantly shorter times to progression than those with single infections: mean difference of 28 months ( $p < 0.05$ ).

**Conclusions:** Anal cytology with HPV co-test should be recommended for high risk patients as HPV genotype can predict development of LSIL/HSIL, even with negative initial study. Providers should be especially wary of progression and shorter progression time in patients with HPV coinfection, where HPVO is most commonly implicated.

**201 The International System for Reporting Serous Fluid Cytopathology: A Study of Inter-Observer Reproducibility**

Lester Layfield<sup>1</sup>, Magda Esebua<sup>1</sup>, Tao Zhang<sup>2</sup>, Zhongbo Yang<sup>3</sup>, Maryna Vazmitsel<sup>2</sup>, Robert Schmidt<sup>4</sup>  
<sup>1</sup>University of Missouri, Columbia, MO, <sup>2</sup>University of Missouri School of Medicine, Columbia, MO <sup>3</sup>Roswell Park Comprehensive Cancer Center, Buffalo, NY, <sup>4</sup>University of Utah/ARUP Laboratories, UT

**Disclosures:** Lester Layfield: None; Magda Esebua: None; Tao Zhang: None; Zhongbo Yang: None; Maryna Vazmitsel: None; Robert Schmidt: None

**Background:** A number of categorization systems have been developed for cytopathology specimens with the aim of providing uniformly used and understood diagnostic terminology and reliable estimates of malignancy risk. The intention of these systems is to improve reproducibility of diagnostic categorization with standardized estimated risks of malignancy and management. Required for the success of these systems is a high level of inter-observer reproducibility in category assignment. Recently, the International System for Reporting Serous Fluid Cytopathology (ISRFC) was proposed with categories non-diagnostic, negative for malignancy (negative), atypia of undetermined significance (AUS), suspicious for malignancy (suspicious) and malignant. Little data exists as to the inter-observer agreement for these categories.

**Design:** A search of the cytology records at the University of Missouri was performed for all pleural fluid specimens obtained between January 2014 and December 2019. A total of 200 specimens were reviewed independently by five board certified cytopathologists. Specimens were characterized as non-diagnostic, negative, AUS, suspicious and malignant. Inter-observer agreement was analyzed using Cohen's kappa.

**Results:** Table 1 shows results of comparisons. Over all observer agreement was 68% and chance corrected agreement (kappa) was 0.51. Agreement was good for categories negative and malignant but poor for AUS and suspicious.



Tabulation of all 600 comparisons:

Rater 1	Rater 2					Total
	1	2	3	4	5	
1	1	0	0	0	0	1
2	6	224	52	11	0	293
3	0	35	30	26	3	94
4	0	16	4	8	8	36
5	0	8	6	19	143	176
Total	7	283	92	64	154	600

**Conclusions:** ISRSFC has performance characteristics similar to other cytologic classifications schemes. Inter-observer agreement is best for the negative (76%) and malignant (81%) categories. Inter-observer agreement is poor for categories suspicious and AUS. This is similar to inter-observer agreement associated with systems for the urinary tract, respiratory tract and salivary gland.

**202 Improving Diagnostic Accuracy & Sensitivity of Bile Duct Brushing Cytology: Pilot Study Using Machine Learning**

Anna Lee<sup>1</sup>, Anjali Saqi<sup>1</sup>, Simon Sung<sup>2</sup>

<sup>1</sup>Columbia University Medical Center, New York, NY, <sup>2</sup>Albert Einstein College of Medicine, Montefiore Medical Center, New York, NY

**Disclosures:** Anna Lee: None; Anjali Saqi: None; Simon Sung: None

**Background:** Bile duct brushing (BDB) samples are frequently utilized to evaluate strictures and diagnose endoscopically identified lesions. While biliary brush cytology has high specificity, its sensitivity is low (ranging between 4% and 60%) and concurrent biopsy and/or fluorescent *in situ* hybridization (FISH) are incorporated to increase diagnostic yield. The aim of this pilot study was to assess the utility of convolutional neural network (CNN) algorithms for improving diagnoses of BDB.

**Design:** A retrospective computerized search was performed for Papanicolaou-stained, ThinPrep slides of BDBs with benign and positive for malignancy diagnoses. All cytological diagnoses were confirmed with surgical pathology biopsy/resection, FISH analysis, and/or clinical history/radiologic follow up. All slides were de-identified and scanned with Leica Aperio AT2 as whole slide images (WSI) .svs files. Patches of 40x images were extracted using open-source GitHub repository code (<https://github.com/ysbecca/py-wsi>) and saved as PNG files. Benign and malignant images were divided randomly into 8:2 ratio for training and validation sets, respectively. Three open-source algorithms, VGG19, Resnet152 and Inception V3, trained with 30 epochs implemented on pytorch 1.5.1 in python 3.8.3 were applied and accuracy, specificity, and sensitivity were calculated for each.

**Results:** From 7 BDB cases, 712 images (274 malignant and 438 benign) were generated. All except one malignant case had histologically confirmed diagnoses of adenocarcinoma. The benign diagnoses had history of autoimmune and/or chronic pancreatitis. Of the 712 images, 570 were used for training and 142 for validation. Resnet 152 had the greatest accuracy (90.8%), sensitivity (76.4%) and specificity (98.9%). (Table 1).

**Table 1:** Accuracy, sensitivity, and specificity of VGG19, Resnet 152, and Inception V3

CNN	Accuracy	Sensitivity	Specificity
VGG19	88.5%	73.7%	97.8%
Resnet 152	90.8%	76.4%	98.9%
Inception V3	84.0%	73.7%	93.7%

**Conclusions:** Our pilot study demonstrates the potential utility of machine learning algorithms for differentiating between benign and malignant BDBs. While the study is limited by small number of training and validation images, preliminary results show significantly improved sensitivity relative to cytology. Future studies that include additional training images are needed to further optimize results and assess performance of indeterminate (atypical and suspicious) diagnoses.

The second and third authors contributed equally to this study.

**203 Upper Urinary Tract Cytology Performance Before and After the Implementation of the Paris System for Reporting Urinary Cytology (TPS)**

Hannah Lee<sup>1</sup>, Nancy Greenland<sup>1</sup>, Laura Tabatabai<sup>1</sup>, Chien-Kuang Ding<sup>1</sup>, Poonam Vohra<sup>1</sup>  
<sup>1</sup>University of California, San Francisco, San Francisco, CA

**Disclosures:** Hannah Lee: None; Nancy Greenland: None; Laura Tabatabai: None; Chien-Kuang Ding: None; Poonam Vohra: None

**Background:** TPS provides a standardized diagnostic approach to evaluate urine cytology. Although these diagnostic criteria are predominantly based on data from the lower urinary tract, they have been recommended for both upper and lower urinary tract specimens. Only a few studies have reported the impact of TPS on UUT cytology. To the best of our knowledge, this is one of the largest studies to evaluate the performance of TPS in UUT specimens.

**Design:** We performed retrospective analysis of 126 UUT cytology specimens from 2010-2019 with concurrent or subsequent histologic specimens for diagnostic correlation. All atypical cases before implementation of TPS were reviewed in a blinded manner by 2 cytopathologists, with diagnoses reassigned to the following TPS categories: negative for high grade urothelial carcinoma (NHGUC), low grade urothelial neoplasia (LGUN), atypical urothelial cells (AUC), suspicious for high grade urothelial carcinoma (SHGUC), and high grade urothelial carcinoma (HGUC).

**Results:** TPS reclassification resulted in specificity of 91% and sensitivity of 75% for the detection of HGUC, and cytology histologic correlation remained similar (73% post-TPS vs 72% pre-TPS). With TPS, the spectrum of diagnoses changed, and the rate of AUC diagnoses decreased from 25% to 18% ( $P = 0.28$ ), increasing the positive predictive value (PPV) for HGUC from 39% to 48%. We found that 9/27 (33%) histologically proven HGUC cases were reclassified as either atypical (6/9, 67%) mainly due to the absence of hyperchromasia or SHGUC (3/9,33%), reflecting an overall shift of downgrading diagnoses with TPS, and leading to a decrease in PPV of HGUC from 87% to 77%. However, when AUC, SHGUC or HGUC interpretations were considered as positive, the PPV in predicting HGUC on histology increased from 77% to 92%. The rate of LGUN diagnosis increased from 0% to 10% due to the presence of fibrovascular cores.

Table 1: Performance of The Paris System for Reporting Urinary Cytology (TPS) compared with a Pre-TPS diagnosis.

	Cytology				
Histology	Benign (58)	LGUN (3)	AUC (23)	SHGUC (7)	HGUC (35)
	(Pre-TPS 57)	(Pre-TPS 0)	(Pre-TPS 31)	(Pre-TPS 0)	(Pre-TPS 38)
Benign	41	0	2	0	4
LGUC	6	2	8	1	3
Atypical	2	0	2	0	1
HGUC	9	1	11	6	27
PPV for HGUC	15%	33%	48%	86%	77%
	(Pre-TPS 16%)	(Pre-TPS 0%)	(Pre-TPS 39%)	(Pre-TPS 0%)	(Pre-TPS 87%)

HGUC, high grade urothelial carcinoma; AUC, atypical urothelial cells; LGUN, low grade urothelial neoplasia; LGUC, low grade urothelial carcinoma; SHGUC, suspicious for high grade urothelial carcinoma; PPV, positive predictive value

**Conclusions:**

1. TPS reclassification resulted in comparable specificity (91%) and sensitivity (75%), similar to the overall reported specificity (90%) and sensitivity (70%) of UUT cytology for the detection of HGUC.
2. TPS decreased the rate of AUC diagnosis, increasing the PPV of AUC for HGUC from 39% to 48%.
3. TPS helped to detect a greater number of LGUN cases.
4. PPV of UUT cytology for predicting subsequent HGUC on histology improved when the AUC and SHGUC diagnostic categories were included in the positive cohort.
5. Using strict TPS criteria in upper urinary tract cytology specimens may decrease the frequency of HGUC diagnoses due to the absence of hyperchromasia in some of the cases.

**204 False-Negative Pap Tests in Women with Biopsy-Proven Endocervical Adenocarcinoma: A Retrospective Analysis with Assessment of Inter-Observer Agreement**

Michelle Lin<sup>1</sup>, Siroratt Narkcham<sup>1</sup>, Angela Jones<sup>2</sup>, Donna Armylagos<sup>1</sup>, Brittany DiPietro<sup>1</sup>, Onyinyechukwu Okafor<sup>2</sup>, Patrick Tracey<sup>2</sup>, Tiffany Vercher<sup>2</sup>, Sara Vasquez<sup>2</sup>, Susan Haley<sup>1</sup>, Suzanne Crumley<sup>1</sup>, Blythe Gorman<sup>1</sup>, Elizabeth Jacobi<sup>1</sup>, Mojgan Amrikachi<sup>1</sup>, Donna Coffey<sup>3</sup>, Dina Mody<sup>1</sup>, Ekene Okoye<sup>1</sup>  
<sup>1</sup>Houston Methodist Hospital, Houston, TX, <sup>2</sup>BioReference Laboratories, Inc., Houston, TX, <sup>3</sup>The Methodist Hospital, Houston, TX

**Disclosures:** Michelle Lin: None; Siroratt Narkcham: None; Angela Jones: None; Donna Armylagos: None; Brittany DiPietro: None; Onyinyechukwu Okafor: None; Patrick Tracey: None; Sara Vasquez: None; Suzanne Crumley: None; Elizabeth Jacobi: None; Dina Mody: None; Ekene Okoye: None

**Background:** The incidence of endocervical adenocarcinoma (EA) is increasing; however, the detection of glandular neoplasia on screening Pap tests continues to pose a challenge for cytologists. The aim of this study was to identify factors contributing to false-negative Pap tests in patients with EA, and to assess the impact of educational instruction on inter-observer agreement in classification of these cases.

**Design:** Available biopsy-proven EA cases (both invasive and in-situ) over a 37-month period with corresponding NILM Pap tests were identified. The Pap tests were assessed in 2 rounds by 12 blinded reviewers (6 cytotechnologists, 6 cytopathologists). The cases were subsequently reviewed and reclassified in a majority-blinded consensus group. Between the two rounds, an educational session on identification of glandular lesions in Pap tests was conducted. Inter-observer agreement was analyzed using Fleiss' kappa and Cohen's kappa calculations.

**Results:** Of 81 EA cases from 71 patients, 24 with corresponding NILM Pap tests from 19 patients were identified; all cases were high-risk HPV positive. Upon consensus review, the cases were reclassified as follows: 9 to a high-risk category (ASC-H or greater), 3 to a low-risk category (ASCUS/LSIL), and 12 kept as NILM. False-negative diagnoses were attributed to sampling variance in 12/24 (50%), interpretive variance in 10/24 (41.7%), and screening variance in 2/24 (8.3%) of cases. Causes of interpretive variance included under-calling neoplastic cells as reactive endocervical cells or endometrial cells, and the presence of obscuring inflammation. The degree of agreement between individual reviewers' diagnoses and the consensus diagnosis improved following educational instruction, with the number of reviewers demonstrating at least moderate agreement with the consensus diagnosis increasing from 4/12 (33%) in round 1 to 8/12 (67%) in round 2 (Table 1). The overall inter-observer agreement also improved from round 1 (Fleiss' kappa = 0.251, 95% confidence interval [CI] 0.214-0.287) to round 2 (Fleiss' kappa = 0.389, 95% CI 0.349-0.429) by a statistically significant margin.

Table 1. Agreement (Cohen's kappa statistic) between individual reviewers' diagnoses and consensus diagnosis.		
	First round	Second round
<b>Cytotechnologists</b>	0.099	0.273

	0.208	0.390
	0.339	0.308
	0.525	0.477
	0.529	0.547
	0.719	0.780
<b>Cytopathologists</b>	0.208	0.200
	0.323	0.495
	0.323	0.704
	0.327	0.472
	0.395	0.556
	0.586	0.643
Kappa: 0.00-0.20 – slight agreement; 0.21-0.40 – fair agreement; 0.41-0.60 – moderate agreement; 0.61-0.80 – substantial agreement; 0.81-1.00 – almost perfect agreement.		

**Conclusions:** Sampling variance accounted for 50% of false-negative Pap tests in patients with EA, highlighting the importance of high-risk HPV co-testing in directing appropriate management for these cases. Educational instruction decreased the rate of interpretive variances, supporting the practice of periodic education initiatives. However, despite this improvement with education, there were still cases not accurately classified in the post-educational round. Thus, high-risk HPV positive Pap tests initially classified as NILM, especially those with hyperchromatic crowded groups or obscuring factors, may benefit from focused rescreening and intradepartmental consultation to improve detection of glandular neoplasia.

**205 Utility of Ultrasonography-Guided Fine Needle Aspiration for the Detection of Intraductal Papilloma of the Breast: Results of a Large Series from a Referral Cancer Center**

Zhonghua Liu<sup>1</sup>, Mohamed Khalil<sup>1</sup>, Savitri Krishnamurthy<sup>1</sup>

<sup>1</sup>The University of Texas MD Anderson Cancer Center, Houston, TX

**Disclosures:** Zhonghua Liu: None; Mohamed Khalil: None

**Background:** In an era in which core needle biopsy (CNB) is the popular technique for evaluating breast lesions, the role of ultrasonography-guided fine needle aspiration (US-FNA) for the investigation of breast lesions that are not suspicious for malignancy is not recognized. We report the utility of US-FNA for detection and clinical management of intraductal papilloma of breast in a large cohort of patients at a referral cancer center.

**Design:** We identified 220 patients with intraductal papilloma diagnosed on US-FNA at MD Anderson Cancer Center from 2015 to 2019. The patients' demographic data, clinical and imaging findings (solitary or satellite of a malignant tumor) were recorded. We performed evaluation of US-FNA samples for cellularity (low [ $<20\%$ ], moderate [ $20-50\%$ ], high [ $\geq 50\%$ ]); fibrovascular cores (present or absent); tissue fragment size (small or large); single-cell intensity (low [ $<20\%$ ], moderate [ $20-50\%$ ], high [ $\geq 50\%$ ]); metaplastic cells (present or absent). The cytological diagnosis was correlated with histopathological diagnosis of concurrent CNB or subsequent surgical resection and/or clinical and imaging follow-up.

**Results:** The median patient age was 59 years (range, 16-84 years). Of the 220 patients, 160 (72.7%) had solitary and 60 (27.3%) had satellite lesions with a history of bloody nipple discharge in 51 (23.2%) patients. All samples had fibrovascular cores; 110 (50%) had small, and 110 had large tissue fragments. Single-cell intensity (including epithelial, myoepithelial, and stromal cells) was low in 188 (85.4%), moderate in 22 (10.0%), and high in 10 (4.5%) samples. Ninety samples (40.9%) had metaplastic cells. Concurrent CNB and subsequent surgical resection were performed in 14 (6.4%) and 51 patients (23.2%); US-FNA diagnosis was correlated with CNB diagnosis in 14 of 14 patients (100%) and with surgical resection in 43 of 51 patients (84.3%). We could not correlate the US-FNA results of 8 satellite lesions that were not sampled in the mastectomy specimen.



**Table 1. Clinical and cytologic features of intraductal papilloma of the breast diagnosed by US-FNA**

Total cases, n	220
Age, median (range), years	59 (16-84)
Presence of nipple discharge, n (%)	51 (23.2%)
Type of presentation	
Solitary lesion, n (%)	160 (72.7%)
Satellite lesion, n (%)	60 (27.3%)
Size of lesion, median (range), cm	0.7 (0.2-12)
Presence of fibrovascular core, n (%)	220 (100%)
Presence of myoepithelial cells, n (%)	220 (100%)
Presence of metaplastic cells, n (%)	90 (40.9%)
Tissue fragment size	
Small, n (%)	110 (50%)
Large, n (%)	110 (50%)
Overall cellularity	
Low, n (%)	71 (32.3%)
Moderate, n (%)	102 (46.4%)
High, n (%)	47 (21.4%)
Intensity of single cells	
Low, n (%)	188 (85.4%)
Moderate, n (%)	22 (10.0%)
High, n (%)	10 (4.5%)
US-FNA diagnosis correlated with histologic diagnosis	
Concurrent CNB, n (%)	14/14 (100%)
Subsequent resection, n (%)	43/51 (84.3%)

**Conclusions:** 1. The presence of fibrovascular cores in association with benign epithelial/myoepithelial clusters is the defining feature for the cytopathological diagnosis of intraductal papilloma. 2. US-FNA with cytopathological examination can be effectively utilized for the detection and clinical management of intraductal papilloma. 3. The US-FNA diagnosis of intraductal papilloma could facilitate clinical and imaging follow-up alone in up to 70% of patients, enabling them to avoid surgery.

**206 Evaluating PD-L1 in Cytology to Determine Eligibility for Anti-PD-1/PD-L1 Immunotherapy in Patients with Head and Neck Squamous Cell Carcinoma**

Zhonghua Liu<sup>1</sup>, Sinchita Roy-Chowdhuri<sup>1</sup>

<sup>1</sup>The University of Texas MD Anderson Cancer Center, Houston, TX

**Disclosures:** Zhonghua Liu: None; Sinchita Roy-Chowdhuri: None

**Background:** Immune checkpoint inhibitors targeting PD-1/PD-L1 pathway have recently emerged as a front-line treatment for head and neck squamous cell carcinoma (HNSCC). Evaluation of PD-L1 expression by immunohistochemistry in histologic samples is used to determine eligibility of HNSCC patients for therapy. Patients with newly diagnosed HNSCC are frequently diagnosed by fine needle aspiration (FNA) of lymph nodes (LN) with metastatic disease. However, evaluation of PD-L1 expression using the proposed combined positive score (CPS)

has not been well-established in cytology specimens. Therefore, in this study we evaluated the feasibility of evaluating PD-L1 CPS in HNSCC patients using FNA cell blocks (CB).

**Design:** A retrospective review of our pathology database from 2014-2020 was performed to identify HNSCC cases with known PD-L1 status on histologic specimens and a matched FNA specimen with tumor on the CB. The CB sections were stained with PD-L1 antibody (clone 22C3) and positive staining was assessed as complete/partial membranous staining in tumor and/or immune cells (lymphocytes and macrophages). All cases were scored using CPS which is the proportion of PD-L1 staining cells (tumor and immune cells) relative to the total number of tumor cells. The tumor proportion score (TPS), which is the proportion of PD-L1 expressing viable tumor cells was also calculated. Concordance was calculated using the histologic specimen as the reference.

**Results:** A total of 21 cases were evaluated in this study. The CPS and TPS for histologic and CB specimens are shown in Table 1. The agreement in CPS between surgical and cytology specimen was 81% (Kappa = 0.7). Since evaluating CPS poses some challenges in FNA specimens due to the inherent difficulty of differentiating tumor associated lymphocytes from those present within the LN, TPS for PD-L1 was also assessed and showed good agreement (76.2%; Kappa = 0.6). The positive predictive value is 100% for both CPS (14/14) and TPS (13/13), while the negative predictive value is 57.1% (4/7) for CPS and 50% (4/8) for TPS assessments.

**Table 1. Concordance of PD-L1 IHC between cytology cell block and histologic specimens**

CPS		Histologic specimen			Agreement	Kappa
		<1	1-49	≥50		
Cell block	<1	4	3	0	81%	0.6923
	1-49	0	9	1		
	≥50	0	0	4		
TPS		Histologic Specimen			Agreement	Kappa
		<1%	1-49%	≥50%		
Cell block	<1%	4	4	0	76.2%	0.6067
	1-49%	0	9	1		
	≥50%	0	0	3		

**Conclusions:** Our results show good correlation of PD-L1 expression between histologic and cytologic HNSCC specimens. The PD-L1 assessment on CB is more reliable when CPS is ≥1 or TPS is ≥1%. Therefore, PD-L1 CPS evaluation is feasible in HNSCC CBs and can act as a surrogate for determining eligibility for anti-PD-1/PD-L1 immunotherapy in cases where a histologic specimen is not readily available.

**207 Optimization of Thyroid Samples for Molecular Testing: Lessons Learned from Indeterminate Thyroid Fine Needle Aspirations with Sub-Optimal Cytology and Molecular Testing Results**

Terrance Lynn<sup>1</sup>, Yi Ding<sup>1</sup>, Madiha Alvi<sup>1</sup>, Michele Zelonis<sup>1</sup>, Sara Monaco<sup>1</sup>  
<sup>1</sup>Geisinger Medical Center, Danville, PA

**Disclosures:** Terrance Lynn: None; Yi Ding: None; Madiha Alvi: None; Michele Zelonis: None; Sara Monaco: None

**Background:** Thyroid nodules sampled with fine needle aspiration (FNA) that have a subsequent indeterminate cytology diagnosis can be challenging for physicians in deciding how to manage patients, and in some institutions, undergo reflex molecular testing (MT). The MT results can help in determining further management if sufficient for analysis. However, indeterminate or failed MT results can be problematic and costly. Thus, this study examines indeterminate thyroid FNAs with MT results to assess ways to optimize the triage of thyroid FNA specimens for MT.

**Design:** Thyroid FNA specimens from June 2017 to December 2019 were retrospectively identified in the pathology LIS (CoPathPlus, Cerner, version 2017.01.1.124) and reviewed for cytology results (using The Bethesda System for Reporting Thyroid Cytopathology) and associated MT reports (ThyroSeq V2 and V3 GC).

**Results:** A total of 519 Thyroid FNA cases with MT were analyzed over the 2.5-year period, of which 351 (68%) were called atypia or follicular lesion of undetermined significance (AUS/FLUS) on cytology. Of the AUS/FLUS cases with MT, 323 (92%) were adequate on cytology, of which 204 (63%) had adequate MT results (167 (52%) negative for mutations; 37 (11%) positive for mutations), and 119 (37%) had suboptimal but negative MT. In the adequate FNA cases with suboptimal MT, it was discovered that triage for MT was variable with respect to the pass submitted for MT and lack of rapid on-site evaluation (ROSE) to guide triage. Of the 28 (8%) AUS/FLUS cases with suboptimal cellularity on cytology, 21 (75%) of these had suboptimal but negative MT results, and 7 (25%) failed testing with no MT results reported. [TABLE 1]

**Table 1. Comparison of thyroid molecular testing adequacy to FNA cytology adequacy, and molecular testing results (Legend: MT, molecular testing).**

<b>Comparison of AUS/FLUS FNA diagnoses with cytology and MT adequacy (n=351)</b>		
	n	%
<b>Cytology Adequate</b>	323	92%
MT Adequate	204	63%
MT Suboptimal	119	37%
MT Failed	0	0%
<b>Cytology Suboptimal</b>	28	8%
MT Adequate	0	0%
MT Suboptimal	21	75%
MT Failed	7	25%
<b>Total</b>	351	100%
<b>Comparison of AUS/FLUS FNA diagnoses with MT results (n=351)</b>		
<b>MT Positive</b>	37	11%
<b>MT Negative</b>	307	87%
MT Negative (adequate)	167	54%
MT Negative (limited)	140	46%
<b>MT Failed</b>	7	2%

**Conclusions:** MT can be helpful for triaging indeterminate thyroid nodules to decide further management. In our experience, the majority (68%) of cases sent for MT have an AUS/FLUS cytology diagnosis, and all cases with suboptimal cellularity on FNA had suboptimal or failed MT. Furthermore, 37% of AUS/FLUS cases with adequate cellularity on FNA had suboptimal MT. In order to optimize results, FNA samples with only focal atypia and compromised cellularity may not be ideal for MT given the low yield and cost. When sending an FNA for MT, ROSE and education of providers on appropriate triage should be considered to optimize the quality and diagnostic yield of the sample for MT.

**208 Sensitivity of Primary HPV Screening for High-Grade Squamous Dysplasia and Carcinoma versus Cotesting in a Community-Based Setting**

Martin Magers<sup>1</sup>, Ranya Hasan<sup>2</sup>, Stephanie Hayden<sup>1</sup>, Sharon Bihlmeyer<sup>2</sup>  
<sup>1</sup>IHA Pathology, Ann Arbor, MI, <sup>2</sup>St. Joseph Mercy Hospital, Ann Arbor, MI

**Disclosures:** Martin Magers: None; Ranya Hasan: None; Stephanie Hayden: None; Sharon Bihlmeyer: None

**Background:** The Pap smear was developed nearly 100 years ago, and it remains a mainstay of cervical cancer detection and prevention, dramatically decreasing the incidence of cervical cancer in the United States in the last 50 years. The causative link between human papillomavirus (HPV) and cervical cancer was discovered in the 1980's, leading to integration of HPV testing in cervical cancer screening guidelines. Until recently, HPV testing was an adjunct to the Pap smear, either as upfront cotesting (i.e., both Pap smear and HPV performed) or as reflex testing based on an atypical Pap smear diagnosis. However, recent guidelines recommend primary HPV screening with HPV-positive results reflexing to a Pap smear for cytologic evaluation. This approach may not detect squamous dysplasia in Pap smears which are negative for HPV by commercially available tests. Thus, we sought to compare the sensitivities of detection of high-grade squamous dysplasia (HSIL) or carcinoma by primary HPV screening versus cotesting.

**Design:** Cervical biopsies with HSIL or carcinoma were correlated with the immediately preceding HPV-cotested Pap smear (i.e., last Pap smear before biopsy occurring  $\leq 6$  months prior to biopsy) at a community practice laboratory from January 2020 to October 2020. HPV testing was performed on the Roche Cobas platform (FDA approved for primary HPV screening), testing for HPV genotypes 16, 18, and "Other" (31, 33, 35, 39, 45, 51, 52, 56, 58, 59, 66, and 68). Cytology was performed using ThinPrep technology. Sensitivities for primary HPV screening and cotesting were calculated.

**Results:** Overall, 140 HSIL biopsies and 3 carcinoma biopsies were identified. Of these, HPV cotesting was performed on 89 of the Pap smears. Of these 89 HPV-cotested Pap smears, 81 were HPV-positive (91%) and 8 were HPV-negative (9%). The diagnoses of the HPV-negative Pap smears were HSIL (n=7, 75%); atypical squamous cells, cannot exclude high-grade dysplasia (n=1, 13%); and atypical glandular cells of undetermined significance (n=1, n=13%). The biopsy diagnoses of the HPV-negative cases were HSIL (n=6, 75%) and squamous cell carcinoma (n=2, 25%). Cotesting demonstrated a sensitivity of 100% for detection of high-grade dysplasia or carcinoma, whereas primary HPV testing had a sensitivity of 91%.

**Conclusions:** Cotesting demonstrated superior sensitivity for detecting cervical HSIL and carcinoma compared to primary HPV screening. Primary HPV screening protocols in the United States should be implemented with caution.

## 209 Risk of Malignancy of Proposed Diagnostic Categories in Lymphoid Tissue Fine-Needle Aspiration Cytology

Vladislav Makarenko<sup>1</sup>, Michelle DeLelys<sup>2</sup>, Robert Hasserjian<sup>1</sup>, Amy Ly<sup>2</sup>

<sup>1</sup>Massachusetts General Hospital, Harvard Medical School, Boston, MA, <sup>2</sup>Massachusetts General Hospital, Boston, MA

**Disclosures:** Vladislav Makarenko: None; Michelle DeLelys: None; Robert Hasserjian: None; Amy Ly: None

**Background:** Despite frequent clinical use, fine-needle aspiration (FNA) cytology for evaluation of lymphoid tissue lacks a uniform cytopathological diagnostic classification, and there is limited data on the clinical implication of such diagnostic categories. Recent publication of the Sydney System has proposed a possible framework for lymph node cytology diagnosis. In this study, we evaluated the diagnostic performance and risk of malignancy associated with the proposed diagnostic categories performed on lymphoid tissue FNA in our institution.

**Design:** All FNA biopsies performed in our institution for the purpose of evaluating patients for suspected lymphoma over a 2-year period (2018-2019) were analyzed retrospectively. One of five diagnostic categories was reported for each case: non-diagnostic, negative for malignancy, atypical, suspicious for malignancy, and positive for malignancy. The cytologic diagnosis was compared with final diagnoses obtained on a subsequent surgical biopsy and/or clinical assessment.

**Results:** A total of 134 cases were included in the study, with 47 (35%) cases definitively diagnosed as lymphoma. FNA was performed for initial diagnosis in 81%, and for diagnosing disease recurrence in 19% of cases. The FNA diagnosis was 85% concordant with the final diagnosis. Likelihood of diagnostic concordance was independent of targeted lesion size, number of needle passes, FNA operator (e.g. radiologist, gastroenterologist, pathologist), and the presence of concurrent flow cytometry. The diagnostic error rate was significantly higher in cases that were not subjected to intra- or interdepartmental consultation ( $\chi^2=3.96$ ,  $p=.046$ ) as well as in cases with



limited specimen adequacy ( $\chi^2=4.77$ ,  $p=.029$ ). The risks of malignancy for each reported category were non-diagnostic – 25%, negative – 4.1%, atypical – 47.6%, suspicious – 87.5%, and positive – 95.8%.

**Conclusions:** Diagnostic performance of FNA cytology of lymphoid tissue is dependent on the quality of the specimen and appears to be improved by consensus review by multiple pathologists. Patients with non-diagnostic specimens should undergo repeat sampling given the significant likelihood of lymphoma in such samples obtained from patients with a clinical suspicion of lymphoma. Understanding the risk of malignancy associated with each FNA diagnostic category in this setting will be helpful in guiding optimal patient management.

**210 Application of the Milan System for Reporting Salivary Gland Cytopathology in Pediatrics: An International, Multi-Institutional Study**

Zahra Maleki<sup>1</sup>, Fabiano Callegari<sup>2</sup>, Austin Wiles<sup>3</sup>, Derek Allison<sup>4</sup>, Irem Kilic<sup>5</sup>, Guido Fadda<sup>6</sup>, Mauro Saieg<sup>7</sup>, Panagiota Mikou<sup>8</sup>, Glen Dixon<sup>9</sup>, Gianluigi Petrone<sup>10</sup>, Kartik Viswanathan<sup>11</sup>, Jeffrey Krane<sup>12</sup>, Syed Ali<sup>13</sup>, Ivana Kholovà<sup>14</sup>, William Faquin<sup>15</sup>, Eva Wojcik<sup>16</sup>, Ashish Chandra<sup>17</sup>, Guliz Barkan<sup>18</sup>, Zubair Baloch<sup>19</sup>, Esther Rossi<sup>20</sup>, Jerzy Klijanienko<sup>21</sup>

<sup>1</sup>Johns Hopkins University School of Medicine, Baltimore, MD, <sup>2</sup>UNIFESP, São Paulo, Brazil, <sup>3</sup>Virginia Commonwealth University Health System, Richmond, VA, <sup>4</sup>University of Kentucky College of Medicine, Lexington, KY, <sup>5</sup>Loyola University Medical Center, Maywood, IL, <sup>6</sup>University Cattolica Sacro Cuore, Rome, Italy, <sup>7</sup>A.C. Camargo Cancer Center, São Paulo, Brazil, <sup>8</sup>Laiko Hospital, Athens, Greece, <sup>9</sup>HCA Healthcare UK, London, United Kingdom, <sup>10</sup>Catholic University of Sacred Heart, Fondazione Policlinico Universitario A. Gemelli, Rome, Italy, <sup>11</sup>New York-Presbyterian/Weill Cornell Medical Center, New York, NY, <sup>12</sup>David Geffen School of Medicine at UCLA, Los Angeles, CA, <sup>13</sup>Johns Hopkins Medical Institutions, Baltimore, MD, <sup>14</sup>University of Tampere, Turku, <sup>15</sup>Massachusetts General Hospital, Harvard Medical School, Boston, MA, <sup>16</sup>Loyola University Medical Center, Chicago, IL, <sup>17</sup>Guy's and St. Thomas' Hospital NHS Foundation Trust, London, United Kingdom, <sup>18</sup>Loyola University Healthcare System, Maywood, IL, <sup>19</sup>Hospital of the University of Pennsylvania, Philadelphia, PA, <sup>20</sup>Fondazione Policlinico Universitario Agostino Gemelli IRCCS-Università Cattolica del Sacro Cuore, Rome, Italy, <sup>21</sup>Institut Curie, Paris, France

**Disclosures:** Zahra Maleki: None; Fabiano Callegari: None; Austin Wiles: None; Derek Allison: None; Irem Kilic: None; Mauro Saieg: None; Panagiota Mikou: None; Glen Dixon: None; Gianluigi Petrone: None; Kartik Viswanathan: None; Jeffrey Krane: None; Ivana Kholovà: None; William Faquin: None; Eva Wojcik: None; Guliz Barkan: None; Zubair Baloch: None; Esther Rossi: None

**Background:** The Milan System for Reporting Salivary Gland Cytopathology (MSRSGC) is a 6-tier diagnostic category system with associated risks of malignancy (ROMs) and management recommendations. Pediatric salivary gland fine-needle aspiration (FNA) is uncommon with a higher frequency of inflammatory lesions and a relatively small proportion of malignancy, which may affect the ROM and subsequent management. This study evaluated the application of the MSRSGC and the ROM for each diagnostic category for 398 pediatric salivary gland FNAs.

**Design:** Pediatric (0-19 years old) salivary gland FNA cytology specimens from 15 international institutions of six countries including United States, England, Italy, Greece, Finland, Brazil, and France were retrospectively assigned to an MSRSGC diagnostic category as follows: nondiagnostic, nonneoplastic, atypia of undetermined significance (AUS), benign neoplasm, salivary gland neoplasm of uncertain malignant potential (SUMP), suspicious for malignancy (SM), or malignant. A correlation with the available histopathologic follow-up was performed, and the ROM was calculated for each MSRSGC diagnostic category.

**Results:** The case cohort of 398 aspirates was reclassified according to the MSRSGC as follows: nondiagnostic, 10.5%; nonneoplastic, 48.2%; AUS, 5.2%; benign neoplasm, 24.6%; SUMP, 5.5%; SM, 2%; and malignant, 14%. The histopathologic follow-up was available for 201 cases (55.5%). The ROMs were as follows: nondiagnostic, 7%; nonneoplastic, 8%; AUS, 23%; benign neoplasm, 3%; SUMP, 20%; SM, 100%; and malignant, 98%. Mucoepidermoid carcinoma was the most common malignancy (14/201) followed by acinic cell carcinoma (11/201) and pleomorphic adenoma was the most common benign neoplasm (75/201), respectively.

Milan System diagnostic category	Total cases	Cases with surgical follow up	Malignant cases	Benign neoplasm	Non-neoplastic	ROM
Non-diagnostic	42	13	1	5	7	7%
Non-neoplastic	150	37	3	10	24	8%
Atypia of undetermined significance (AUS)	21	13	3	6	4	23%
Neoplasm- Benign	98	66	2	62	2	3%
Neoplasm- Uncertain Malignant Potential (SUMP)	22	15	3	12	0	20%
Suspicious for Malignancy	9	8	8	0	0	100%
Malignant	56	49	48	0	1	98%
<b>Total</b>	<b>398</b>	<b>201</b>	<b>68</b>	<b>95</b>	<b>38</b>	<b>33.8%</b>

The case cohort of 398 aspirates was reclassified according to the MSRSGC as follows: nondiagnostic, 10.5%; nonneoplastic, 48.2%; AUS, 5.2%; benign neoplasm, 24.6%; SUMP, 5.5%; SM, 2%; and malignant, 14%. The histopathologic follow-up was available for 201 cases (50.5%). The ROMs were as follows: nondiagnostic, 7%; nonneoplastic, 8%; AUS, 23%; benign neoplasm, 3%; SUMP, 20%; SM, 100%; and malignant, 98%. Mucoepidermoid carcinoma was the most common malignancy (14/201) followed by acinic cell carcinoma (11/201) and pleomorphic adenoma was the most common benign neoplasm (75/201), respectively.

**Conclusions:** This multi-institutional study shows that the ROM of each MSRSGC category in pediatric salivary gland FNA is relatively similar to that reported for adult salivary gland FNA, although the reported rates for the different MSRSGC categories were variable across institutions. Thus, the MSRSGC can be reliably applied to pediatric salivary gland FNA.

**211 Human Papillomavirus Positive and Cytology Negative Women: An Analysis According to Race**

Daniel Miller<sup>1</sup>, Ashleigh Graham<sup>2</sup>, Katelynn Davis<sup>3</sup>, Harsimar Kaur<sup>2</sup>, Marissa White<sup>3</sup>, Zahra Maleki<sup>3</sup>, Erika Rodriguez<sup>3</sup>

<sup>1</sup>Saint Louis University Hospital, St. Louis, MO, <sup>2</sup>Johns Hopkins University, Baltimore, MD, <sup>3</sup>Johns Hopkins University School of Medicine, Baltimore, MD

**Disclosures:** Daniel Miller: None; Ashleigh Graham: None; Katelynn Davis: None; Harsimar Kaur: None; Marissa White: None; Zahra Maleki: None; Erika Rodriguez: None

**Background:** The majority of cervical cancers occur in women who are not up-to date with cervical cancer screening guidelines or did not receive appropriate clinical follow-up after an abnormal screening test result. The rate of follow-up of women with negative cytology (PAPneg) and positive high risk Human Papillomavirus (hrHPV) is considered low despite the increased risk of CIN3+ lesions. Herein we compare follow-up results in black and white women.

**Design:** We performed a retrospective case review of all women who had pap tests in two calendar years. We identified all women who had cytology negative, hrHPV positive results, then completed a review of the pathology system to determine follow up surgical pathology correlation and follow up pap test results. We assessed these data according to race cohorts of black and white women.

**Results:** 1,728 women had negative cytology in the setting of an hrHPV infection (PAPneg/HPVpos). Of these patients, 53% (n=915) were black and 47% (n=813) were white. See table 1. HPV16 was more common in white women (146 vs 103, p < 0.01); HPV18 was more common in black women (61 vs 36, p = 0.04); and non-16/18

hrHPV was more common in black compared to white women (798 vs 670,  $p = 0.02$ ). 503 patients had no follow-up and there was no difference with respect to race (30% of black and 27% white cohorts). A total of 1,055 women (61%) had a follow-up PAP test, including 549 black and 506 white women. The range of cytologic diagnoses were similar between the two race cohorts. However, co-testing showed HPV16 to be more common in white (59 vs 35,  $p < 0.01$ ) and non-16/18 hrHPV more common in black women (250 vs 219,  $p < 0.01$ ); while HPV18 was more common in black women, this difference did not reach statistical significance (15 vs 12,  $p > 0.05$ ). 768 patients had colposcopy after their pap test with mean interval being 7.2 months for both cohorts. The surgical pathology results were similar for both cohorts, although HSIL on endocervical curettage (ecc) was more common in black compared to white women (21 vs 7,  $p=0.01$ ).

**Table 1. Black and White Women with a Cytology Negative HPV Positive PAP Test, 2017-2019**

	Black	White	p-value
Total # Patients	915	813	
Median Age (mean)	39 (42.5)	37 (41)	0.05*
HPV 16+	103	146	<0.01
HPV18+	61	36	0.04
HPVother+	798	670	0.02
HPV16/HPV18	5	1	n.s.
Patients who had Colpo	397	371	n.s.
Range Mo. PAP to Colpo	0 - 32	0 - 33	n.s.
Median	3	3	n.s.
Mean	7.2	7.2	n.s.
STDEV	7.4	7.5	n.s.
HPV16+ who underwent Colpo w/ 12 mo.	68 (65%)	91 (62%)	n.s.
HPV18+ who underwent Colpo w/ 12 mo.	43 (70%)	23 (63%)	n.s.
non-16/18 who underwent Colpo w/ 12 mo.	180 (22%)	174 (26%)	n.s.
Bx	229	234	n.s.
BX HSIL	15	21	n.s.
BX LSIL	21	16	n.s.
BX Benign	194	191	n.s.
BX AIS	0	3	n.s.
ECC	365	325	n.s.
ECC HSIL	21	7	0.01
ECC LSIL	18	18	n.s.
ECC Benign	315	296	n.s.
ECC Atypical Glands	0	2	n.s.
ECC AIS	0	0	n.s.
Follow Up PAP	549	506	n.s.
# Months (median)	14	13	n.s.
Range of Months	1 to 36	1 to 32	n.s.
NIEL	454	425	n.s.
ASC-US	59	40	n.s.
ASC-H	8	4	n.s.
LSIL	21	31	n.s.
HSIL	2	1	n.s.
AGC	1	0	n.s.
2nd PAP HPV16+	35	59	<0.01
2nd PAP HPV18+	15	12	n.s.
2nd PAP HPVother	250	219	<0.01

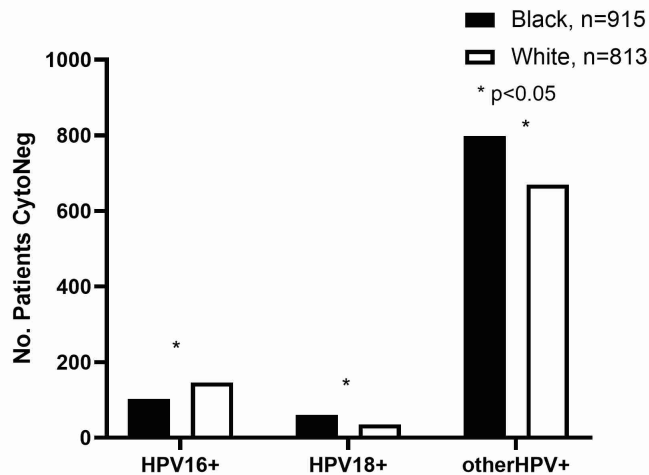


Figure 1-211

**Conclusions:** Follow-up of women with PAPneg/HPVpos remains a challenge (61%). There was no disparity in follow up when both cohorts were compared. However black women had a higher number of HSIL on ecc.

**212 Fine Needle Aspiration Findings of Extragonadal Germ Cell Tumors and Diagnostic Pitfalls**

Fatima Mir<sup>1</sup>, Ifeanyi Nwadukwe<sup>1</sup>, Matthew Thomas<sup>1</sup>, Patrick McIntire<sup>1</sup>, Christopher Przybycin<sup>1</sup>, Jordan Reynolds<sup>1</sup>

<sup>1</sup>Cleveland Clinic, Cleveland, OH

**Disclosures:** Fatima Mir: None; Ifeanyi Nwadukwe: None; Matthew Thomas: None; Patrick McIntire: None; Christopher Przybycin: None; Jordan Reynolds: None

**Background:** Extragonadal germ cell tumors(EGCTs), either primary or as metastasis are rare. Unlike at gonadal sites, fine needle aspiration(FNA) is an accepted alternative to surgical intervention as a first diagnostic modality for diagnosis of EGCTs. Because gonadal GCTs are barely diagnosed by FNA and EGCTs are rare, the literature on cytologic characteristics of these tumors is very limited and leads to missed/misinterpreted diagnosis. We aim to present our experience with FNAs for the diagnosis of EGCTs, both primary and metastasis from gonadal sites and to discuss diagnostic pitfalls encountered in cytologic interpretation.

**Design:** EGCTs diagnosed on cytology were retrieved from our pathology database. The following data was recorded: patient age and gender, clinical presentation, site of involvement, prior diagnoses and procedure details, time from primary to metastatic disease if applicable, cytologic findings, and follow-up histopathology if available.

**Results:** During a 20-year period(2000-October 2020), a total of 27 cases of EGCTs diagnosed on cytology were identified(26 males, 1 female; 4d-73yrs). The most common site of involvement was mediastinum(7/27), followed by retroperitoneum, fluids, neck, inguinal, lung, liver, thyroid, peripancreatic, abdominal. 6 cases(22%) were primary and 21 cases(78%) were secondary EGCTs. Of the primaries, 2/6 were seminomas and 4/6 were non-seminomatous tumors. 7/21 secondary EGCTs were seminomas followed by teratoma(5/21), yolk sac tumor(4/21), mixed GCT(2/21), undifferentiated(2/21) and 1 choriocarcinoma. In 3/21 secondary EGCTs, the metastases presented with an occult primary. 1/3 cases showed regressed primary testicular tumor. In the remaining 18 secondary EGCTs, the time of presentation of metastases from the initial diagnosis ranged from 1 month to 20 years. EGCT was misinterpreted as “poorly differentiated carcinoma” in 2/27 cases. In 2/27 cases, the primary testicular tumor was mixed malignant germ cell tumor and the metastatic focus showed only mature teratomatous component following chemotherapy.

**Conclusions:** Metastatic germ cell tumor may be the first clinical presentation in a patient with an occult or regressed primary tumor, and should be included as a differential in “cancer of unknown primary”. Cytology alone can be misleading as EGCTs can mimic poorly differentiated carcinomas; clinical presentation, serum tumor



markers, immunocytochemistry should all be taken into consideration before making a diagnosis. Mature teratoma may be the only remaining germ cell tumor component post-treatment. Diagnosis and appropriate management with complete surgical excision is needed in these cases since teratoma can give rise to other malignant GCTs.

**213 Digital Image Analysis Reveals that Plasmacytoid Variant of High-Grade Urothelial Carcinoma has an Average N:C Ratio Below 0.5 in Urinary Cytology**

Fatima Mir<sup>1</sup>, Meredith Nichols<sup>1</sup>, Maria Luisa Policarpio-Nicolas<sup>2</sup>, Jordan Reynolds<sup>1</sup>, Patrick McIntire<sup>1</sup>  
<sup>1</sup>Cleveland Clinic, Cleveland, OH, <sup>2</sup>Cleveland Clinic Foundation, Cleveland, OH

**Disclosures:** Fatima Mir: None; Meredith Nichols: None; Maria Luisa Policarpio-Nicolas: None; Jordan Reynolds: None; Patrick McIntire: None

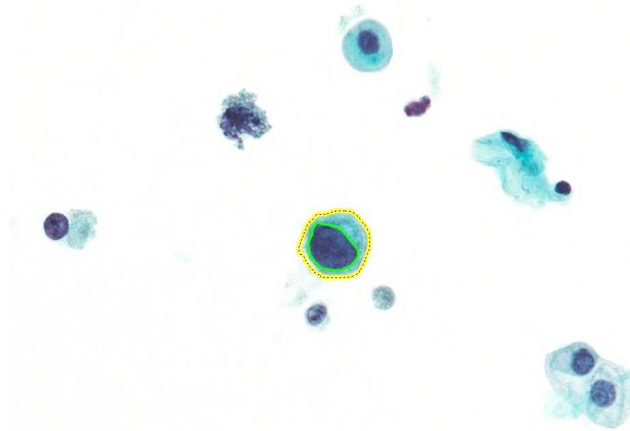
**Background:** The Paris System for Reporting Urinary Cytology (TPS) was first published in 2016 and was designed to standardize the practice. TPS emphasizes diagnosing high-grade urothelial carcinoma (HGUC). N:C ratios are critical for establishing the diagnostic categories in TPS. Major criteria for the atypical urothelial cell (AUC) category requires N:C ratio of  $\geq 0.5$ . The suspicious for high-grade urothelial carcinoma (SHGUC) and positive for HGUC categories require N:C of  $\geq 0.7$ . While these cut-off points have contributed to the major success of TPS, they do not address rare variants of HGUC. Specifically, the plasmacytoid variant of HGUC is a morphologically distinct entity, which is composed of eccentrically placed nuclei and increased cytoplasm. The purpose of this study was to utilize digital image analysis to calculate N:C ratios in urine specimens with plasmacytoid variant of HGUC.

**Design:** Urine specimens with diagnoses of SHGUC or HGUC with biopsy proven plasmacytoid variant HGUC follow-up within 30 days of the index case were identified. ThinPrep slides were reviewed along with biopsy specimens to ensure the cytomorphology was concordant. Whole-slide images were scanned at a 40x magnification and digital annotations of the nuclear and cytoplasmic membranes were performed (**Figure 1**). Cells with degeneration artifact, unclear cytoplasmic borders and disrupted nuclear/cytoplasmic borders were excluded.

**Results:** The final cohort consisted of 5 cases of plasmacytoid HGUC in urine specimens. The average age of the patients were 69.8 years (range: 56-83 years). Two of the patients were female (40%, 2/5) and three were male (60%, 3/5). Two specimens were of the upper urinary tract (40%, 2/5) and three were of the bladder (60%, 3/5). 30 HGUC cells were analyzed per case for a total of 150 cells. The results of the individual cases are available in **Table 1**. The average nuclear circumference was 39.9  $\mu\text{m}$ , nuclear area was 103.5  $\mu\text{m}^2$ , cytoplasmic circumference was 61.6  $\mu\text{m}$  and cytoplasmic area was 235.0  $\mu\text{m}^2$ . The average N:C ratio was 0.44.

Case	Nuclear circumference (um)	Nuclear area (um <sup>2</sup> )	cytoplasmic circumference (um)	Cytoplasmic area (um <sup>2</sup> )	N:C ratio
1	55.5	161.1	73.7	345.5	0.47
2	37.2	83.0	59.0	211.9	0.39
3	34.1	76.4	54.0	163.7	0.47
4	32.6	77.1	58.5	208.6	0.37
5	40.0	120.1	62.6	245.6	0.49
average	39.9	103.5	61.6	235.0	0.44

Figure 1 - 213



**Conclusions:** While morphologically the plasmacytoid variant of HGUC may be diagnosed in urine specimens, the average N:C ratio is below the threshold for AUC category (<0.5) in TPS.

#### 214 Thyroid Malignancy in Effusion, Our Institutional Experience

Fatima Mir<sup>1</sup>, Renuka Malenie<sup>1</sup>, Maria Luisa Policarpio-Nicolas<sup>2</sup>

<sup>1</sup>Cleveland Clinic, Cleveland, OH, <sup>2</sup>Cleveland Clinic Foundation, Cleveland, OH

**Disclosures:** Fatima Mir: None; Renuka Malenie: None; Maria Luisa Policarpio-Nicolas: None

**Background:** Malignant effusions secondary to thyroid malignancies are extremely rare. Because of the paucity of the literature on cytologic characteristics of these tumors in fluid cytology, it could be a diagnostic challenge. Our aim is to examine the incidence of thyroid malignancy involving effusion cytology, review the cytologic features, ancillary tests and patient's clinical demographic.

**Design:** A computerized search for fluid cytology with thyroid malignancy diagnosis from 2000-2020 was performed. All available cases were reviewed. The following data were collected: patients' age and gender, original histologic diagnosis, cytology and immunohistochemical findings.

**Results:** Of the 47,593 non-gynecologic fluid specimens processed in our laboratory from 2000-2020, there were only 9 thyroid malignancies in the pleural fluid. No cases were seen in the peritoneal and pericardial cavity. The original histologic type of all 9 cases was papillary carcinoma. There were 5 females and 4 males with an age range of 55-86 years (median=74). The cytologic findings showed malignant cells with large nuclei, round to irregular nuclear borders, small inconspicuous to prominent nucleoli, and occasional intracytoplasmic vacuoles (Figure 1). Some of the tumor cells showed fuzzy cytoplasmic borders. The tumor cells were arranged singly, in clusters/acinar and some with scalloped borders easily mimicking adenocarcinoma and mesothelioma. Only two cases showed Psammoma bodies. In 8/9 cases, the cytomorphic diagnosis was rendered utilizing immunohistochemical stains performed on the cell block (PAX-8, TTF-1 and thyroglobulin in 6 cases and thyroglobulin in 2 older cases) [Figure 2]. Immunohistochemistry was not performed in one case and the diagnosis was rendered after the cytologic material was compared with a prior pleural biopsy.

Figure 1 - 214

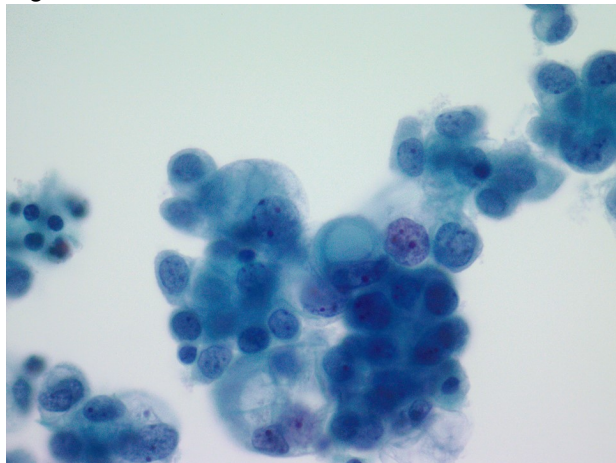
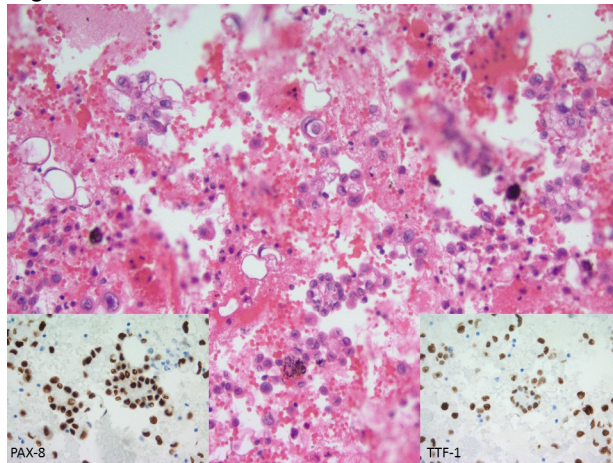


Figure 2 - 214



**Conclusions:** The incidence of thyroid malignancy in fluid cytology is extremely rare (<0.01%). It often involves the pleural cavity and the most common histologic type is papillary carcinoma. The cytologic findings are nonspecific and could easily mimic adenocarcinoma or mesothelioma. Psammoma bodies are not always present. In pleural fluid, immunohistochemical stains PAX-8 and thyroglobulin are useful markers supportive of thyroid primary, in the right clinical setting.

## 215 Development and Validation of a Dual Color/Multiplex Stain for MUC4 and STAT6 for Assessment of Cytologic/Small Biopsy Samples of Spindle Cell Lesions

Daniel Neal<sup>1</sup>, Natalie Overby<sup>1</sup>, Steven Smith<sup>2</sup>, Raghavendra Pillappa<sup>1</sup>

<sup>1</sup>VCU Health System, Richmond, VA, <sup>2</sup>VCU School of Medicine, Richmond

**Disclosures:** Daniel Neal: None; Natalie Overby: None; Steven Smith: None; Raghavendra Pillappa: None

**Background:** Two useful immunohistochemical (IHC) stains emergent in recent years include STAT6 and MUC4, for the identification of solitary fibrous tumors (SFTs; STAT6), low grade fibromyxoid sarcoma (LGFMS; MUC4) and most recently, meningiomas (MUC4). Small biopsy and cytology differential diagnoses of spindle cell tumors is challenging, and the differential diagnosis (including that of CNS SFT/hemangiopericytoma versus meningioma), often includes multiple lesions in this group. In light of treatment differences and to maximize tissue preservation, we sought to develop a dual color STAT6/MUC4 multiplex stain for aspirates, cores, and small biopsies in this differential.

**Design:** We developed and validated an automated dual color multiplex stain using anti-STAT6 (clone EP325/YE361; predilute, brown chromogen), and anti-MUC4 (clone 8G7; predilute, red chromogen). Testing included a cohort of retrospectively-identified cases of well characterized SFTs, LGFMSs, and meningiomas, confirmed diagnostically by IHC and/or molecular diagnostics. The validation cohort included these lesions and other spindle cell lesions in the differential.

**Results:** A total of 61 samples (14 LGFMSs, 11 SFTs, 5 desmoid-type fibromatoses, 5 intramuscular myxomas, 10 meningiomas, 6 neurofibromas, 5 schwannomas and 5 synovial sarcomas) were tested. Overall, 14/14 LGFMSs were positive for MUC4; all LGFMSs were negative for STAT6. In contrast, 10/11 SFTs were positive for STAT6; all were negative for MUC4. Dual stain concordance was 100% when comparing available send out IHC and molecular testing. Lastly, 8/10 meningiomas were MUC4 positive, as were at least focal cells in all 5 cases of monophasic synovial sarcoma. The dual stain cocktail was completely negative in all cases of desmoid fibromatosis, intramuscular myxoma, neurofibroma and schwannoma. No sample showed positivity for both marker.

**Conclusions:** This dual stain for STAT6/MUC4 is facile and useful in clinical scenarios where small specimens would require separate IHCs to address the SFT, LGFMS, and/or meningioma differential. As seen previously in

biphasic and even focally in monophasic synovial sarcoma, focal MUC4 positivity actually supports synovial sarcoma diagnosis as evidence of epithelial differentiation, and with other markers may help secure that diagnosis. In the head and neck, the SFT versus meningioma differential is also a promising emerging use of these markers.

**216 Utility of Concurrent Common Bile Duct (CBD) Brushing Cytology and Endoscopic Ultrasound-Guided Fine Needle Aspiration (EUS-FNA) for Solid Pancreatic Neoplasms**

Quoc Nguyen<sup>1</sup>, Nivedita Suresh<sup>2</sup>, Kamal Khurana<sup>3</sup>

<sup>1</sup>SUNY Upstate Medical University, Syracuse, MA, <sup>2</sup>University of Rochester Medical Center, Rochester, NY, <sup>3</sup>SUNY Health Science Center, Syracuse, NY

**Disclosures:** Quoc Nguyen: None; Nivedita Suresh: None; Kamal Khurana: None

**Background:** Accurate preoperative cytopathological diagnosis is important for management of pancreatic masses. Both endoscopic ultrasound-guided fine needle aspiration (EUS-FNA) and common bile duct (CBD) brushing cytology have been used for diagnosis of pancreatic solid neoplasms. However, none of the prior studies have focused on concurrent use of these two methods to provide accurate preoperative diagnosis of pancreatic neoplasms. This study aims at retrospectively determining the usefulness of concomitantly performed EUS-FNA and CBD brushing for cytopathological diagnosis of solid pancreatic neoplasms.

**Design:** Computerized search of laboratory information system for patients whose underwent concurrent EUS-FNA of the pancreas and CBD brushing from January 2018 to October 2019 was performed. Cytology reports were reviewed for positive for malignancy, suspicious for malignancy, atypical cytology, and benign. Histological and clinical follow-up was available in all cases. Negative cases had at least one year of clinical or radiologic follow up. Sensitivity and specificity for the two methods (separately and combined) were calculated. For calculation purposes, atypical/suspicious cases were considered true positive if the final outcome were malignant.

**Results:** Sixty-five patients were included in this study (mean age is 68.5 years, and male to female ratio is 36:29). Based on surgical and clinical follow up, 38 (58.5%) malignant pancreatic neoplasms were identified and the remaining 27 (41.5%) lesions were benign. Sensitivity and specificity of EUS-FNA alone was 86.8 and 100%, respectively. CBD brushing alone yielded a sensitivity and specificity of 52.6% and 100%, respectively. Five of the 38 (13.15%) malignant pancreatic tumors were exclusively detected on CBD brushing cytology. Combined EUS-FNA and CBD brushing had 100% sensitivity and specificity.

**Conclusions:** EUS-FNA is superior to CBD brushing cytology for diagnosis of solid pancreatic neoplasms. However, combination of these methods results in improved diagnostic accuracy.

**217 Immunophenotypical Analysis of SMARCA4 (BRG1) Deficient Non-Small Cell Lung Carcinoma Diagnosed on Cytology Specimens**

Oluwaseun Ogunbona<sup>1</sup>, Daniel Lubin<sup>2</sup>, Michelle Reid<sup>2</sup>, Keriann Van Nostrand<sup>3</sup>, Frank Schneider<sup>3</sup>, Qiuying Shi<sup>3</sup>

<sup>1</sup>Emory University School of Medicine, Atlanta, GA, <sup>2</sup>Emory University Hospital, Atlanta, GA, <sup>3</sup>Emory University, Atlanta, GA

**Disclosures:** Oluwaseun Ogunbona: None; Daniel Lubin: None; Michelle Reid: None; Keriann Van Nostrand: None; Frank Schneider: None; Qiuying Shi: None

**Background:** Inactivation of SMARCA4/BRG1 (Brahma-related gene 1), a member of the SWItch/Sucrose Non-Fermentable (SWI/SNF) subfamily of ATP-dependent chromatin remodeling complexes, has increasingly been demonstrated in a subset of non-small cell lung carcinomas (NSCLCs). Cytomorphologic features of BRG1-deficient lung neoplasms have only rarely been reported.

**Design:** Four cytology specimens of BRG1-deficient NSCLC were identified. Cytomorphology was reviewed for features that could prospectively prompt BRG1 testing in this setting.



**Results:** Four BRG1-deficient carcinoma cases were identified. Patients ranged in age from 61- 71 years with a M:F of 1:1. Two had a history of previous carcinomas (one laryngeal squamous and the other a renal cell carcinoma) diagnosed >35 years earlier and the other two had >40 pack/year smoking history. Cytologically, tumors were epithelioid and poorly differentiated featuring marked large pleomorphic cells, moderate to abundant cytoplasm, nuclei with coarse to vesicular chromatin, and prominent nucleoli. Three cases showed loosely cohesive cells and two cases had focal plasmacytoid/rhabdoid morphology. Two cases showed intracytoplasmic mucin. All cases demonstrated BRG-1 loss, were positive for AE1/AE3 and CK7, and negative for TTF-1 and p40/p63. One case was positive for synaptophysin. One had metastasized to the thigh at the time of diagnosis.

**Tumor size and Immunophenotypical analysis**

Case #	Tumor size (cm)	BRG-1	INI-1	AE1/3	CK7	TTF-1	Napsin A	p40	p63	Synaptophysin
1	4.9	Lost	Retained	+	+	-	-	-	NR	+
2	5.2	Lost	Retained	+	+	-	+, rare cells	-	NR	-
3*	3.5	Lost	NR	+	+	-	-	NR	-	NR
4	2.1	Lost	Retained	+	+	-	-	-	NR	-

NR: not run  
\* referral case

Figure 1 - 217

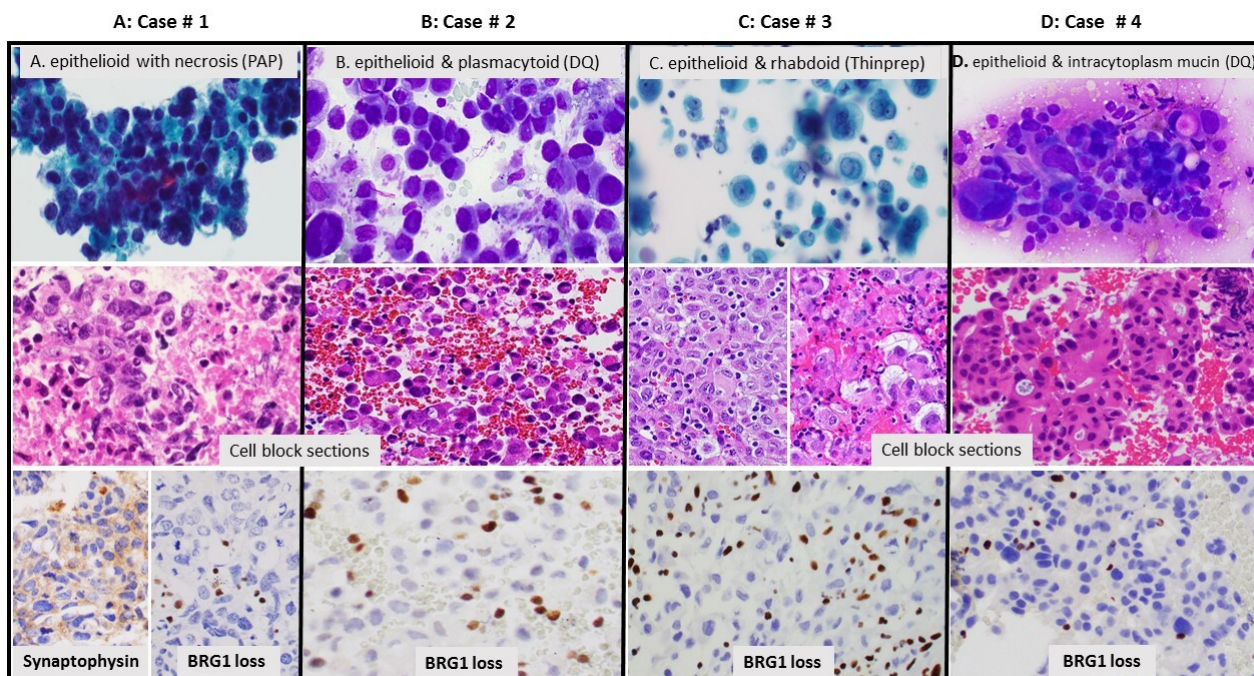


Figure: Cytomorphologic features and immunohistochemistry staining for BRG-1 deficient carcinoma

**Conclusions:** BRG1-deficient NSCLCs appeared to exhibit high-grade cytological features, with rhabdoid morphology in two cases, and lacked expression of lung adenocarcinoma/squamous markers in all cases. Increased awareness of the cytomorphologic and immunophenotypic features of this entity can ensure diagnostic consideration on fine needle aspiration (FNA) thereby avoiding delayed diagnosis. Carcinomas with neuroendocrine features should be included in this differential.

**218 Automated Detection of Atypical Cells in Urine Cytology Using Deep Anomaly Detection**

Inyoung Paik<sup>1</sup>, Han Suk Ryu<sup>2</sup>, Tae-Yeong Kwak<sup>3</sup>, Sun Woo Kim<sup>1</sup>, Hyeyoon Chang<sup>1</sup>

<sup>1</sup>Deep Bio Inc., Seoul, South Korea, <sup>2</sup>Seoul National University College of Medicine/Hospital, Seoul, South Korea, <sup>3</sup>Deep Bio Inc., Guro-gu, South Korea

**Disclosures:** Inyoung Paik: *Employee*, Deepbio Inc.; Han Suk Ryu: *None*; Tae-Yeong Kwak: *Employee*, Deep Bio Inc.; Sun Woo Kim: *Stock Ownership*, Deep Bio Inc.; Hyeyoon Chang: *Employee*, Deepbio Inc.

**Background:** Urine cytology is a commonly used test for the evaluation of patients with various urological symptoms. It is also an important test for initial diagnosis and follow-up for a patient suspected or with urothelial carcinoma. It is a time-consuming and labor-intensive task for cytopathologists and cytotechnicians to find atypical or malignant cells in hundreds or thousands of cells. Also, there are concerns about low interobserver agreement even by well-trained cytopathologists or cytotechnicians.

Deep learning is one of the most powerful tools to evaluate and classify images. We can expect great benefit if automated detection or screening by a deep learning model is worked. But labelling each cell rises another problem. We propose deep learning-based anomaly detection model, which requires only slide-level diagnosis.

**Design:** The 1,161 Urine cytology glass slides from a single institution were collected and scanned using Aperio AT2 digital slide scanner (Leica Biosystems Imaging, Inc., Vista, CA, United States). Hospital diagnosis is used as ground-truth. 976 of them were benign and 187 of them were abnormal. The data were randomly sampled into training/validation/test set at a ratio of 0.7 : 0.15 : 0.15 = 812 : 174 : 175.

We used a deep semi-supervised anomaly detection framework. We used a 2-model ensemble of MNasNet for embedding and metric loss was applied to separate benign and abnormal data. For each iteration, Randomly sampled ImageNet data and Gaussian noise image was added as abnormal data. Unlike usual, we used metric loss which pulls the abnormal images to the origin and sends benign images as far as possible from the origin. Also, strong L2 weight decay was applied to keep abnormal data near the origin.

**Results:** Sample image patches that classified as benign (Figure 2, first row) and abnormal (Figure 2, 2nd row) are shown. The model's abnormal detection AUC was 0.857. Since not every image patch from an abnormal slide is not abnormal, we randomly sampled 300 image patches classified as benign, and 300 patches classified as abnormal. Compared with ground truth by a pathologist, the model's sensitivity and specificity were 0.879 and 0.617. (Table 1)

	(Pathologist) Benign	(Pathologist) Abnormal
(Model) Benign	283	17
(Model) Abnormal	176	124

Figure 1 - 218

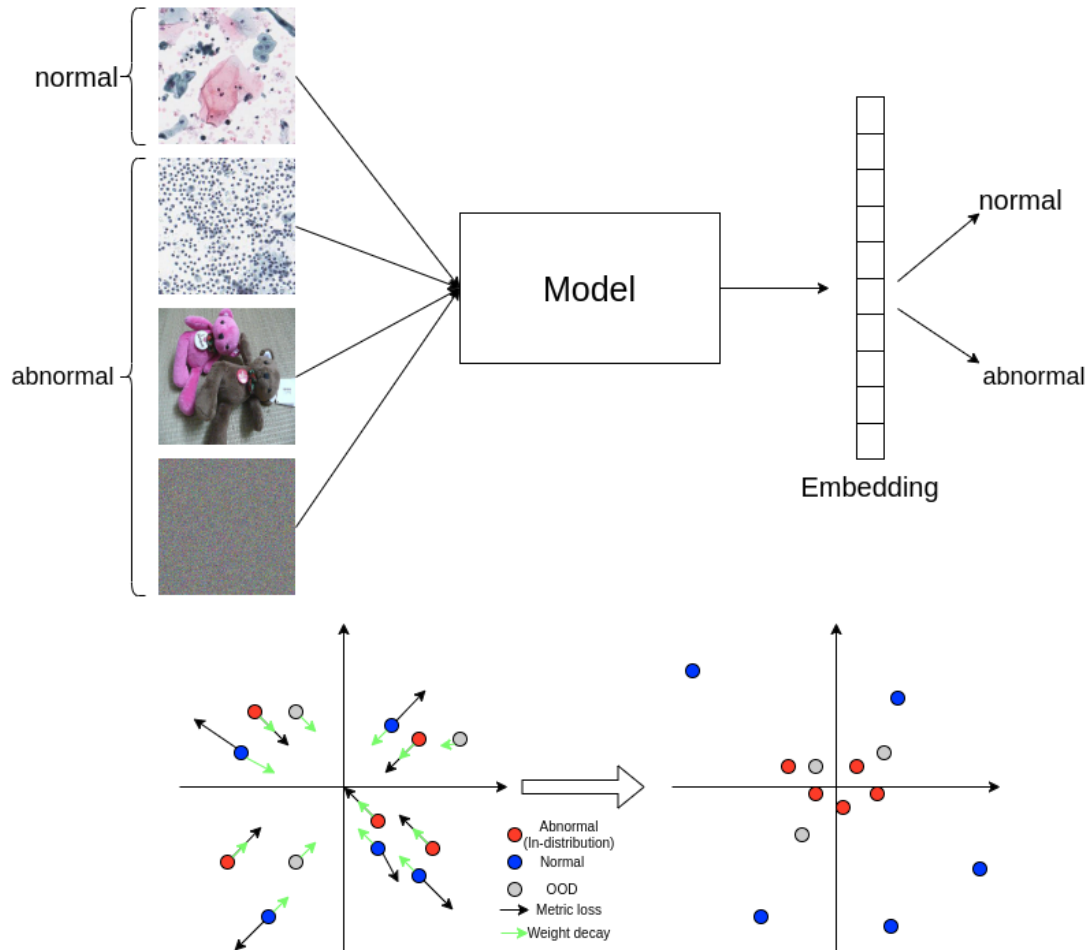
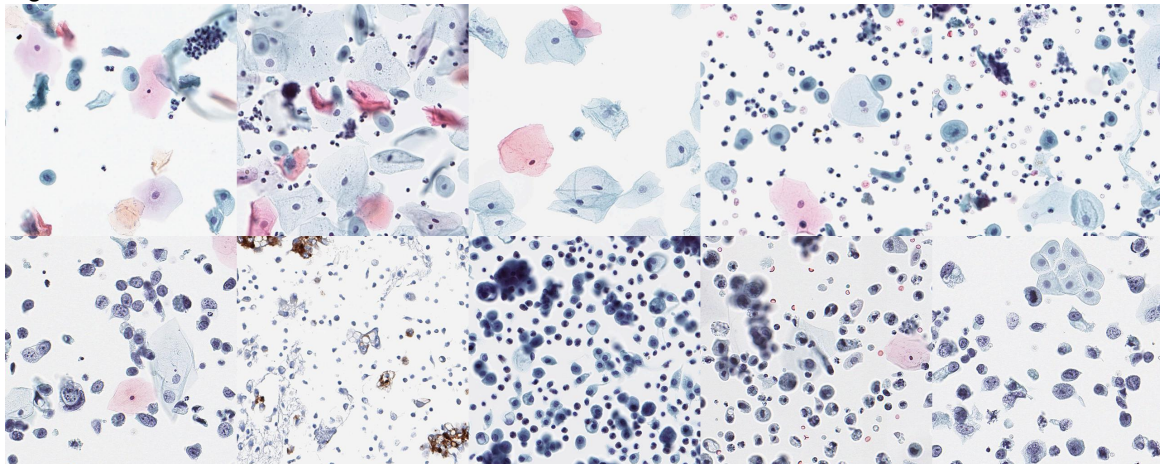


Figure 2 - 218



**Conclusions:** Although performance still needs to be improved, our study suggests the possibility that deep learning models can reduce human labor through screening in urine cytology.



**219 Cytologic Features of Gynecologic and Non-Gynecologic Neoplasms with Rhabdomyosarcomatous Differentiation**

Fanni Ratzon<sup>1</sup>, Lu Wang<sup>1</sup>, Abeer Salama<sup>1</sup>, Liz Edmund<sup>1</sup>, Marina Baine<sup>1</sup>, Rajmohan Murali<sup>1</sup>

<sup>1</sup>Memorial Sloan Kettering Cancer Center, New York, NY

**Disclosures:** Fanni Ratzon: None; Lu Wang: None; Abeer Salama: None; Liz Edmund: None; Marina Baine: None; Rajmohan Murali: None

**Background:** Rhabdomyosarcoma (RMS) is the most common soft tissue sarcoma of childhood and can be found rarely in adults. RMS may also be seen as a heterologous element in gynecologic carcinosarcomas. Histologic features of RMS and carcinosarcomas with a RMS component have been well-described. Cytologic diagnosis may be challenging because of their rarity and morphologic overlap with other entities particularly in the absence of characteristic ‘rhabdoid’ morphology.

**Design:** Tumors with a histologically confirmed RMS component in women, diagnosed between 2003 and 2019 with available cytologic specimens were identified. Cytomorphologic characteristics (listed in the Table) were independently evaluated by a cytopathology fellow, a cytotechnologist and a cytopathologist, and consensus was reached on any discrepant parameters.

**Results:** The study cohort consisted of tumors from 18 women, aged 3-75 (median 31) years. The 6 gynecologic cases included 4 carcinosarcomas with heterologous RMS (67%), embryonal RMS (1, 17%) and RMS not otherwise specified (1, 17%). The 12 non-gynecologic tumors included alveolar RMS (6, 50%), embryonal RMS (2, 17%), spindle cell RMS (2, 17%), pleomorphic RMS (1, 8%) and RMS, not otherwise specified (1, 8%). Cytologic features are detailed in the Table. No intracytoplasmic vacuoles or diffusely eosinophilic cytoplasm indicating myogenic differentiation nor multinucleation were found. One case (spindle cell RMS) exhibited bizarre cell shapes (‘tadpole’) cells. Mitotic figures and necrosis were rare. Four peritoneal washings in patients with carcinosarcomas with RMS showed malignant cells, which (in the absence of identifiable distinctive rhabdoid features) may have represented the carcinomatous component of the primary tumor. Two cases (RMS, not otherwise specified and alveolar RMS) showed a small round cell population, raising a cytomorphologic differential diagnosis including such as lymphoma and small cell carcinoma, among others.

Age at Diagnosis	Histologic finding/ Site	Cytologic specimen/ Site	Cellularity	Cellular arrangement/Single cells	Nuclear/ Cytoplasmic ratio	Nuclear shape	Chromatin pattern	Nuclear irregularities	Conspicuous Nucleoli
10	RMS-S /Paraspinal	Fluid/Trunk	Moderate	Single cells	Moderate/	Spindle occasional bizarre/ 'tadpole' cells	Vesicular	Irregular	-
73	RMS-P /Forearm	FNA/Forearm	Moderate	Single cells	Low to moderate	Round/oval	Coarse	Irregular	+
64	RMS-A /Paranasal sinus	TP/Sacrum	Moderate	3D clusters/ Single cells	Low to high	Round/oval	Coarse	Irregular /lobulated	+
21	RMS-A /Foot	TP/ Foot	Moderate	3D clusters/ Single cells	Moderate	Round/oval	Coarse	Irregular /lobulated	+
22	RMS NOS /Cheek	FNA/Cheek	High	Single cells	High	Oval	Fine	Irregular /lobulated	-
18	RMS-A /Calf	FNA/Tibia	High	Loosely cohesive aggregates/ Single cells	High	Round/oval	Coarse	Irregular /lobulated	-
4	RMS-A /Hand	FNA/ Pancreas	Moderate	Small clusters/ Single cells	High	Round	Coarse	Mildly irregular	-
8	RMS-A /Pancreas	Fluid/ Pleura	Low	Single cells	High	Round	Coarse	Irregular /lobulated	+
3	RMS-E / Spinal cord	Fluid/ CSF	Low	Single cells	High	Round	Fine	Irregular	-

7	RMS-E /Pelvic peritoneum	Fluid/ Peritoneum	Moderate	3D clusters/ Single cells	High	Round/oval	Coarse	Irregular	-
75	RMS-E/Maxilla /Gingiva	FNA/ Neck level II LN	Moderate	3D clusters/ Single cells	High	Round/oval	Coarse	Irregular	-
40	RMS-A/Groin	FNA/ Groin	Moderate	3D clusters/ Single cells	High	Round/oval	Coarse	Irregular	-
3	RMS-E/Vagina	Fluid/Urine	Moderate	Small 3D clusters/ Single cells	High	Round/oval	Coarse	Irregular	-
70	RMS NOS /Ovary	TP/ Lung	Moderate	Loosely cohesive aggregates/ Single cells	Low to moderate	Round/oval	Coarse	Irregular	+
65	CS-RMS/Uterus	TP/ Peritoneum	Moderate	Small clusters/ Single cells	Moderate	Round/oval	Coarse	Irregular	+
64	CS RMS/Uterus	Fluid/ Pelvic washing	Moderate	Small 3D clusters	Moderate	Round/oval	Coarse	Smooth	-
69	CS-RMS/Uterus	Fluid/ Pelvic washing	Low	Single cells	High	Round/oval	Coarse	Irregular	+
50	CS-RMS/Uterus	Fluid/ Pelvic washing	Low	Small clusters/ Single cells	Moderate	Round	Coarse	Irregular	+

Abbreviations: CS carcinosarcoma; CS-RMS carcinosarcoma with heterologous rhabdomyosarcoma element; CSF cerebrospinal fluid; FNA fine needle aspiration; RMS NOS Rhabdomyosarcoma, not otherwise specified; RMS-A alveolar RMS; RMS-E embryonal RMS; RMS-S Spindle cell RMS; RMS-P Pleomorphic RMS; TP touch preparation

**Conclusions:** Pathognomonic ‘rhabdoid’ morphologic features of RMS such as rhabdoid/strap/tadpole cells and cytoplasmic striation are exceedingly rare in cytologic specimens from patients with RMS and carcinosarcomas with an RMS component. Careful search for these features, allied with a high index of suspicion in specimens exhibiting a ‘small round cell tumor’ morphology may (with the help of confirmatory ancillary tests, such as immunochemistry and molecular analysis) aid accurate diagnosis.

**220 Analysis of Salivary Gland Cyto-Histologic Discrepancies in a Major Cancer Center**

Fanni Ratzon<sup>1</sup>, Marina Baine<sup>1</sup>, Dominique Feliciano<sup>1</sup>, Bin Xu<sup>1</sup>, Nora Katabi<sup>1</sup>, Oscar Lin<sup>1</sup>, Xiao-Jun Wei<sup>1</sup>  
<sup>1</sup>Memorial Sloan Kettering Cancer Center, New York, NY

**Disclosures:** Fanni Ratzon: None; Marina Baine: None; Dominique Feliciano: None; Bin Xu: None; Nora Katabi: None; Oscar Lin: *Consultant, Hologic; Consultant, Janssen*; Xiao-Jun Wei: None

**Background:** Fine needle aspiration biopsy (FNA) plays a critical role in the management of patients with salivary gland lesions. Definitive diagnosis can be difficult due to the wide range of lesions that can have overlapping morphologic features, leading to potential interpretation errors. We therefore aimed to analyze the cytologic-histologic discrepancies identified in the quality assurance program of a major cancer center in cases of salivary gland FNA and their potential causes.

**Design:** Salivary gland FNA performed over a period of 12 years were reviewed and correlated with subsequent salivary gland surgical resections. The cytologic diagnoses for these cases were re-categorized according to the Milan system for reporting salivary gland cytopathology (MSRSGC) based on the original reports. The cases were analyzed for potential cyto-histologic discrepancies (overcall and undercall, respectively) defined as those in which the primary cytologic diagnosis could potentially result in unnecessary surgery or delay of treatment.

**Results:** The final diagnoses from a total of 2586 cases of salivary gland were reviewed. Subsequent resections were available for comparison in 669 (25.9%) cases. Of the 669 cases, 28 (4.2%) were classified as non-diagnostic and 71 (10.6%) as atypical. The surgical resection matched the MSRGC diagnostic category (non-neoplastic, neoplastic-benign, and neoplastic-malignant) in 499 cases (74.9%). The remaining 71 (10.6%) cases had diagnostic discrepancies (overcalls or undercalls). The overall findings are summarized in Table 1. The overall incidence was 2.5% (17/669), and the undercall incidence was 8.1 % (54/669). A detailed analysis showed that 17 of 46 (37%; 2/17, 11.8% overcalls; 15/17, 88.2% undercalls) misinterpreted malignancies were neoplasms containing a major myoepithelial component. In the malignant cases that were interpreted as non-neoplastic on



FNA, 5 of 13 (38.5%) were lymphomas that were not initially worked up with flow cytometry studies. Of the 26 malignant cases that were undercalled as neoplastic-benign, 10 (38.5%) were cases originally diagnosed as pleomorphic adenomas that were diagnosed as carcinoma ex-pleomorphic adenoma on resection. Oncocytic features, mucoid background and inflammation were also identified as features associated with cyto-histologic discrepancies.

Cytologic diagnosis	Histologic diagnosis			Total Cases	Discrepant Cases
	Non-neoplastic	Neoplastic Benign	Neoplastic Malignant		
1. Non - diagnostic	8	11	9	28	0
2. Non - neoplastic	40	15	13	68	28
3. Atypical	16	25	30	71	0
4a. Neoplasm Benign	1	74	26	101	27
4B. Neoplasm of uncertain potential (SUMP)	10	49	81	140	10
5. Suspicious for malignancy	3	1	36	40	4
6. Malignant	1	1	219	221	2
<b>Total</b>	79	176	414	669	71
<b>Distribution and incidence of discrepancies</b>					
	<b>Undercall</b>	<b>Overcall</b>	<b>TOTAL DISCREPANCY</b>		
<b>Number of Cases</b>	54	17	71/669		
<b>Incidence (%)</b>	8.1%	2.5%	10.6%		

**Conclusions:** Myoepithelial-rich lesions, lymphomas are the most common entities associated with underdiagnosis in salivary gland cytopathology. Carcinomas ex-pleomorphic adenoma diagnosis can be challenging in cytology specimens. The use of category 4B in the MSRSGC is appropriate for lesions with abundant myoepithelial cells.

**221 SATB2 and CDX2 Expression in Pancreaticobiliary Adenocarcinoma and Metastatic Esophageal and Colorectal Adenocarcinoma on Cytology Specimens**

Shuyue Ren<sup>1</sup>, Alan Tsai<sup>2</sup>

<sup>1</sup>Cooper University Hospital, Camden, NJ, <sup>2</sup>Cooper Medical School of Rowan University, Camden, NJ

**Disclosures:** Shuyue Ren: None; Alan Tsai: None

**Background:** SATB2, special AT-rich sequence binding protein-2, is a transcriptional regulator and has been shown to be a highly sensitive and specific marker of normal colorectal epithelium and colorectal adenocarcinoma. SATB2 and CDX2 have been used as markers of colorectal origin; however, their expression is not entirely specific. Cytology aspiration specimen is often the first diagnosis for a malignancy of unknown primary but, it is challenging to determine the origin. The primary aim of this study was to evaluate the expression of SATB2 and CDX2 on cytology specimens in primary and metastatic pancreaticobiliary adenocarcinoma, metastatic esophageal adenocarcinoma and metastatic colorectal adenocarcinoma.

**Design:** From our cytopathology database, 68 cytology specimens from 2019 to 2020 were selected. There were 7 cases of pancreatic adenocarcinoma; 11 cases of metastatic pancreaticobiliary adenocarcinoma to liver, lymph node, bone and ascites; 5 cases of metastatic esophageal adenocarcinoma to liver, lymph node and pleural fluid; 45 cases of metastatic colorectal adenocarcinoma to liver, lymph node, lung, omentum, bone, pleural fluid, ascites and pelvis. SATB2 and CDX2 immunohistochemical stains were performed with adequate controls on the cell block materials of the 68 specimens.

**Results:** The SATB2 and CDX2 immunohistochemical staining results are summarized in table 1. SATB2 and CDX2 both showed nuclear staining and the patterns were focal or diffuse. Overall, CDX2 showed more frequent and less specific expression than SATB2 in all types of examined adenocarcinoma. There were 2 cases negative for SATB2 in 45 metastatic colorectal adenocarcinoma and they were liver metastasis of rectal primary. CK7 was positive in all 18 and CK20 was focally positive in 8 of the 18 cases of pancreaticobiliary adenocarcinoma. CK7 and CK20 were both positive in 4 of the 5 cases of metastatic esophageal adenocarcinoma.

TABLE 1. SATB2 and CDX2 expression in adenocarcinoma on cytology specimens

	Primary pancreaticobiliary	Metastatic pancreaticobiliary	Metastatic esophageal	Metastatic colorectal
SATB2+/CDX2+	1 (14.3%)	2 (18.2%)	3 (60%)	43 (95.6%)
SATB2+/CDX2-	0	1 (9.1%)	0	0
SATB2-/CDX2+	4 (57.1%)	5 (45.6%)	2 (40%)	2 (4.4%)
SATB2-/CDX2-	2 (28.6%)	3 (27.3%)	0	0
Total SATB2+	1 (14.3%)	4 (36.4%)	3 (60%)	43 (95.6%)
Total CDX2+	5 (71.4%)	7 (63.6%)	5 (100%)	45 (100%)
<b>TOTAL</b>	<b>7</b>	<b>11</b>	<b>5</b>	<b>45</b>

**Conclusions:** This is the first study to evaluate SATB2 and CDX2 expression on cytology specimens in metastatic gastrointestinal and pancreaticobiliary adenocarcinoma. SATB2 and CDX2 expression is sensitive for colorectal adenocarcinoma, but not entirely specific. Our results showed that these markers were also frequently expressed in metastatic esophageal adenocarcinoma. SATB2 expression was identified in a small portion of pancreaticobiliary adenocarcinoma compared to CDX2. SATB2 was observed to be expressed in mores cases of metastatic pancreaticobiliary adenocarcinoma (36.4%) than pancreatic primary adenocarcinoma (14.3%).

**222 Utility of Cell Block Preparation for Bronchoalveolar Lavage Specimens: An Institutional Review of Cases Over Five Years**

FNU Sakshi<sup>1</sup>, Salvatore Luceno<sup>1</sup>, Danial Mir<sup>1</sup>, Hamza Ashmila<sup>1</sup>, Suad Taraif<sup>1</sup>  
<sup>1</sup>Temple University Hospital, Philadelphia, PA

**Disclosures:** FNU Sakshi: None; Salvatore Luceno: None; Danial Mir: None; Hamza Ashmila: None; Suad Taraif: None

**Background:** Bronchoalveolar lavage (BAL) is commonly used to investigate a variety of disease processes in the lower respiratory system including surveillance for opportunistic infections in lung transplant patients. At our institution, analysis of BAL specimens is routinely done using a combination of Liquid-based cytology (LBC), Cytospin and cell block (CB) preparations. While the use of a CB to increase the diagnostic yield of BAL specimen for cancer diagnosis has been established, the utility of CB in the transplant setting has not been thoroughly evaluated. In this study, we aim to evaluate and the contribution of CB to the cytological evaluation of BAL specimens.

**Design:** All BAL specimens examined between 2015-2020 were retrospective retrieved from our departmental archives. The following clinicopathologic data was collected: age, gender, volume of specimen, gross characteristic of specimen, cytologic preparation type, cytologic diagnosis, cell block diagnosis, change in diagnosis on cell block, concurrent surgical specimen diagnosis, history of transplant, and history of malignancy. Cytological findings on LBC and Cytospin were compared with those on CB.

**Results:** 617 BAL specimens were reviewed (Table 1). Most specimens were reported as benign/negative for malignancy (n=573, 92.9%). Specimens reported as non-diagnostic (n=4, 0.6%), atypical (n=18, 2.9%), positive for *pneumocystis jiroveci* (n=13, 2.1%) and suspicious/positive for malignancy (n=9, 1.4%) constituted the remaining cases in the diagnostic cohort. CB could not be made in 26/617 specimens (4.2%) due to insufficient material, in 44/617 cases (7.1%) CB was non-diagnostic, in 175/617 specimens (28.4%) CB was reviewed simultaneously with LBC and Cytospin, hence the additional diagnostic value of CB in those cases cannot be verified. However, evaluation of 372/617 cases (60.3%) revealed no change in diagnosis on the subsequent CB examination when compared with the LBC and Cytospin preparations. 302 specimens (49%) were from patients with prior history of transplant (surveillance BAL specimens).

<b>Bronchoalveolar Lavage Specimens Summary</b>			
<b>Cytologic Diagnosis</b>	<b># of Cases (n=617) (%)</b>	<b>Age, years Mean (range)</b>	<b>Gender M=Male F=Female</b>
Non-diagnostic (ND)	4 (0.6)	64 (64)	2M/2F
Benign/Negative for malignancy (NFM)	573 (92.9)	59.8 (20-89)	326M/247F
Positive for <i>P. jiroveci</i>	13 (2.1)	51.92 (26-74)	12M/1F
Atypical	18 (2.9)	63.8 (43-86)	10M/8F
Suspicious for malignancy (SFM)/Malignant (PFM)	9 (1.4)	66.9 (59-81)	6M/3F
	<b>GMS/special stain performed</b>	<b>Change in Diagnosis on CB</b>	
<b>No CB/Non-contributory CB (n=70); 26 – CB not made, 44 – CB non-contributory</b>	Yes	Cannot be assessed	
<b>CB reviewed simultaneously with LBC/Cytospin/Both (n=175)</b>	Yes	Cannot be assessed	
<b>Subsequent CB preparation (n=372)</b>	Yes	No (100%)	

**Conclusions:** The study identified no significant contributions from a CB when utilized as an adjunct to concurrent conventional preparations (LBC/Cytospin with routine GMS stain) in BAL specimens in the transplant setting. CB preparation can be considered on selective basis if there is suspicion for malignancy. Reallocating resources to exclude CB preparations on BAL specimens can be considered without compromising patient care.

**223 Pericardial Fluid Cytology: An Institutional Review of Cases Over Twenty Years**

FNU Sakshi<sup>1</sup>, Israh Akhtar<sup>2</sup>, Nirag Jhala<sup>1</sup>, Suad Taraif<sup>1</sup>, Aileen Grace Arriola<sup>1</sup>

<sup>1</sup>Temple University Hospital, Philadelphia, PA, <sup>2</sup>Temple University Hospital, Fox Chase Cancer Center, Philadelphia, PA

**Disclosures:** FNU Sakshi: None; Israh Akhtar: None; Nirag Jhala: None; Suad Taraif: None; Aileen Grace Arriola: None

**Background:** Pericardial fluid (PF) is an uncommon body fluid specimen and interpretation can be challenging. This is evidenced by prior studies demonstrating a poorer concordance rate in the diagnostic accuracy of PF compared to other body fluids. In this study, we retrospectively reviewed institutional PF cases to see whether any clinicopathologic parameters relate to diagnostic categories and compare PF to pleural fluid (PLF) cases.

**Design:** PF (1999-2019) and PLF (2/1/19-9/28/20) cases were retrieved and the following data collected: diagnosis, age, gender, fluid volume, immunocytochemical stains (ICC) performed, subsequent submission of PF, and malignancy history. Diagnostic categories were revised to fit the international system for reporting serous fluids (TIS) (nondiagnostic/ND, negative for malignancy/NFM, atypia of undetermined significance/AUS, suspicious for malignancy/SFM, and malignant/PFM). Association of categorical and continuous values was assessed with chi-square and student T-test, respectively; 0.05 p-values were considered significant.

**Results:** 380 cases were identified (Table). ND cases had a lower mean fluid volume (95mL) compared to other categories (253mL) (p-value=0.26). ICC were more frequently performed in AUS, SFM, and PFM cases compared to NFM. Similarly, such cases often had a known malignancy vs. NFM (SFM+PFM, 85% and AUS, 38% vs. NFM, 24%). Lung was the most common primary (28/53, 53%) followed by breast (3/53, 6%). A significant number of cases were not further classified after ICC (14/53, 26%). Subsequent submission of additional PF was not significantly different in AUS+SFM+PFM vs. NFM. Compared to a similarly sized cohort of PLF, AUS rate was higher and ICC more frequently utilized in PF vs. PLF (p-value<0.05). However, there was no significant difference in the use of ICC for AUS cases between the two groups. ICC confirmed the atypical cells as mesothelial in nature in 35% and 50% of PF and PLF cases, respectively. Finally, a gross description of bloody PF was not significantly different in cases of PFM+SFM (82%) as compared to AUS+NFM (70.2%) (p-value=0.11).

<b>Pericardial Fluid Summary and Analysis</b>			
<b>Diagnostic Category</b>	<b># of Cases (n=380) (%)</b>	<b>Age, years Mean (range)</b>	<b>Gender</b>
Non-diagnostic (ND)	2 (0.5)	71 (71)	0 M/2 F
Negative for malignancy (NFM)	274 (72.1)	57 (14-92)	119 M/155 F
Atypical (AUS)	41 (10.8)	59 (29-88)	16 M/25 F
Suspicious for malignancy (SFM)	10 (2.6)	53 (25-76)	4 M/2 F
Malignant (PFM)	53 (14)	56 (20-85)	26 M/27 F
	<b>AUS, SFM, and PFM Diagnosis (n=104)</b>	<b>NFM Diagnosis (n=274)</b>	<b>p-value</b>
<b>Immunostains</b>	71 (68%)	36 (13%)	<b>&lt;0.00001</b>
Performed	33 (32%)	238 (87%)	
Not Performed			
<b>Prior history of malignancy</b>	54 (52%)	63 (23%)	<b>&lt;0.00001</b>
Present	31 (30%)	197(72%)	
Absent	19 (18%)	14 (5%)	
Unknown			
<b>Subsequent Pericardial Fluid Sent</b>	13 (12.5%)	31 (11.3%)	0.748117
	91 (87.5%)	243 (88.7%)	



Yes			
No			
<b>Pericardial vs. Pleural Fluid Analysis</b>			
	<b>Pericardial fluid (n=380)</b>	<b>Pleural fluid (n=307)</b>	<b>p-value</b>
<b>Diagnosis</b>	41 (10.8%)	19 (6.2%)	<b>0.033717</b>
Atypical	339 (89.2%)	288 (93.8%)	
Non-atypical			
<b>Immunostains</b>	107 (28%)	47 (15%)	<b>0.000059</b>
Performed	273 (72%)	260 (85%)	
Not Performed			
	<b>AUS Pericardial Fluid (n=41)</b>	<b>AUS Pleural Fluid (n=19)</b>	<b>p-value</b>
<b>Immunostains for Atypical</b>	23 (56.1%)	8 (42.2%)	0.313017
Performed	18 (43.9%)	11 (57.8%)	
Not Performed			

**Conclusions:** This study uncovered that AUS rates were higher in PF vs. PLF. ICC use did not refine the diagnosis in a significant number of AUS and malignant PF. Hence, the threshold for atypia should remain higher in PF vs. other body fluids. This emphasizes the need for systematic guidelines in reporting PF cytology and investigating the application of TIS AUS criteria for such specimens to avoid overdiagnosis of atypia.

**224 Assessing Morphologic Features in Malignant Pleural Mesothelioma in Cytology Specimens: Reliability, Utility and Implications**

Abeer Salama<sup>1</sup>, Marina Baine<sup>1</sup>, Prasad Adusumilli<sup>1</sup>, Darren Buonocore<sup>1</sup>, Michael Offin<sup>1</sup>, Marjorie Zauderer<sup>1</sup>, Natasha Rekhtman<sup>1</sup>, William Travis<sup>1</sup>, Oscar Lin<sup>1</sup>, Jennifer Sauter<sup>1</sup>  
<sup>1</sup>Memorial Sloan Kettering Cancer Center, New York, NY

**Disclosures:** Abeer Salama: None; Marina Baine: None; Prasad Adusumilli: None; Darren Buonocore: None; Michael Offin: None; Marjorie Zauderer: None; Natasha Rekhtman: None; William Travis: None; Oscar Lin: *Consultant*, Hologic; *Consultant*, Janssen; Jennifer Sauter: None

**Background:** Morphologic features including architectural patterns, nuclear grade and necrosis assessed in histologic specimens have been shown to have prognostic significance in epithelioid malignant pleural mesothelioma (MPM). However, cytology specimens are often the first, or occasionally the only, pathology available for patients with MPM. The aim of this study is to investigate the reliability of assessing these morphologic features in cytology specimens.

**Design:** Architectural patterns (tubulopapillary, trabecular, micropapillary, solid and pleomorphic), nuclear atypia (1-3) and presence/absence of necrosis were retrospectively assessed in cytology specimens (20 touch preparations (TP), 4 FNA, and 16 fluids) and in paired surgical pathology specimens from patients (n=40) with MPM. Diagnoses were confirmed on histology by WHO criteria. All available cytology slides for each case including aspirate smears, ThinPrep and cell block slides were reviewed. Agreement between cytology and histology was determined using unweighted Kappa scores. Discordant cases were re-reviewed by at least 2 (and up to 4) thoracic pathologists and/or cytopathologists with expertise in MPM.

**Results:** Interpretation of nuclear atypia in cytology specimens showed strong agreement with surgical biopsies (Kappa=0.84, p<0.0001). Presence of necrosis and assessment of architectural patterns showed fair agreement (Kappa=0.22 and 0.3, respectively). However, in one case with a focal pleomorphic pattern identified on histology, areas of tumor cells with pleomorphic features were also seen on cytology material. Upon re-review, most discordant cases were due to sampling differences among cytology and surgical pathology specimens.

**Table1:** Assessment of morphologic features in paired cytology and histology specimens of epithelioid malignant pleural mesothelioma.

	<b>Kappa*</b>	<b>p-value</b>
<b>Surgical vs cytology</b>		
Nuclear atypia	0.84	<0.001
Necrosis	0.22	0.08
Architecture	0.03	0.51
<b>Nuclear atypia by specimen type</b>		
Surgical vs Touch preparation (n=20)	0.86	<0.001
Surgical vs Fluids (n=16)	0.89	<0.001
Surgical vs FNA (n=4)	1.0	<0.001

\*p-value corresponds to a two-sided hypothesis test comparing interpretations on paired cytology and histology specimens (>0.5 moderate agreement,>0.7 good agreement,>0.8 strong agreement).

**Conclusions:** Nuclear grading of epithelioid MPM is accurate in cytology specimens and has strong agreement with histologic grade, while assessment of necrosis and architectural patterns in cytology specimens is more limited. Further study investigating identification of pleomorphic pattern in cytology specimens is warranted, due to its potential importance in clinical management decisions.

**225 A Large Community Hospital Experience: Does High-Risk HPV Testing Improve Accuracy in Detection of CIN2+ Lesions in ASC-H Postmenopausal Women?**

Christine Salibay<sup>1</sup>, Zhengshan (Allen) Chen<sup>2</sup>, Wafaa Elatre<sup>2</sup>, Sue Martin<sup>1</sup>, Tiannan Wang<sup>3</sup>  
<sup>1</sup>Keck School of Medicine of USC, Los Angeles, CA, <sup>2</sup>LAC+USC Medical Center, Los Angeles, CA, <sup>3</sup>University of Southern California, Keck School of Medicine of USC, LAC+USC Medical Center, Los Angeles, CA

**Disclosures:** Christine Salibay: None; Zhengshan (Allen) Chen: None; Wafaa Elatre: None; Sue Martin: None; Tiannan Wang: None

**Background:** A Pap test diagnosis of ASC-H for a woman of any age results in a colposcopy regardless of high risk human papilloma virus (hrHPV) testing results, which has been implemented for years according to the ASCCP 2012 and 2019 guidelines. Reflex HPV testing with an ASC-H diagnosis is not recommended due to the perceived high 5-year cancer risk. New studies have shown HPV-negative ASC-H patients are at low risk for CIN2+ lesions on colposcopic follow-up. To decrease the burden of diagnostic work-up and to avoid over-treatment in postmenopausal women, we herein assess the efficacy of reflex HPV testing in postmenopausal women with ASC-H cytology and histologic follow-up in the Los Angeles County community hospitals.

**Design:** We retrospectively reviewed cases over five years (June 1, 2015 to August 25, 2020) with a PAP smear diagnosis of ASC-H in women aged ≥ 45 years old. Histopathologic follow-up, hrHPV testing and genotyping results were collected and analyzed.

**Results:** Of 108 patients with a diagnosis of ASC-H, 92.6% (100/108) were clinically postmenopausal with ages ranging from 45 to 79 years old. Eight women were excluded due to no follow-up biopsy and HPV results were

available for 85 women. 75.2% identified as Hispanic and 25.9% were non-Hispanic. 37.6% (32/85) were HPV negative and 62.4% (53/85) were HPV positive. Thirty-one (36.5%) women were found to have CIN2+ lesions on follow-up biopsy. Five HPV negative women (5.9%) had CIN2+ lesions. Of the women with CIN2+ lesions, 13 patients (15.3%) were hrHPV 16/18/45 positive and 13 patients (15.3%) were hrHPV-other subtype positive. A positive HPV was 3.1 times increased risk of developing CIN2+ lesions (95% CI 1.34 to 7.35, p=0.008). hrHPV 16/18/45 was 2.3 times increased risk developing CIN2+ lesion than hrHPV-other subtype (95% CI 1.9 to 32.7, p=0.048).

**Table 1. Detection Rate of CIN2+ Lesions in Postmenopausal Women with ASC-H and hrHPV Genotype Results**

HPV Results	Total No. (%)	CIN2+ No.	Negative / CIN1 No.	P-value	RR <sup>1</sup>	95% CI <sup>2</sup>
HPV positive	53 (62.4)	26	19 / 8	0.0084	3.13	1.34 - 7.35
HPV 16/18/45	19 (35.8)	13	5 / 1	0.0005	3.97	1.82 - 8.65
HPV other	34 (64.2)	13	14 / 7	0.0224	1.65	1.07 - 2.54
HPV negative	32 (37.6)	5	18 / 9	-	-	-

<sup>1</sup>RR = relative risk, <sup>2</sup>CI = confidence interval

**Conclusions:** Postmenopausal women with ASC-H Pap results have a higher CIN2+ detection rate if HPV positive with hrHPV 16/18/45 patients showing an increased risk of developing CIN2+ lesions versus hrHPV-other subtype. Triaging ASC-H postmenopausal women with HPV co-testing or hrHPV genotyping, which provides additional risk stratification, should be considered as optimal clinical practice for cervical cancer screening. Of note, our patients of predominant Hispanic ethnicity have equal incidences of hrHPV 16/18/45 and hrHPV-other genotypes suggesting other hrHPV genotypes may carry an equal or higher risk of progression of CIN in varying ethnicities, particularly in postmenopausal women.

**226 A Novel Approach for Computational Classification of Pancreatobiliary Cytopathology**

Briana Santo<sup>1</sup>, Xiaobing Jin<sup>2</sup>, Pinaki Sarder<sup>1</sup>

<sup>1</sup>SUNY Buffalo, Buffalo, NY, <sup>2</sup>University at Buffalo, SUNY, Buffalo, NY

**Disclosures:** Briana Santo: None; Xiaobing Jin: None; Pinaki Sarder: None

**Background:** Pancreatobiliary cytology (PBC) remains a challenging field. Cytology specimens acquired from endoscopic retrograde cholangiopancreatography (ERCP) or pancreatic fine needle aspiration (FNA) procedures are requisite for accurate detection of malignancy. However, diagnoses of atypical and suspicious categories are often rendered due to variability in visual assessment of minute cytomorphologic features (e.g., membrane irregularity). Precise prediction of benign, atypical and malignant (B-A-M) categories from digitized cytopathology specimens is essential to improve diagnostic accuracy and patient outcomes. To this end, we developed an AI-assisted tool for computational classification of PBC specimens based on biologically-inspired cytomorphologic features.

**Design:** Thinprep slides of cytological specimens from B-A-M categories were digitized and screened by a cytopathologist to provide ground-truth identification of representative cells [Aperio Versa, Leica, 40X]. Both intra-nuclear and whole-cell image patches were automatically extracted from screened cells. Color and morphological image processing techniques were applied to (i) characterize nuclear texture from intra-nuclear patches, (ii) segment nuclei from whole-cell patches, and (iii) engineer morphometrics from whole nuclei. Nuclear texture was analyzed to detect nuclear hyperchromicity. Shape signatures were engineered from segmented nuclei to quantify the differential irregularity of B-A-M nuclei. A supervised machine learning model, K-Nearest Neighbor (KNN) multiclass, was trained to identify cells as B-A-or-M based on our feature set. 10-fold cross validation was used to assess model performance; The train/test split was 70/30.

**Results:** Computationally-derived textural and morphologic features enabled differentiation of PBC categories (**Fig 1a**) and our model's performance in B-A-M specimen classification (**Fig 1b**).

**Fig 1b: Table w/ performance metrics**

Class	Benign	Atypical	Malignant
Accuracy	0.6667	1.0000	0.6667

Fig 1b) Model performance for classification of PBC specimens as B-A-or-M.

Figure 1 - 226

**Fig 1a: Scatterplot of training and testing**

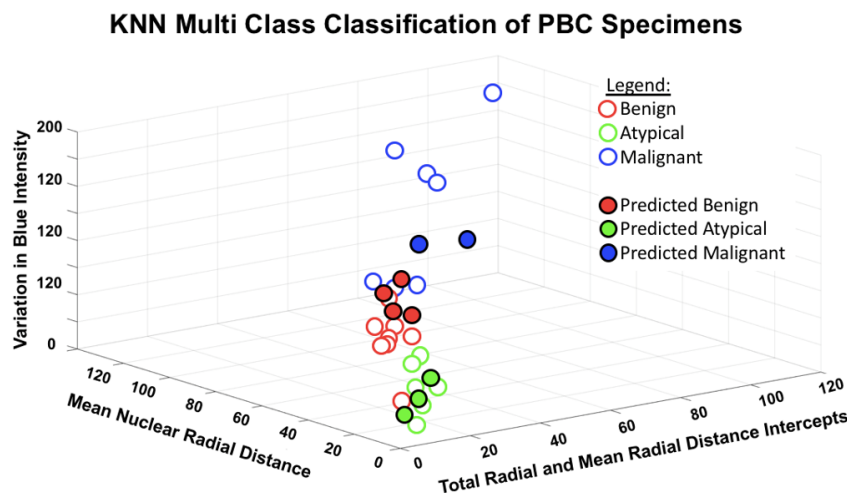


Fig 1a) Classification based on textural and cytomorphologic features. Intra-nuclear texture was quantified as the variation in blue pixel intensity. Nuclear shape signatures were engineered from whole-nuclei. Morphologic metrics were derived from shape signatures including the mean radial distance from the nucleus center to boundary, as well as the quantity of intercepts between all radial and the mean radial nuclear distance.

**Conclusions:** We have demonstrated a novel computational method for automated analysis and classification of PBC specimens. Given recent collection of PBC data from a comprehensive patient cohort ( $n = 60$ , 20 each of B-A-M), conference presentation will feature cohort-wide analysis and expansion of our cytomorphologic feature set. In the current study, our method successfully differentiated atypical from benign and malignant cells, and has potential for application in clinical practice to increase diagnostic accuracy.

**227 High Grade Squamous Intraepithelial Lesions (HSIL) on Cervical Pap Tests with Concomitant Negative High Risk HPV (hrHPV) Test Results**

Mrinal Sarwate<sup>1</sup>, Dawn Underwood<sup>2</sup>, Erica Kaplan<sup>2</sup>, Gary Procop<sup>2</sup>, Jennifer Brainard<sup>2</sup>  
<sup>1</sup>Cleveland Clinic Foundation, Cleveland, OH <sup>2</sup>Cleveland Clinic, Cleveland, OH

**Disclosures:** Mrinal Sarwate: None; Dawn Underwood: None; Erica Kaplan: None; Gary Procop: None; Jennifer Brainard: None

**Background:** Co-testing of women 30 years of age and older with a hrHPV test and Pap is a currently approved method for cervical cancer screening. A recent 2020 update of American Cancer Society cervical cancer screening guidelines recommends primary HPV testing alone as a preferred method of screening for average risk patients

between the ages of 25 to 65 years. We decided to study our experience with HSIL pap tests that are hrHPV negative and correlate with surgical pathology follow up.

**Design:** We reviewed Thin Prep® (Marlborough, MA) Pap tests performed at our institution over a period of 46 months between 10/12/2016 to 08/31/2020 with a HSIL Pap and negative hrHPV test. All hrHPV tests were performed directly on the ThinPrep PreservCyt® Solution using the Roche cobas®HPV test (Basel, Switzerland) which detects 14 hrHPV types and provides individual results on the highest risk genotypes HPV 16 and HPV 18. HrHPV tests were repeated in a subset. Surgical pathology specimens from these patients were reviewed. All diagnoses of HSIL were reviewed for consensus among our subspecialty Gynecologic Pathology group. An immunohistochemical stain (IHC) for p16 (Ventana Medical Systems, Tucson, AZ) and chromogenic in situ hybridization (CISH) (Advanced Cell Diagnostics, Newark, CA) for hrHPV was performed in HSIL cases with available paraffin blocks. CISH detects 18 hrHPV types including HPV types 26, 53, 73 and 82 which are not included in the Roche cobas®test.

**Results:** There were 1056 HSIL Pap tests in 235,035 total Paps during the study period. Of these, 45 were hrHPV negative (4.3%) A repeat hrHPV test was performed in 22 (49%) with a negative result in all cases. All HSIL Paps in our study were re-reviewed by multiple authors and a diagnosis of HSIL was confirmed in all but one case (98%). Surgical pathology follow up was available in 36 cases (80%), which consisted of 11 benign, 1 LSIL and 24 HSIL cases. Results of p16 IHC and hrHPV CISH are summarized in Table 1.

	<b>p16 (block positivity)</b>	<b>hrHPV CISH</b>
Positive	19	8
Negative	2	5
Total number tested	21	13

**Conclusions:** :

- HPV testing alone would miss 45 cases of HSIL in our study population over a 46 month period.
- Repeating the hrHPV test confirmed the negative result in all cases tested.
- Review of hrHPV negative HSIL Paps is prudent to prevent over-treatment.
- Patients with HSIL Paps, negative hrHPV tests and benign follow up may have small HSIL lesions not visible by colposcopy.
- Gynecologic pathology consensus review together with ancillary studies supports a HSIL diagnosis in the majority of cases with available surgical pathology follow up.
- hrHPV CISH results suggest the possibility of a causative HPV type other than those included in the Roche cobas® hrHPV test in a subset of patients.

**228 Comparison of Risk of Malignancy of Indeterminate Thyroid Nodules Analyzed by Utilizing Histologic Findings versus Molecular Data: Experience of Large Health Care System**

Deepika Savant<sup>1</sup>, Nidhi Kataria<sup>1</sup>, Swachi Jain<sup>1</sup>, Bhumika Vadalia<sup>1</sup>, Alanna Chiu<sup>2</sup>, Kasturi Das<sup>3</sup>, Seema Khutti<sup>4</sup>

<sup>1</sup>Donald and Barbara Zucker School of Medicine at Hofstra/Northwell, New York, NY, <sup>2</sup>Donald and Barbara Zucker School of Medicine at Hofstra/Northwell, Lake Success, NY, <sup>3</sup>Northwell Health, Greenvale, NY, <sup>4</sup>Donald and Barbara Zucker School of Medicine at Hofstra/Northwell, Greenvale, NY

**Disclosures:** Deepika Savant: None; Nidhi Kataria: None; Swachi Jain: None; Bhumika Vadalia: None; Alanna Chiu: None; Kasturi Das: None; Seema Khutti: None

**Background:** ThyroSeq version 3(TV3) is the most widely used molecular test in guiding management of thyroid nodules with intermediate cytologic diagnosis (Bethesda III or IV). TV3 identifies genetic mutations associated with thyroid carcinomas in cytology samples and classifies them as either “negative”, “currently negative” or “positive”. Many of the thyroid nodules with intermediate category cytologic diagnosis do not undergo excision and option for



calculating traditional cytologic-histologic correlation (CHC) is limited. Aim of our study was to evaluate molecular derived risk of malignancy (MDROM) in our institution.

**Design:** All thyroid cytology cases of the indeterminate categories (Category III – Atypia of undetermined significance, Category IVA – Suspicious for follicular neoplasm and IVB Suspicious for neoplasm- Hurthle cell neoplasm) from January 2019- June 2020 with adequate TV3 reports (TV3R) were included in the study. Details of probability of carcinoma in numerical values from each TV3R were tabulated and the mean of risk of malignancy (ROM) for each category was calculated. Surgical follow-up of these cases was also noted. The cytohistologic correlation (CHC) was established with rate of malignancy derived in two ways, first- with total number of molecular tested lesions (M) as denominator and second -percentage of malignant cases confirmed with only resected cases as denominator (R). NIFTP was considered as a malignant outcome since it requires a surgical excision.

**Results:** Our cohort consisted of 132 cases with adequate TV3R. We had 95 cases of Category III – Atypia of undetermined significance, 26 cases of Category IV A– Suspicious for follicular neoplasm and 11 cases of Category IVB Suspicious for neoplasm- Hurthle cell neoplasm. The estimated MDROM was 24.3%, 31.7% and 55.1% respectively. Out of 132 cases, 39 cases underwent excision. Upon CHC, the malignancy rates with all cases of molecular testing as denominator were as follows- 11.6% for category III, 34.6% for Category IVA and 27.3% for Category IVB. The malignancy rates with denominator restricted to only excised cases were 55% for category III, 62.9% for Category IVA and 50% for Category IVB. The results are summarized in Table 1.

Table 1. Categorization of molecular reports in each category with molecular derived Risk of malignancy (MDROM) and CHC details

	Total Cases (n)	ThyroSeq 3 report details			Number of excised cases (n)	Histologic diagnosis in excised cases			MDROM	CHC M-R
		Negative (n)	Currently negative (n)	Positive (n)		Benign (n)	NIFTP (n)	Malignant (n)		
Category III	95	51	11	33	20	9	7	4	24.3	11.6 - 55
Category IVA	26	11	2	13	13	4	1	8	31.7	34.6- 62.9
Category IVB	11	2	0	9	6	3	0	3	55.1	27.3 - 50
Total	132	64	13	55	39	16	8	15		

**Conclusions:** MDROM can be used as an alternative method to calculate risk of malignancy in cases with intermediate cytologic diagnosis.

**229 Novel Epigenetic Imprinting Alteration Biomarkers Occur Earlier Than Morphological Changes in Lung Lesions**

Rulong Shen<sup>1</sup>, Tong Cheng<sup>2</sup>, Xing Li<sup>2</sup>, John Pineda<sup>2</sup>, Hongyu Yu<sup>3</sup>, Wenbin Huang<sup>4</sup>, Shaohua Lu<sup>5</sup>, Jian Zhou<sup>6</sup>, Jie Hu<sup>6</sup>, Encheng Li<sup>7</sup>, Ming Ding<sup>8</sup>, Xiaonan Wang<sup>2</sup>, Han Si<sup>2</sup>, Panying Shi<sup>2</sup>, Ning Zhou<sup>9</sup>, Chunxue Bai<sup>6</sup>

<sup>1</sup>The Ohio State University Wexner Medical Center, Columbus, OH, <sup>2</sup>Epigenetics Laboratory, Chinese Alliance Against Lung Cancer, Wuxi, China, <sup>3</sup>Changzheng Hospital, China, <sup>4</sup>Nanjing First Hospital, <sup>5</sup>Fudan University Zhongshan Hospital, Shanghai, China, <sup>6</sup>Zhongshan Hospital, Fudan University, Shanghai, China, <sup>7</sup>The Second Hospital of Dalian Medical University, Dalian, China, <sup>8</sup>Zhongda Hospital, School of Medicine, Southeast University, Nanjing, China, <sup>9</sup>Epigenetics Laboratory, Chinese Alliance Against Lung Cancer, Dalian, China

**Disclosures:** Rulong Shen: None; Xing Li: None; John Pineda: None

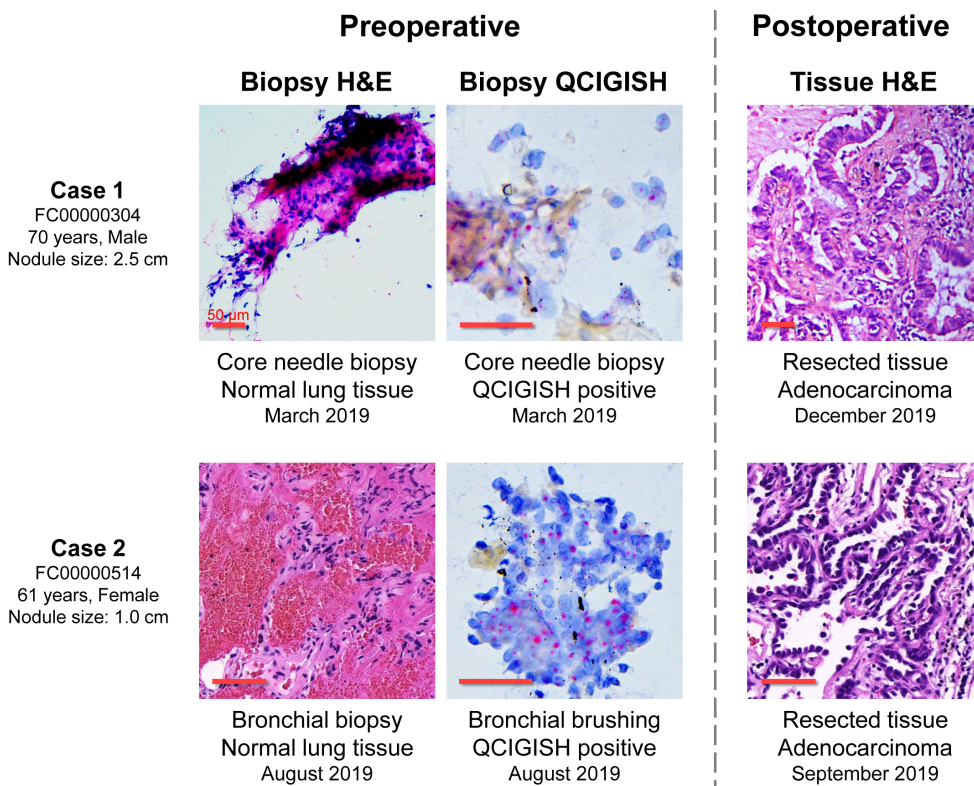
**Background:** Early lung cancer diagnosis presents a critical factor associated with better patient survival. Precise and definitive cancer diagnosis of lung lesions continues to be a clinical challenge for routine diagnostic biopsies in

the absence of sufficient morphological evidences. Epigenetic changes, including imprinting alterations, often occur in early cancers prior to morphology. Here, we investigated the expression alterations of certain imprinting genes as novel diagnostic and predictive biomarkers for lung cancers.

**Design:** We evaluated a total of 351 lung lesion specimens gathered from six Chinese medical centers. We retrospectively applied quantitative chromogenic imprinted gene *in-situ* hybridization (QCIGISH) on 225 postoperative tissue specimens to directly visualize the transcription sites and quantitatively analyze the allelic expression alterations of an imprinted gene panel (*GNAS*, *GRB10*, *SNRPN* and *HM13*), based on which, a malignancy diagnostic grading model was developed. The model was blindly validated on an independent cohort of 126 patients. From this number, we particularly investigated 44 patients who were initially evaluated as indeterminate or benign from cytology or small biopsy pathology, but with final diagnoses determined after monitoring the cases within a 24-month clinical follow-up period.

**Results:** QCIGISH demonstrated excellent overall sensitivity (100%, 8/8) and specificity (94%, 34/36) for the investigation set of 44 cases following a 2-year period. The 34 QCIGISH-negative cases were confirmed benign after the 2-year clinical follow-up. For the 10 QCIGISH-positive cases, results showed that within 2 years, subsequent clinical diagnoses indicated a progressing tumor for 8 of them (with the other 2 cases still under continuous monitoring) which were verified as malignant from CT follow-up evaluation and postoperative histopathology. The malignancies for the 8 cases were effectively predicted by QCIGISH at least 2 weeks to 8 months prior to cancer clinical diagnoses.

Figure 1 - 229



**Conclusions:** With highly sensitive and specific epigenetic imprinting alteration-based biomarkers and a clinically-efficient technique, QCIGISH was presented as an effective tool for a more accurate and definitive diagnosis of pathologically indeterminate and certain benign lung cytology and small biopsy specimens. Early lung cancer detection could drive better clinical outcomes by permitting timely treatment which could ultimately improve lung cancer survival rates.

**230 Hypochromasia: Shedding Light on the “Lightness” of High Grade Urothelial Carcinoma**

Evan Stern<sup>1</sup>, Momin Siddiqui<sup>2</sup>

<sup>1</sup>New York-Presbyterian/Weill Cornell Medical Center, New York, NY, <sup>2</sup>Weill Cornell Medicine, New York, NY

**Disclosures:** Evan Stern: None; Momin Siddiqui: None

**Background:** The Paris system (TPS) has provided a standardized classification system for reporting urinary cytology, specifically high grade urothelial carcinoma (HGUC). While hyperchromasia is considered a well described feature of HGUC, there exists little data on hypochromasia as a finding in HGUC. The focus of our study is to highlight the incidence of hypochromasia in HGUC and whether it should also be included as part of the definitive criteria for diagnosing HGUC.

**Design:** We reviewed all cases of HGUC diagnosed at our institution for a three year interval (2017-2019) using the current criteria set forth by TPS. All cases were examined with a single Thinprep slide and had concurrent biopsy or resection specimens to confirm the diagnosis within 30 days. The presence of nuclear hypochromasia was evaluated, and cases where it was identified were further stratified based on the percent of tumor cells displaying nuclear hypochromasia. Cases showing nuclear hypochromasia in 5% or greater of the total tumor cells in each case are considered “positively identified” for nuclear hypochromasia.

**Results:** Our data set consisted of 119 cases of HGUC with twelve cases having a positive identification for nuclear hypochromasia (12/119, Figure 1 and 2). Nuclear hypochromasia in 50% or more of the tumor cells was identified in four of 119 cases (3.4%) of HGUC (Table 1). Eight out of 119 cases (6.8%) were found to have nuclear hypochromasia in 5-49% of the total tumor cells (Table 1). In total, we found nuclear hypochromasia within 5% or more of the tumor cells in 12 out of 119 cases (10.2%) of HGUC. The remainder of the cases are negative for nuclear hypochromasia. No cases were identified in our data set where nuclear hypochromasia was an isolated feature within the tumor cells.

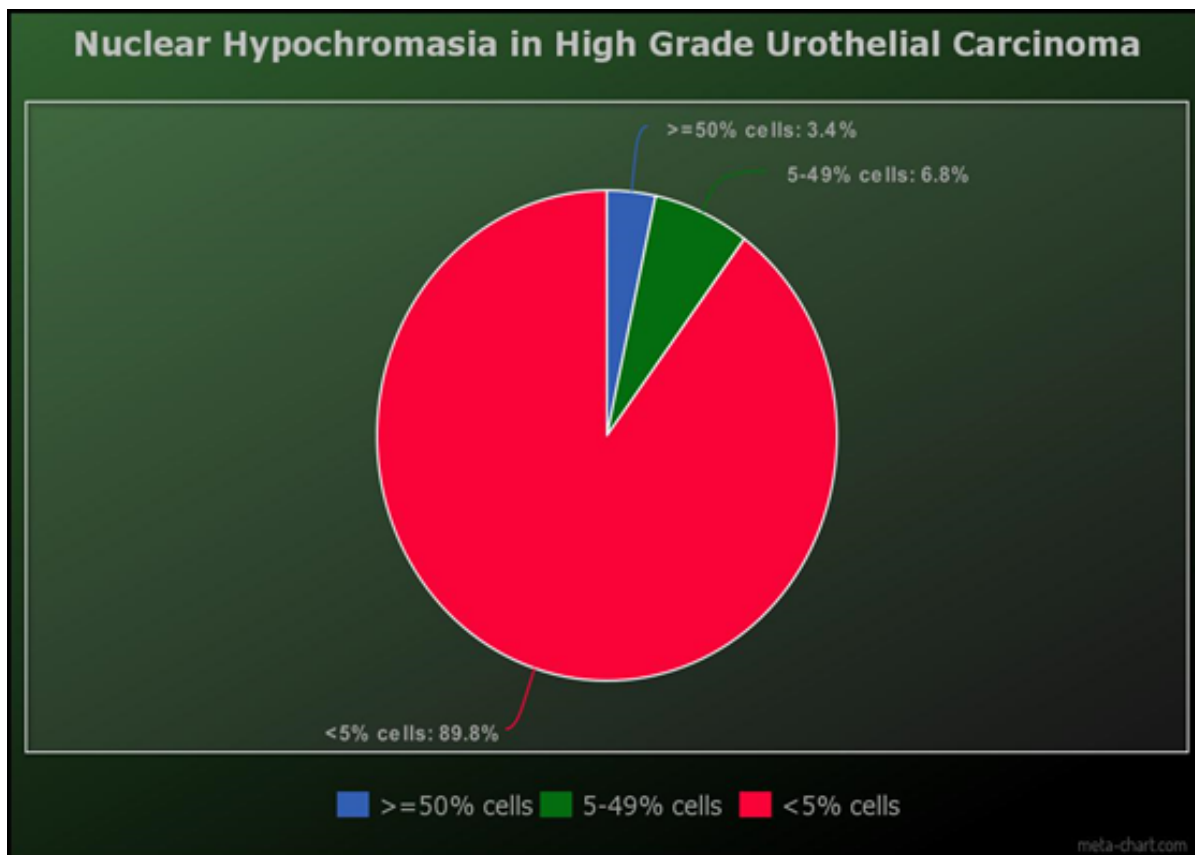


Figure 1 - 230

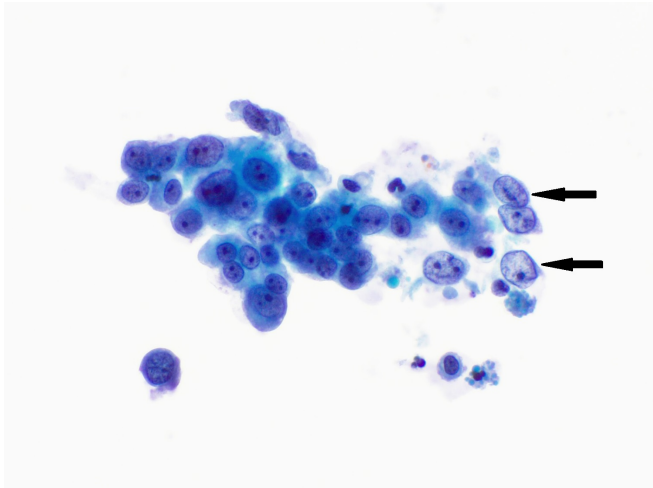
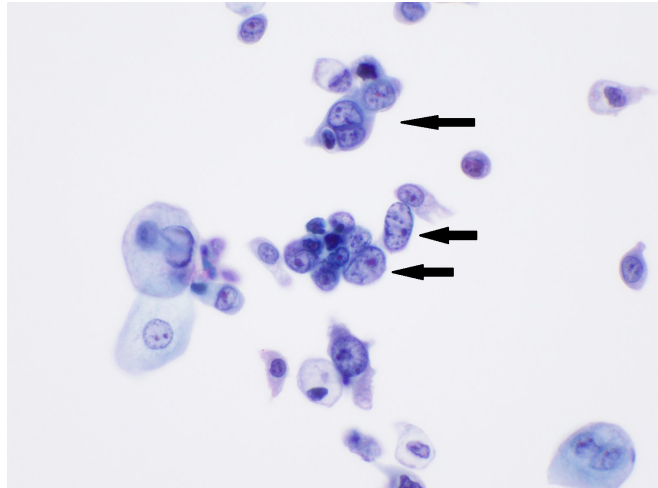


Figure 2 - 230



**Conclusions:** TPS and use of nuclear hyperchromasia as a feature of HGUC is affirmed. However, nuclear hypochromasia, while not diagnostic in isolation, is present in urines and washings of a sub-set of patients with HGUC (10.2%). Further studies into this topic would be beneficial. In conclusion, the presence of nuclear hypochromasia in conjunction with hyperchromatic nuclei, should be considered as a diagnostic feature of HGUC.

**231 Nuclear Expression of NR4A3 by Immunohistochemistry Distinguishes Acinic Cell Carcinoma from its Mimics on Fine-Needle Aspiration Samples**

Xiaoyu Tang<sup>1</sup>, Jianhui Shi<sup>1</sup>, Fan Lin<sup>1</sup>, Haiyan Liu<sup>1</sup>  
<sup>1</sup>Geisinger Medical Center, Danville, PA

**Disclosures:** Xiaoyu Tang: None; Jianhui Shi: None; Fan Lin: None; Haiyan Liu: None

**Background:** Diagnosis of acinic cell carcinoma (AciCC) on fine-needle aspiration (FNA) specimen can be challenging due to cytologic mimics of salivary gland neoplasm with oncocytic cytomorphology and even normal acinar tissue. Recently, a recurrent and specific rearrangement [t(4; 9)(q13; q31)] was identified in the majority of AciCC, which results nuclear overexpression of NR4A3 (nuclear receptor subfamily 4 group A member 3) by immunohistochemistry (IHC). In the current study, we evaluated the expression of NR4A3 by IHC on cell block sections of 40 FNA cases of salivary gland neoplasm with oncocytic cytomorphology, to assess the utility of nuclear expression of NR4A3 in distinguishing AciCC from its mimics on cytology FNA samples.

**Design:** Forty cases of cytology FNA of salivary gland neoplasms showing oncocytic cytomorphology and with followup confirmed diagnoses on surgical resections were retrieved from the archives of laboratory medicine at our institution, including AciCC (N=11), mucoepidermoid carcinoma (n=6), mucinous cystadenoma (n=1), oncocytoma/oncocytosis (n=2), secretory carcinoma (n=1), salivary duct carcinoma (n=2) and Warthin tumor (n=17). Immunohistochemical evaluation of NR4A3 (sc-393902, Santa Cruz Biotechnology Inc.) was performed on cytology cell block sections. The staining distribution was recorded as negative (0 to <5% of tumor cell staining) and positive (>5% of tumor cell staining).

**Results:** The staining results are summarized in Table 1. NR4A3 nuclear expression was identified in 91% (10/11) of AciCC (Fig. 1). All other tumors were negative for NR4A3 (Fig. 2). In addition, the normal acinar tissue showed no nuclear expression for NR4A3 (Fig. 2). Nuclear expression of NR4A3 by IHC has a sensitivity of 91% and specificity of 100% for AciCC.



Table 1. Summary of Expression of NR4A3 in 40 Cytology FNA Cases of Salivary Gland Neoplasms

Diagnosis	Number of Cases	NR4A3 IHC Positive Cases (%)
Acinic cell carcinoma	11	10 (91%)
Mucoepidermoid carcinoma	6	0
Mucinous cystadenoma	1	0
Oncocytoma/Oncocytosis	2	0
Salivary duct carcinoma	2	0
Secretory carcinoma	1	0
Warthin's Tumor	17	0

Figure 1 - 231

Fig. 1 H&E and NR4A3 IHC staining on two cases of acinic cell carcinoma (top x20, bottom x40). Case on bottom shows abundant lymphoid cells I background. H&E, hematoxylin and eosin; IHC, immunohistochemistry.

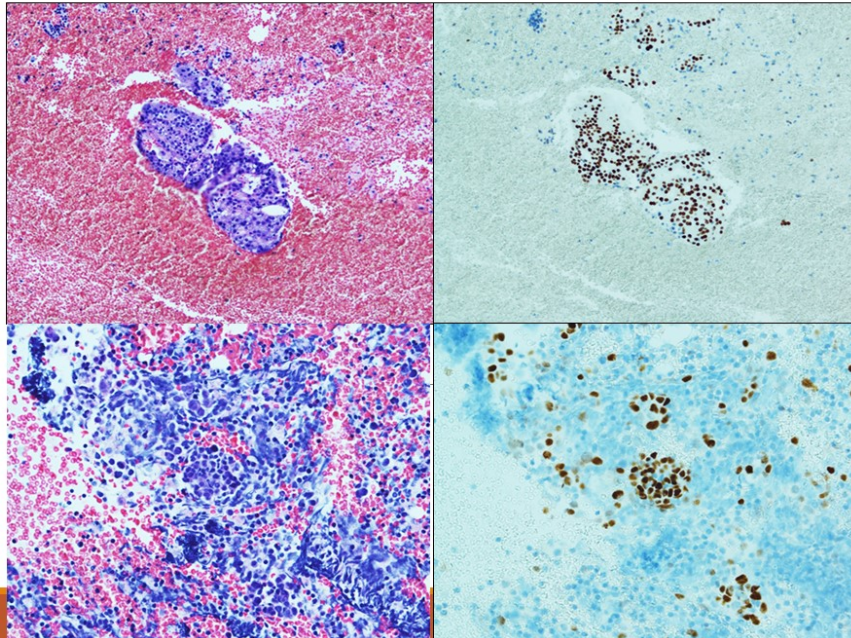


Figure 2 - 231

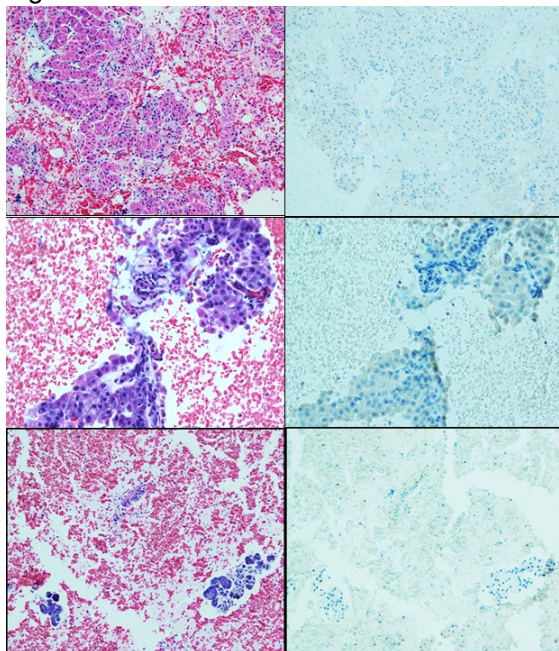


Fig. 2 H&E and NR4A3 IHC staining on selected cases and normal acinar tissue (40). (top) Oncocytoma / Oncocytosis; (mid) mucoepidermoid carcinoma; (bottom) Normal acinar tissue in a case of Warthin's tumor. H&E, hematoxylin and eosin; IHC, immunohistochemistry.



**Conclusions:** Our data demonstrate that nuclear expression of NR4A3 by IHC is highly sensitive and specific for AciCC, and distinguishes AciCC from its mimics; therefore, NR4A3 by IHC can be utilized in cytology FNA samples where the diagnosis of AciCC is considered. Additional large series of study may be necessary to validate our findings.

**232 Adrenal Gland FNA Reporting: A Multi-Institutional Proposal for a Standardized System**

Levent Trabzonlu<sup>1</sup>, Lucy Jager<sup>2</sup>, Seena Tabibi<sup>3</sup>, Margaret Compton<sup>4</sup>, Vivian Weiss<sup>4</sup>, Yonca Kanber<sup>5</sup>, Valentina Robila<sup>6</sup>, Tatjana Antic<sup>7</sup>, Zahra Maleki<sup>8</sup>, Elizabeth Morency<sup>2</sup>, Guliz Barkan<sup>9</sup>  
<sup>1</sup>Loyola University Medical Center, Maywood, IL, <sup>2</sup>Feinberg School of Medicine/Northwestern University, Chicago, IL, <sup>3</sup>Johns Hopkins University, Baltimore, MD, <sup>4</sup>Vanderbilt University Medical Center, Nashville, TN, <sup>5</sup>McGill University Health Centre, Montréal, Canada, <sup>6</sup>Virginia Commonwealth University Health System, Richmond, VA, <sup>7</sup>University of Chicago, Chicago, IL, <sup>8</sup>Johns Hopkins University School of Medicine, Baltimore, MD, <sup>9</sup>Loyola University Healthcare System, Maywood, IL

**Disclosures:** Levent Trabzonlu: None; Lucy Jager: None; Seena Tabibi: None; Margaret Compton: None; Yonca Kanber: None; Valentina Robila: None; Tatjana Antic: None; Zahra Maleki: None; Guliz Barkan: None

**Background:** With the development of new technologies (e.g. endoscopic ultrasonography (EUS)) and the changing patient profiles, cytopathology departments receive increasing numbers of adrenal gland fine-needle aspiration (AG-FNA) specimens. In this multi-institutional study, we analyzed archival AG-FNA cases and attempted to formulate a diagnostic reporting system.

**Design:** Retrospective electronic medical records were reviewed for AG-FNA cases performed at six tertiary care centers from 1995 to 2020. The patients demographics, clinical histories, laterality, and FNA procedure approach were tabulated. The cytology diagnoses were grouped in 6 categories: Unsatisfactory (UNSAT), Negative for malignancy/Benign cortical elements (NEG), Neoplasm of unknown malignant potential – noncortical (NUMP-NC), Atypical (ATY), Suspicious for malignancy (SM), and Malignant (MAL). If available, histopathology results of concurrent/follow-up biopsies/resections were documented.

**Results:** Five hundred and five AG-FNA cases were evaluated from 277 male and 228 female patients. The mean patient age was 65.3 (range 1-108). Overall adequacy rate was 92.7%, with 91.8% for percutaneous FNAs and 93.5% for EUS-guided FNAs (p>0.05). The cytology diagnosis was NEG in 28.9% of the cases and MAL in 57.8%. Seventy-three cases (14.5%) had histology follow-up and showed 94.7% and 94.4% concordance in the NEG and MAL cases, respectively. Four out of 9 NUMP-NC cases had histopathology follow-up and all were diagnosed as pheochromocytoma in histology. There were 3 ATY and 5 SM cases with histopathology follow-up in our cohort. All SM cases and 2 ATY cases were diagnosed as malignant in histology, leaving only one case of ATY not diagnosed malignant in the follow-up. The final diagnosis was "fibroconnective tissue with focal necrosis" for this case (Table). The ATY and SM cases had low cellularity, and lacked qualitative/quantitative evidence of a definitive malignancy on the cytology specimens.

	n	Histopathology diagnosis	Risk of malignancy
Unsatisfactory	37 (7.3%)	6 (8.2%)	1 (16.7%)
Negative for malignancy/Benign cortical elements	146 (28.9%)	19 (26%)	1 (5.3%)
Neoplasm of unknown malignant potential - noncortical	9 (1.7%)	4 (5.4%)	0 (0%)
Atypia of undetermined significance	15 (2.9%)	3 (4.1%)	2 (66.7%)
Suspicious for malignancy	6 (1.1%)	5 (6.8%)	5 (100%)
Malignant	292 (57.8%)	36 (49.3%)	34 (94.4%)
Total	505	73	

**Conclusions:** We propose a 6-tier diagnostic scheme for AG-FNAs: UNSAT, NEG, NUMP-NC, ATY, SM, MAL. In our multi-institutional cohort the risk of malignancy was 94.4% in malignant cases (34/36). Only two cases with discordance had insufficient tissue in the histopathology specimens. There was no difference between EUS-guided and percutaneous AG-FNA. Further studies are recommended to validate and universalize this approach.

**233 Clinical Impact of Endoscopic Ultrasound-Guided Fine Needle Aspirations of Cystic Pancreatic Lesions**

Cindy Wang<sup>1</sup>, Ward Reeves<sup>1</sup>, Ricardo Lastra<sup>1</sup>, Anna Biernacka<sup>1</sup>, Uzma Siddiqui<sup>1</sup>, Irving Waxman<sup>1</sup>, Tatjana Antic<sup>1</sup>

<sup>1</sup>University of Chicago, Chicago, IL

**Disclosures:** Cindy Wang: None; Ward Reeves: None; Ricardo Lastra: None; Anna Biernacka: None; Uzma Siddiqui: None; Irving Waxman: None; Tatjana Antic: None

**Background:** Cystic pancreatic lesions (CPLs) range from benign to malignant. Evaluation of those lesions often includes endoscopic ultrasound-guided fine needle aspirations (EUS-FNA). In recent years, the incidence of CPLs has increased due to the widespread use of advanced imaging studies. Although it is considered a safe procedure, EUS-FNA has associated risks such as bleeding, pancreatitis, and infection. Adequate sampling of the cyst lining is required to make a cytopathological diagnosis. Often these specimens are “non-diagnostic” or “cyst contents.” Due to the anatomy of the CPL, the diagnostic needle travel through normal tissues, such as stomach and duodenum, which may introduce benign mucinous epithelium into the FNA specimen, thus making diagnosis difficult.

**Design:** We searched our archive for CPL cases obtained by EUS-FNA from 2005-2015. Demographics, cytology, and surgical pathology diagnoses of the CPLs were collected via electronic medical record.

**Results:** The study cohort comprised of 724 FNA specimens from 624 patients, of which 261 were male and 363 female. Eighty-four patients had multiple specimens (range 2-4). Of 724 cytology specimens, 187 were “non-diagnostic (ND)” (26%), 351 were “benign” (49%), 83 had “atypical cells” (11%), 42 were “suspicious for neoplasm” (6%), and 61 had definite diagnosis of “neoplasm or malignancy” (8%); see figure 1. Of the 61 definite diagnoses, there were 59 patients, of which 17 had resections (29%). Of the 17 resections, 3 had surgical diagnosis of adenocarcinoma (18%), 6 PEN (35%), 6 IPMN (35%), 1 MCN (6%), and 1 benign cyst (6%). Of the 565 patients with non-definitive diagnosis, 90 had resections (16%), of which 5 had diagnosis of adenocarcinoma (5.6%), 2 PEN (2.2%), 40 IPMN (44%), 15 cystadenoma (18%), 7 MCN (7.8%), 1 solid pseudopapillary tumor (1.1%), 2 adenoma (2.2%), and 18 benign (20%). Of a total of 149 resected cases, there were 8 adenocarcinoma (5.4%), 46 IPMN (31%), 8 PEN (5.4%), 8 MCN (5.4%), 15 cystadenoma (10%), and 19 benign cystic lesions (13%); see table 1. IPMN was the most common diagnosis followed by other neoplasms with low-malignant potential in both definitive and non-definitive diagnosis categories.

Figure 1 - 233

**Distribution of EUS-FNA Specimens (n=724)**

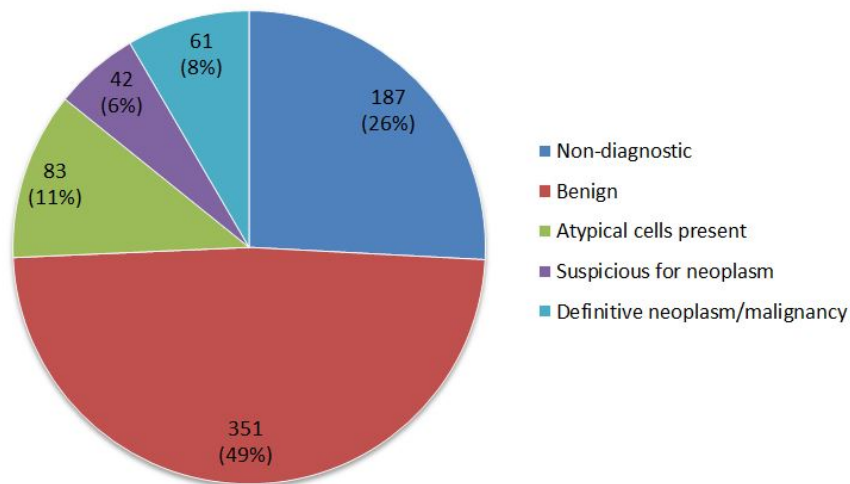


Figure 1: Distribution of cytologic diagnosis of all EUS-FNA specimens.

Figure 2 - 233

Table 1: Distribution of surgical resection diagnosis based on the initial EUS-FNA cytologic diagnosis

Surgical Diagnosis of Resection Specimen	EUS-FNA with Definitive Cytologic Diagnosis (n=17)	EUS-FNA with Non-Definitive Cytologic Diagnosis (n=90)
Adenocarcinoma	3 (18%)	5 (6%)
Intraductal papillary mucinous neoplasm (IPMN)	6 (35%)	40 (44%)
Pancreatic endocrine neoplasm (PEN)	6 (35%)	2 (2%)
Mucinous cystic neoplasm (MCN)	1 (6%)	7 (8%)
Cystadenoma (serous or mucinous)	-	15 (18%)
Adenoma	-	2 (2%)
Benign cystic lesions	1 (6%)	18 (20%)

**Conclusions:** There is a statistically significant difference in resection rates of patients with and without a definitive diagnosis ( $p=0.016$ ). However, the majority of patients with definite cytologic diagnosis (71%) did not receive a resection, and the majority of patients without a definite diagnosis (76%) who had resections fell in either benign (44%) or neoplastic with low malignant potential (54.7%) category. These findings suggest that definitive cytologic diagnosis or lack of thereof did not significantly contribute to surgical management's clinical decision.

**234 Cervical Cancer Screening During COVID-19: Impact of Delayed Follow-Up Evaluation of Unsatisfactory Pap Tests**

Nicole Williams<sup>1</sup>, Priti Sooin<sup>1</sup>

<sup>1</sup>Penn State Health Milton S. Hershey Medical Center, Hershey, PA

**Disclosures:** Nicole Williams: None; Priti Sooin: None

**Background:** During the spring of 2020, many hospital systems suspended elective medical procedures and non-essential outpatient office visits to preserve personal protective equipment and mitigate the spread of novel coronavirus-19, including delayed cancer screening. Cervical cancer screening guidelines were recently updated in 2019 with interim guidance for delayed screening due to COVID-19 published in 2020. We evaluated the significance of delayed cervical cancer screening by looking at outcomes for patients with unsatisfactory pap smears in our hospital system with a retrospective study.

**Design:** All unsatisfactory pap smears reported during the year 2016 were evaluated for follow up by retrospective chart review. There were 300 cases of unsatisfactory Pap smears with concurrent high-risk HPV DNA test results included in this study. Data regarding repeat Pap test time interval, diagnosis, age distribution, and subsequent high-risk HPV DNA test results were mined from the electronic medical record and compared to the American Association of Colposcopy and Cervical Pathology guidelines.

**Results:** The follow-up rate of unsatisfactory pap smears was 75.4% within our system after four years. Only 46.6% of these cases had repeat Pap tests within the recommended guidelines of 4 months. 30.9% had a repeat Pap test within 4-12 months, 16.8% cases within 12-24 months, and 5.7% had follow-up greater than 24 months later.

Repeat Pap tests were negative for intraepithelial lesion in 75.2% of the cases, ASCUS and ASC-H in 1.3% of cases each, LSIL and AGUS in 0.4%, and atrophy reported in 13% of cases. There was a 7.6% repeat unsatisfactory Pap test classification. High-risk HPV positivity increased from 0.07% to 1.2% in repeat Pap tests.

**Conclusions:** A large proportion of cases initially classified as unsatisfactory were negative for intraepithelial lesion on repeat Pap test evaluation. Additionally, an increase in high-risk HPV positivity on follow-up may represent insufficient epithelial component in the initial sample; nonetheless, the percentage remained relatively low. The patients were not subjected to substantial risk from delayed screening due to an unsatisfactory Pap test. Considering the modifications in screening guidelines during the COVID-19 pandemic, this study supports the safety of delayed screening in low-risk populations. Nevertheless, a risk-based approach to each patient is warranted, balancing the potential risks of delayed diagnosis versus risks associated with Covid-19.

**235 Utility of URO17™ (Keratin 17) Immunohistochemistry in ThinPrep Processed Urine Specimens**

Juan Xing<sup>1</sup>, John Cucci<sup>2</sup>, Catherine Cao<sup>3</sup>, Michael Matthews<sup>2</sup>, Liron Pantanowitz<sup>4</sup>

<sup>1</sup>UPMC Shadyside Hospital, Pittsburgh, PA, <sup>2</sup>Acupath Laboratories, Inc., Plainview, NY, <sup>3</sup>University of Pittsburgh, Pittsburgh, PA, <sup>4</sup>University of Michigan, Ann Arbor, MI

**Disclosures:** Juan Xing: None; Catherine Cao: None; Michael Matthews: None; Liron Pantanowitz: None

**Background:** Keratin 17 (K17) is an oncoprotein that drives cell cycle progression in multiple cancers. Studies have shown that K17 is a specific and sensitive biomarker for urothelial neoplasia. We evaluated the utility of a commercially available K17 immunostain (URO17™) in 60 ThinPrep processed urine cytology specimens.

**Design:** Following institutional review board approval, deidentified unstained ThinPrep slides prepared from 60 residual urine specimens of 58 patients were sent to Acupath Laboratory, Inc. (Plainview, NY) for URO17™ immunostaining (Figure 1). Cytology diagnoses included 18 high-grade urothelial carcinoma (HGUC), 2 suspicious for HGUC (SHGUC), 20 atypical urothelial cells (AUC) and 20 negative for HGUC (NHGUC) cases. URO17™ results were interpreted by a pathologist as positive, negative, equivocal or non-contributory. Sensitivity, specificity, positive predictive value (PPV) and negative predictive value (NPV) of URO17™ were compared to the results of histological diagnoses and cystoscopic findings, respectively.

**Results:** Fifty-eight (97%) cases had definitive URO17™ results, 54 (93%) patients had cystoscopies and 28 (48%) had histological follow-up (Table 1). URO17™ was equivocal in 1 (2%) case and non-contributory in 1 (2%) case. Compared to histological diagnoses sensitivity, specificity, PPV and NPV of URO17™ were 94%, 27%, 65% and 75%. Sensitivity, specificity, PPV and NPV of URO17™ were 75%, 100%, 100% and 33% in HGUC/SHGUC cases and 43%, 0%, 75% and 0% in AUC cases. Compared to cystoscopic findings sensitivity, specificity, PPV and NPV of URO17™ were 66%, 70%, 78% and 56%. Sensitivity, specificity, PPV and NPV of URO17™ were 67%, 100%, 100% and 90% in NHGUC cases, 50%, 57%, 67% and 40% in AUC cases and 80%, 67%, 92% and 40% in HGUC/SHGUC cases.

**Table 1.** Results of URO17™ immunostaining, cystoscopic findings and histological follow-up in 60 ThinPrep processed urine cytology specimens.

Cytology Diagnoses (n=60)	URO17 (n=60)				Cystoscope (n=54)		Histopathology (n=28)	
	Positive	Negative	Equivocal	NC <sup>4</sup>	Abnormal	Normal	Neoplasia	Negative
HGUC/SHGUC <sup>1</sup>	14 (70%)	6 (30%)	0 (0%)	0 (0%)	17 (89%)	2 (11%)	16 (89%)	2 (11%)
AUC <sup>2</sup>	8 (40%)	11 (55%)	1 (5%)	0 (0%)	12 (67%)	6 (33%)	8 (89%)	1 (11%)
NHGUC <sup>3</sup>	6 (30%)	13 (65%)	0 (0%)	1 (5%)	5 (19%)	12 (71%)	0 (0%)	1 (100%)

HGUC/SHGUC<sup>1</sup>: High-grade urothelial carcinoma/suspicious for high-grade urothelial carcinoma. AUC<sup>2</sup>: Atypical urothelial cells. NHGUC<sup>3</sup>: Negative for high-grade urothelial carcinoma. NC<sup>4</sup>: Non-contributory.



Figure 1 - 235

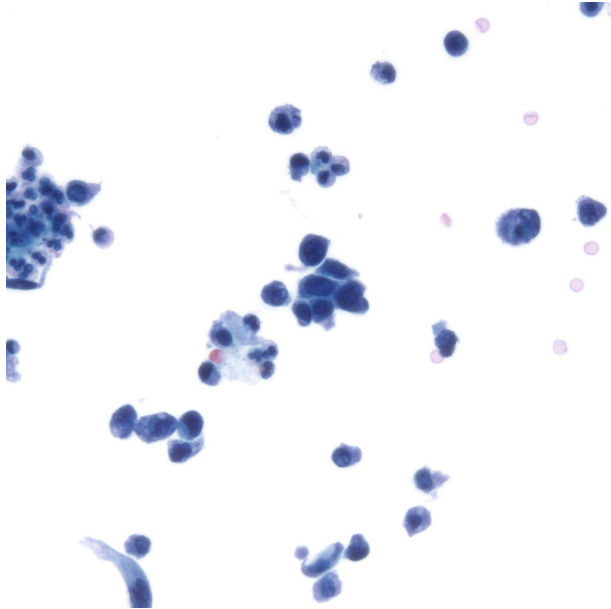
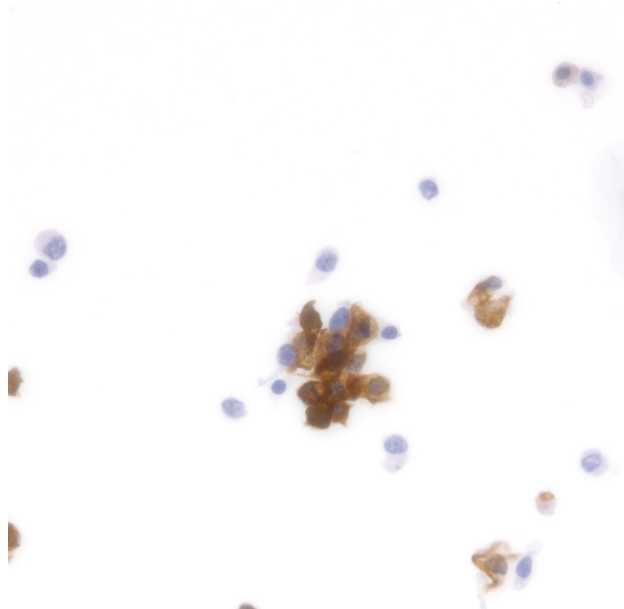


Figure 2 - 235



**Conclusions:** URO17<sup>TM</sup> immunostain can be reliably performed and interpreted in ThinPrep processed urine specimens. Our study showed that URO17<sup>TM</sup> was a sensitive, but less specific marker for using histological diagnoses as a gold standard. URO17 demonstrated moderate sensitivity and specificity when compared to cystoscopic findings. Cytology and URO17<sup>TM</sup> double positive results were highly specific for urothelial neoplasia. Cytology and URO17<sup>TM</sup> double negative results were highly specific for negative cystoscopic findings. URO17<sup>TM</sup> demonstrated significant potential as a cost-effective, non-invasive, risk stratification tool to use in conjunction with traditional ThinPrep urine cytology.

**236 Bile Duct Brushing Cytology: A 10 Year Experience in An Academic Center**

Jack Yang, Ashley Cross<sup>1</sup>, Alex Clavijo<sup>2</sup>, Nathan Ryan<sup>2</sup>, Patricia Houser<sup>2</sup>, Olga Chajewski  
<sup>1</sup>Ralph H. Johnson VA Medical Center, Charleston, SC, <sup>2</sup>Medical University of South Carolina, Charleston, SC

**Disclosures:** Jack Yang: None; Ashley Cross: None; Alex Clavijo: None; Nathan Ryan: None

**Background:** Bile duct brushing is an important tool used to evaluate patients with obstructive jaundice. Differentiating cytologic atypia caused by inflammation from cancerous lesions on bile duct brushings can be a diagnostic challenge. A significant number of bile duct brushings are reported as indeterminate. From 2008 to 2014, 36.8% of all bile duct brushings at our institution were diagnosed as Atypical or Suspicious for Malignant Cells. As a quality control project, we performed a clinical, histologic, and cytologic correlation study and subsequently re-defined the morphological criteria for cytologic diagnosis. In the present study, we evaluated the effect of our new criteria on the bile duct brushing cytology reporting.

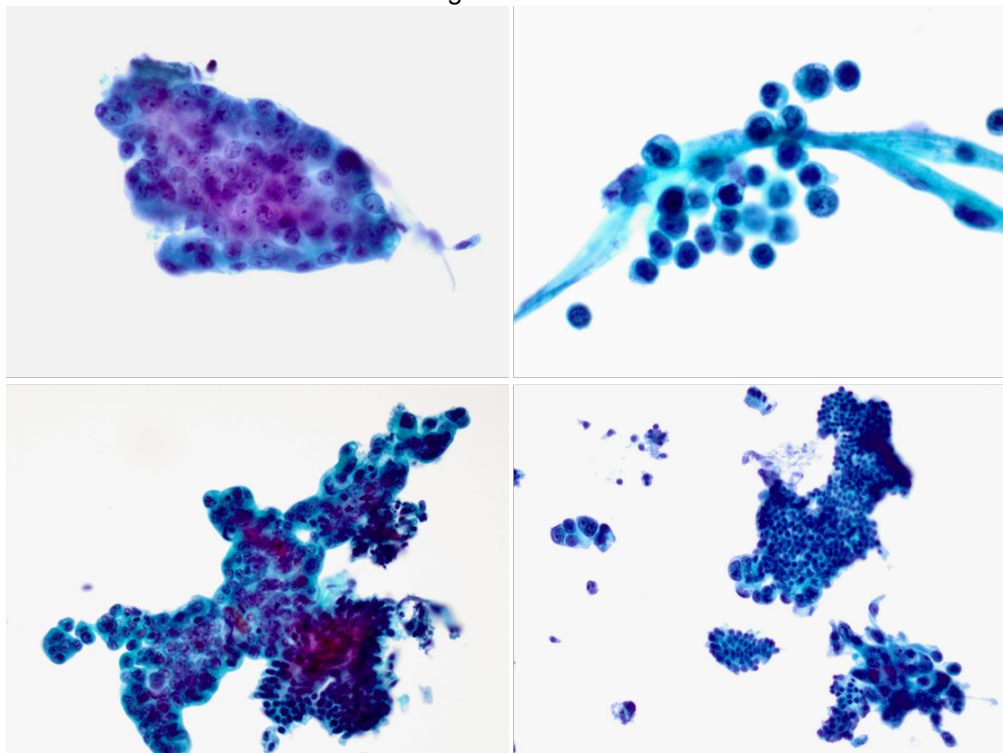
**Design:** Phase I included 95 bile duct brushings with a cytologic diagnosis of Atypical Cells during the period of 2008 to 2014. Based on the histologic and clinical correlation, these cases were classified into Benign and Malignant groups. The Malignant group demonstrated unique cytologic features which included 3-Dimensional groups of atypical cells with cytoplasmic vacuoles, single highly atypical cells, significant anisonucleosis (4:1 ratio), and two distinct populations of epithelial cells (Figure). Phase II evaluated the change in reporting after implementation of the aforementioned criteria in daily practice (2015 to 2018).

**Results:** Results of cytologic, histologic, and clinical correlation are shown in Table. A total of 348 cases were obtained during the period of 2008 to 2014. Cytologic diagnoses included 4 (0.2%) Unsatisfactory, 154 (44.3%) Benign, 95 (27.3%) Atypical, 33 (9.55%) Suspicious, and 62 (17.8%) Malignant. Atypical and Suspicious categories

accounted for 36.8% of the cases. Of those originally cytologically classified as Benign and Atypical, 32 (20.8%) and 48 (50.5%), respectively, were subsequently found to be malignant histologically or clinically. A total of 229 cases were examined in 2015 to 2018. Cytologic diagnoses included 1 Unsatisfactory (0.4%), 149 (65.7%) Benign, 39 (17.0%) Atypical, 15 (6.6%) Suspicious, and 25 (10.9%). Atypical and Suspicious categories decreased to 23.6% of the cases. Of those originally cytologically classified as Benign and Atypical, 35 (23.5%) and 24 (61.5%), respectively, were subsequently found to be malignant.

CYTOLOGY DIAGNOSIS	CLINICAL DIAGNOSIS				NO FOLLOW UP	TOTAL
	BENIGN	MALIGNANT				
		CHOLAGIOMYOCARCINOMA	PANCREATIC CA	OTHER CA		
2008 - 2014						
UNSAT	2	1	0	0	1	4 (0.2%)
NEGATIVE	91	12	17	3	31	154 (44.3%)
ATYPICAL	34	16	27	5	13	95 (27.3%)
SUSPICIOUS	1	12	12	2	6	33 (9.5%)
MALIGNANT	1	20	28	4	9	62 (17.8%)
	129	61	84	14	60	348
2015 - 2018						
UNSAT	0	0	1	0	0	1 (0.4%)
NEGATIVE	88	16	19	1	25	149 (65.1%)
ATYPICAL	9	14	7	3	6	39 (17.0%)
SUSPICIOUS	3	5	5	0	2	15 (6.6%)
MALIGNANT	1	13	7	2	2	25 (10.9%)
	95	48	39	12	35	229

Figure 1 - 236



**Conclusions:** Implementation of strict malignant criteria significantly reduced the number of cases categorized cytologically as Atypical, with only a mild increase in false negative cases.

**237 Performance of the Afirma Genomic Sequencing Classifier versus Gene Expression Classifier in Bethesda Category III Thyroid Nodules: An Institutional Experience**

Lin Zhang<sup>1</sup>, Brian Smola<sup>2</sup>, Richard Cantley<sup>1</sup>, Madelyn Lew<sup>3</sup>, Judy Pang<sup>3</sup>, Xin Jing<sup>3</sup>

<sup>1</sup>Michigan Medicine, University of Michigan, Ann Arbor, MI, <sup>2</sup>Michigan Medicine, Ann Arbor, MI, <sup>3</sup>University of Michigan, Ann Arbor, MI

**Disclosures:** Lin Zhang: None; Brian Smola: None; Richard Cantley: None; Madelyn Lew: None; Judy Pang: None; Xin Jing: None

**Background:** One of the major challenges in the management of thyroid nodules is associated with thyroid nodules with indeterminate cytologic interpretation. The Afirma gene expression classifier (GEC) and Afirma genomic sequencing classifier (GSC), as an adjunct to cytology, improve the risk assessment and reduce unnecessary surgery by further stratifying indeterminate thyroid nodules into benign or suspicious categories. The current Afirma GSC was developed in 2017, aiming to improve specificity and positive predictive value of the Afirma test. There are limited independent studies comparing the diagnostic performance of GSC vs. GEC.

**Design:** The retrospective study included thyroid nodules categorized as Atypia of undetermined significance/Follicular lesion of undetermined significance (Bethesda category III) in our institution and were simultaneously tested with GEC (January 2013 - July 2017) or GSC (August 2017 - March 2020). For each individual patient, the Afirma test result, follow-up clinical and/or radiological result (at least >4 months after result), as well as subsequent surgical pathologic result (if surgically treated) were collected and analyzed. Diagnostic parameters, including sensitivity, specificity, positivity predictive value (PPV), negative predictive value (NPV), and diagnostic accuracy were calculated to compare the performance between GEC and GSC.

**Results:** The study evaluated 265 Bethesda category III thyroid nodules tested with either GEC (n = 131) or GSC (n = 134). The sensitivity and NPV were 100% for both cohorts. In comparison to GEC cohort, GSC cohort demonstrated a greater specificity (83.2% vs. 54.8%),  $p < 0.05$ , a higher PPV (30% vs. 11.1%,  $p < 0.05$ ) and an improved diagnostic accuracy (84.3% vs. 57.2%,  $p < 0.05$ ).

**Conclusions:** Implementation of GSC improved diagnostic specificity, PPV and accuracy while maintaining high sensitivity and NPV. The substantial increase (28%) in diagnostic specificity associated with GSC may potentially avoid unnecessary surgical intervention of Bethesda category III thyroid nodules.